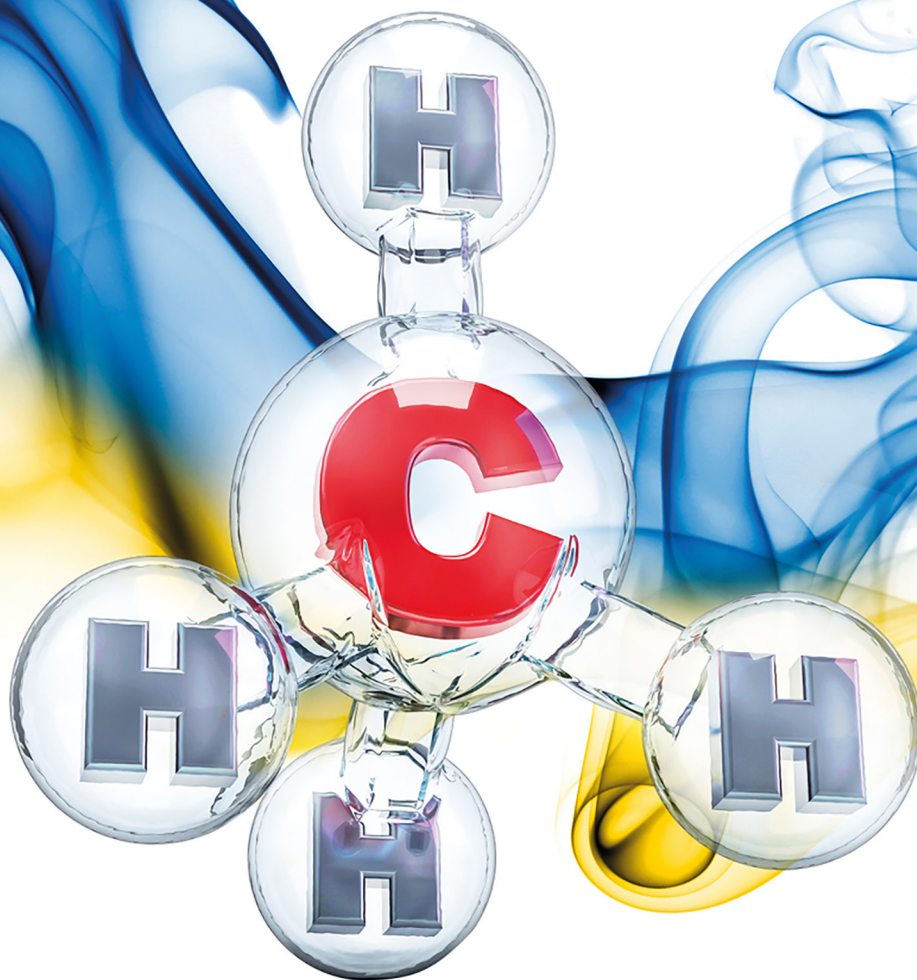


Vasyl Holinko | Roman Dychkovskiy | Artur Dyczko | Marcin Popczyk



# Methane from Underground Coal Mines in Ukraine

Elements of Acquisition  
and Management Processes

Gliwice 2024

<https://doi.org/10.32056/KOMAG/Monograph2024.3>

**Vasyl Holinko**  
**Roman Dychkovskiy**  
**Artur Dyczko**  
**Marcin Popczyk**

**Methane from Underground Coal Mines  
in Ukraine  
Elements of Acquisition and Management Processes**



*Monografia opublikowana na licencji [Creative Commons Uznanie autorstwa -  
- Użycie niekomercyjne 4.0 Międzynarodowe](https://creativecommons.org/licenses/by-nc/4.0/) (CC BY-NC 4.0)*

**Authors:**

Vasyl Holinko, profesor  
Dnipro University of Technology, Dnipro, Ukraine

Roman Dychkovskiy, profesor  
Dnipro University of Technology, Ukraine  
AGH University of Krakow, Poland

Artur Dyczko, Ph. D. Eng.  
Instytut Gospodarki Surowcami Mineralnymi i Energią PAN (Mineral and Energy Economy Research  
Institute of the Polish Academy of Sciences), Poland

Marcin Popczyk  
Politechnika Śląska (The Silesian Technical University in Gliwice), Poland

**Reviewed Scientific Monograph:**

Henryk Badura, Ph. D. Eng.  
Politechnika Śląska (The Silesian Technical University in Gliwice), Poland

Zbigniew Lubosik, Ph. D.  
Główny Instytut Górnictwa Państwowy Instytut Badawczy w Katowicach, Poland

**Cover design:**

NAVIGATOR OLANA PIOTR TURKOT

Copyright by *Instytut Techniki Górniczej KOMAG, Gliwice 2024*  
(*KOMAG Institute of Mining Technology, Gliwice 2024*)

**Editor:**

*Instytut Techniki Górniczej KOMAG, ul. Pszczyńska 37, 44-101 Gliwice, Polska*  
(*KOMAG Institute of Mining Technology*)

**ISBN 978-83-65593-40-5**

## Contents

<b>Introduction</b> .....	4
<b>1. Methane from hard coal mines in Ukraine</b> .....	5
1.1. Complex methane production and hazards of its exploration .....	5
1.2. Operating conditions and modes of operation of explosion hazard control devices .....	7
1.3. Analyze existing methods of methane content control .....	10
1.4. Analysis of existing explosion hazard controls .....	20
1.5. Conclusions .....	22
References .....	23
<b>2. Investigation of electrothermal processes in primary converters of methane analyzers</b> .....	26
2.1. Theoretical analysis of heat transfer process in methane sensors .....	26
2.2. Analysis of operation modes of bridge circuits in methane analyzers .....	33
2.3. Selection of power supply mode for thermoconductometric sensors in methane analyzers .....	36
2.4. Study of influence of gas medium parameters on temperature modes of thermocouples in bridge circuits of methane analyzers .....	43
2.5. Conclusions .....	47
References .....	48
<b>3. Theory development of control methods of methane content in gas mixtures</b> .....	49
3.1. Theoretical evaluation of methane analyzer errors from unmeasured components of mine atmosphere .....	49
3.2. Justification of the thermoconductometric method of control using different thermal modes of sensing elements .....	53
3.3. Justification of the control method using thermocatalytic methane sensor with unequal electrothermal parameters of sensing elements .....	61
3.4. Development and justification of the control method using a two-chamber thermocatalytic methane sensor .....	69
3.5. Justification of the design and operating modes of two-chamber sensor thermocouples .....	73
3.6. Selection and justification of gas mixtures composition control methods for universal wide-range methane analyzers .....	76
3.7. Conclusions .....	87
References .....	89
<b>4. Monitoring of explosion hazard control devices and the ways of their further improvement (written with the participation of Oleksandr Holinko)</b> .....	91
4.1. Development of zero-readings automatic control methods of thermocatalytic gas analyzers .....	91
4.2. Development of automatic control methods of thermocatalytic sensor sensitivity .....	97
4.3. Improving the speed of automatic gas protection systems .....	101
4.4. Conclusions .....	106
References .....	106
<b>Abstract</b> .....	108

## **Introduction**

The presented research addresses one of the critical challenges and opportunities in the energy sector: the management of methane emissions from underground coal mines in Ukraine. Methane, a potent greenhouse gas, has a global warming potential significantly higher than carbon dioxide, making its capture and utilization a priority in mitigating climate change. This research provides an in-depth examination of the current state of methane management in Ukraine, a country with a long history of coal mining and significant methane emissions associated with this industry.

The focus of this research is twofold. First, it explores the methods and technologies available for the acquisition of methane from underground coal mines. This involves a detailed analysis of the techniques used to capture methane, the infrastructure required, and the operational practices that ensure efficient and safe extraction. Second, the study delves into the various elements of methane management, highlighting best practices, regulatory frameworks, and the economic implications of methane utilization.

Ukraine's coal mining sector, characterized by its deep and gassy mines, presents unique challenges and opportunities for methane management. The findings of this research are particularly relevant in the context of Ukraine's ongoing efforts to modernize its energy sector, enhance energy security, and reduce greenhouse gas emissions. By effectively managing methane emissions, Ukraine can not only improve mine safety and reduce environmental impact but also harness methane as a valuable energy resource, contributing to the country's energy mix.

This research draws on a wealth of data, field studies, and expert insights to provide a comprehensive overview of the methane management landscape in Ukraine. It evaluates the effectiveness of current policies and practices and offers practical recommendations for improving methane capture and utilization. The study also compares Ukraine's approach with international best practices, identifying areas where Ukrainian mines can benefit from global experiences and innovations.

The importance of this research cannot be overstated. As the world grapples with the dual challenges of energy security and climate change, the effective management of methane emissions represents a crucial intersection of these issues. For Ukraine, with its significant coal resources and ambitious climate commitments, the findings and recommendations of this study have the potential to drive meaningful progress in both environmental stewardship and energy efficiency.

We commend the researchers for their meticulous work and their commitment to addressing such a vital issue. This research not only contributes to the scientific understanding of methane management but also provides actionable insights that can guide policymakers, industry stakeholders, and environmental advocates in Ukraine and beyond. It is my hope that this study will serve as a catalyst for improved methane management practices, fostering a more sustainable and secure energy future for Ukraine.

*Vasyl Holinko, Roman Dychkovskiy, Artur Dyczko, Marcin Popczyk*

## 1. Methane from hard coal mines in Ukraine

### 1.1. Complex methane production and hazards of its exploration

Coal mines are a very complex production system with particularly hazardous working conditions. Complex mining and geological conditions of the majority of coal deposits in Ukraine determine the presence of a large number of hazardous and harmful production factors, which significantly affect the life and health of workers and lead to a high level of injuries and occupational diseases in the industry. Accidents with group accidents associated with gas and dust explosions, underground fires and gas dynamic phenomena are particularly dangerous.

Depending on the nature of the course and the consequences caused, accidents associated with methane ignitions are usually divided into three groups: explosions, flashover and combustion [1,2]. In an explosion, there is a rapid combustion of the methane-air mixture, which results in a significant increase in temperature and pressure. The rapid compression of gases leads to the formation of an air shock wave, as a result of the spread of which there are mechanical injuries to people, destruction or damage to mine workings, structures and equipment. The flash occurs during rapid combustion of a relatively small volume of methane-air mixture. The amount of energy released is insufficient to generate a shock wave capable of having a destructive effect on objects and equipment and causing mechanical injuries to people. It is considered that the air overpressure, which is safe for a person, does not exceed 0.01 MPa [3]. This value of overpressure is usually taken as the boundary between explosion and methane flash. During normal combustion there is a calm deflagration combustion of methane without shock wave formation.

Usually, when analyzing coal mine accidents, methane explosions and methane combustion events are difficult to distinguish and are often combined into one group of events. There are 1-2 methane explosions annually at coal mines in Ukraine. The largest number of explosions occurs in preparatory workings ventilated by local ventilation fans, which is primarily due to fan shutdowns and various defects in the ventilation system. A significant number of explosions also occur in the cleaning workings and outgoing workings from the mine face and panels. The main causes of these explosions are related to the failure of ventilation of the workings by the main ventilation fans, sudden release of methane into the workings caused by gas dynamic phenomena (sudden emissions, breakthroughs, fumaroles), formation of local methane accumulations and accumulation of methane in the workings [4].

Ventilation failures in dead-end mine workings most often occur as a result of stoppage of local ventilation fans [2]. In this case, gasification starts with methane filling of domes and voids and formation of methane accumulations under the roof at the face of the workings. The section of the dead-end excavation adjacent to the mouth is ventilated by turbulent diffusion, while the rest of the excavation is unstable natural ventilation due to the temperature gradient and methane concentration difference. In horizontal mine workings there are usually two flows: at the soil to the face, at the roof to the mouth, the speed of which depends on many factors and ranges from tenths to tens of meters per minute. The rate of increase of methane concentration in the excavation depends on its parameters and the intensity of gas emission, which, in turn, depends on the methane content of the coal and the surrounding rocks, the thickness of the uncovered seams, the amount of stripped coal, the speed of excavation and other factors.

The calculations usually take into account methane emission from the exposed surface of the formation at the 20 m long bottom-hole section, from the stripped coal and from the mine walls along its entire length. The highest rate of increase in methane concentration in the workings is observed if the ventilation of the workings was disrupted during blasting operations.

Maximum methane emission in bottom hole space  $I_{h.s.max}$  is observed after coal blasting. According to [5] it can be calculated as

$$I_{h.s.max} = 0.05\gamma S_c I_{bl}(x - x_0), \quad (1.1)$$

where:

- $\gamma$  – coal density, t/m<sup>3</sup>;
- $S_c$  – coal face area, m<sup>2</sup>,

$l_{bl}$  – face movement per blasting, m,

$x, x_0$  – respectively, methane content and residual methane content of coal,  $\text{m}^3/\text{t}$ .

During the first 30 minutes after coal blasting, the intensity of methane emission from the blasted coal  $I_{in}$  can be determined by the formula:

$$I_{in} = \frac{1.8I_{h.s.\max}}{1.8 + T}, \quad (1.2)$$

where:

$T$  – time elapsed after detonation of charges, min.

In case of stopping the fan at such intensity of methane emission already in 1 min after the explosion the concentration of methane in the bottom-hole space becomes explosive.

Characteristic changes in the flow rate and methane concentration in the bottom-hole space of a dead-end mine during blasting operations and insufficient air supply due to damage of ventilation pipes are shown in Fig. 1.1 [6]. In this situation, the methane concentration in the bottom-hole space becomes explosive within a few minutes.

Often gasification of dead-end mine workings occurs as a result of coal and gas emissions during concussive explosion. In this case, already within the first 6-10 s, the concentration of methane in the bottom-hole space exceeds the lower explosive limit of the mixture [6].

The main causes of gasification of mine workings at mine sites are ventilation failures, local accumulations of methane and methane accumulation in the mined-out spaces. Thus, after the air flow rate is reduced by 3 or more times within 5-15 min, local accumulations of methane with explosive concentrations are formed in ventilation workings [6]. Gradually these accumulations increase in length and height.

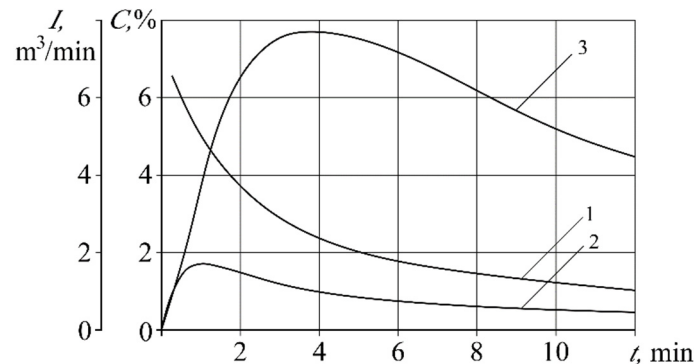


Fig. 1.1. Graph of change of flow rate and methane concentration in the bottom-hole space of a dead-end mine after blasting of charges on coal at  $I_{h.s.\max} = 7.5 \text{ m}^3/\text{min}$ :  
1 – flow rate; 2 and 3 – concentration at air flow rate of 320 and 30  $\text{m}^3/\text{min}$ , respectively

Due to the decrease in turbulent diffusion intensity and reduction of air leakage through the mined-out space, areas with high methane concentration appear in its stagnant zone. At the same time, in the outgoing ventilation jet of the site, the growth of methane concentration may not be observed for a long time, and starts only after several hours after the air flow rate is reduced. After the normal ventilation regime is restored, methane accumulated in the excavated space is intensively carried out into the ventilation workings, and its concentration may reach explosive values.

Modeling of the processes of gasification in the cleaning workings and in the workings coming from the cleaning faces under gas dynamic phenomena [7] showed that in the absence of debris, the concentration of methane in the longwall face after ejection can reach maximum (100 vol.%) in tenths of minutes, and in the workings coming from the cleaning faces the concentration of methane for a long time can exceed tens of percent. The blockages occurring during the release lead to a significant reduction in the air flow rate through the cleanup face, which sometimes increases the time of gasification to several hours [8]. Subsequently, when

the ventilation mode is restored, a transient gas-dynamic process occurs at the mine site, which can last for several hours and even days [8].

In methane explosions, the main impact factors are the shock wave, high-temperature explosion products and toxic gases produced during the explosion, as well as insufficient oxygen content in the air of mine workings due to its participation in combustion processes. Particularly severe consequences occur if a methane explosion initiates a coal dust explosion. Explosive dust-air mixture is mainly formed by the blowing up of dust deposited on the surface of the mine workings, caused by the dynamic effect of the shock wave during the ignition of methane.

The sources of ignition of explosive mixtures are various thermal impulses, flames or sparks generated during technological work in mines, as well as spontaneous combustion of coal and other self-igniting substances when they are used in mines [1, 3].

In large explosions, the number of fatally injured on average is several dozen people, and the average material damage from the explosion exceeds tens of millions of hryvnias, which necessitates the development of measures aimed at prevention and prophylaxis of methane and dust explosions in coal mines.

## **1.2. Operating conditions and modes of operation of explosion hazard control devices**

Explosion control devices in mine workings and equipment of coal mines are operated under very difficult conditions, which are characterized by the possibility of formation of an explosive environment, a wide range of temperature and atmospheric pressure changes, high relative humidity and dustiness of the mine atmosphere, variability of gas composition and air flow velocity. In addition, portable explosion control devices, as well as those installed on mobile machinery and equipment, are subjected to significant dynamic and vibration loads. All of this predetermines special requirements for the design of explosion control devices, as well as requirements for their performance, reliability, mechanical strength, corrosion resistance, etc.

Existing means and systems of control of explosion hazard in mine workings and equipment of coal mines are usually divided into the following groups [9]:

- episodic portable devices;
- portable automatic devices;
- stationary automatic devices;
- automatic remote control systems.

Operating conditions and modes of operation of portable and stationary control devices differ significantly. The operating conditions of stationary means used in the systems of automatic gas protection of mine workings and used to control explosion safety in degassing systems are also significantly different. Taking this into account, let us analyze the conditions for three groups of control devices:

- portable devices;
- stationary means of explosion hazard control of mine workings of mines;
- stationary means of explosion hazard control of degassing systems.

In the operation of portable instruments, it is usually envisaged that they should be serviced on the surface every working shift or every day before each delivery to the mine. Given that the instruments are serviced on the surface, their operating conditions cover the entire possible range of changes in environmental parameters in the mine workings and rooms of the surface complex of the mine:

- ambient temperature from 5 °C to 35 °C (278-308) °K;
- atmospheric pressure 87.8-119.7 kPa;
- relative humidity of ambient air up to 100 % at 35 °C (without condensation);
- atmospheric dustiness up to 1000 mg/m<sup>3</sup>;
- air velocity not more than 8 m/s.

Since the devices may be operated in potentially explosive atmospheres, they must have the explosion protection of the proper level (Intrinsically safe).

The composition of the mine atmosphere where the devices are operated differs significantly from the composition of the atmospheric air on the surface. Under normal operating conditions, methane (up to 2 vol.%)

and carbon dioxide (up to 1 vol.%) may be present in the mine atmosphere, and the oxygen content may be reduced to 20 vol.%. In case of emergency gasification of mine workings, the concentration of methane can reach tens of percent, and the concentration of oxygen as a result of dilution of air with mine gas can be significantly reduced.

In addition to methane, mine gas usually contains its higher homologues: ethane, propane, butane and in small quantities hydrogen. Due to the fact that the content of these components in mine gas usually does not exceed 5 vol.%, they are usually neglected when analyzing the explosive properties of mixtures.

In the presence of burning centers in the collapsed rock mass, the concentration of hydrogen increases and carbon monoxide enters the mine atmosphere [10]. In the case of developed fires, the content of carbon monoxide and hydrogen in the mine air reaches 2.0 vol.%, and sometimes more. The analyzed mixture in this case contains several combustible components, and its explosive properties increase.

In addition to these gases, other harmful gases may be present in the mine atmosphere, in particular, sulfur dioxide, hydrogen sulfide, nitrogen oxides, etc. Sulfur dioxide is formed mainly by combustion of sulfur contained in significant amounts in many grades of coal. It enters the mine atmosphere during fires and blasting operations. Hydrogen sulfide is formed due to decay of organic substances, interaction of sulfate water with methane, decomposition of pyrite enters the mine atmosphere from cracks and mineral springs. Significant amount of it can also be allocated at carrying out of explosive works and at endogenous fires. In some cases concentration of hydrogen sulfide can reach tenths of volume percent.

Significant quantities of nitrogen oxides are produced during blasting operations. The main form of oxides entering the mine atmosphere at the initial moment after the explosion is nitrogen oxide NO. In the mine air in the presence of water vapor and sulfur dioxide, which act as catalysts, nitrogen oxide combines with air oxygen and converts to the form of nitrogen dioxide NO<sub>2</sub>. High concentrations of nitrogen oxides (up to tenths of a percent) are observed only after blasting. Later, as a result of intensive interaction of nitrogen oxides with water, their concentration in mine air decreases rapidly.

Operation of portable devices under conditions significantly different from normal conditions is usually possible during the time required for personnel to exit from the gassed workings to a fresh ventilation stream and may last up to several hours. In case of debris formation, which makes it difficult for workers to leave the emergency area, the operation of these devices under conditions significantly different from normal may last until the batteries in the power supply unit are completely discharged, i.e. actually 8-10 hours.

In the presence of blockages, the air flow rate in the workings is significantly reduced, which leads to their gasification. The time of gasification depends on the intensity of gas emission and the air flow rate. Usually, there is a linear relationship between the air flow rate and methane concentration in the outgoing face jet. On this basis, at the initial methane concentration in the workings of 1 vol.%, as a result of air flow rate change, the methane content in the places where workers may be located may be within the range of explosive concentrations for a long time, which may lead to overheating of sensitive elements of existing thermocatalytic sensors and failures in the operation of explosion hazard control devices.

Portable devices in the process of operation may be exposed to transportation and technological vibration. Accidental blows on the device case, falling from a height, short-term flooding with water, filling with coal fines, etc. are also possible. Stationary means of explosion hazard control of mine workings measure the concentration of methane in the place of installation of sensors of gas analyzers. According to [11] sensors of stationary gas analyzers should be installed in the outgoing jets of mine workings, in bottom-hole spaces of dead-end workings, in dead-ends of ventilation workings, extinguished after the mine face and other places.

Maintenance of stationary means of explosion hazard control in mine workings is carried out directly in the places of their installation. Their operating conditions cover the entire possible range of changes in environmental parameters in mine workings. Usually, in order to unify the requirements to explosion safety monitoring devices, the range of change of such environmental parameters as ambient temperature, atmospheric pressure, relative humidity of the ambient air and dustiness of the atmosphere for stationary means of explosion hazard monitoring of mine workings is the same as for portable devices.

Significant changes in gas composition are observed in isolated areas of mine workings when extinguishing complex developed fires by isolation methods. In isolated workings the oxygen content decreases, the concentration of methane, carbon dioxide, carbon monoxide, sulfur dioxide, hydrogen increases, and in addition, unsaturated hydrocarbons, products of thermal decomposition of combustibles and materials may be present in the gas mixture. At present, when managing the process of extinguishing isolated fires, the control of gas composition, characterizing the explosive properties of the mixture, is carried out by sampling and subsequent laboratory analysis or with the help of mine chromatographs. Existing stationary gas analyzers in this situation are inoperable.

Very severe operating conditions are characteristic of the control devices installed in the bottom-hole spaces of mine workings, as well as on mining and transportation equipment, where the control devices may be exposed to machine elements and mechanisms, water, falling pieces of coal and rock, and increased levels of vibration. In addition, explosion safety controls installed on transportation equipment may be operated at higher air velocities. In the case of counter direction of air and vehicle movement, this velocity can be up to 20 m/s [12].

The operating conditions of stationary explosion control devices of degassing systems may differ significantly from the operating conditions of explosion control devices installed in mine workings. An important parameter determining the operating conditions of stationary means of explosion hazard control of degassing systems is pressure. It should be noted that the means of control installed before the vacuum pump, operate at a pressure below atmospheric, and after the vacuum pump – under increased pressure. The value of rarefaction or overpressure can vary in wide enough limits depending on the length and condition of degassing pipelines, presence of air suction into degassing wells through the destroyed rock massif and leaky wellhead and other reasons.

Sensors of stationary explosion monitoring devices are usually installed directly in the mixture to be analyzed. Sensors installed before the vacuum pump can operate at a vacuum of 16-86 kPa. The pressure behind the vacuum pump when the methane-air mixture is released into the atmosphere is almost equal to atmospheric pressure, and during the subsequent use of the mixture it reaches 150 kPa.

In addition to methane, the captured gas mixtures contain various gaseous impurities that affect the explosive properties of methane and change the operating conditions of gas analyzer sensors. The lower explosivity limit of the gas mixture is usually determined by the Le Chatelier formula [13]:

$$C_c = \frac{100}{\frac{C_1}{N_1} + \frac{C_2}{N_2} + \dots + \frac{C_n}{N_n}}, \quad (1.3)$$

where:

$C_1, C_2, \dots, C_n$  – concentration of combustible components present in the mixture, % ( $C_1 + C_2 + \dots + C_n = 100\%$ );

$N_1, N_2, \dots, N_n$  – lower explosive limit of the corresponding combustible components, %.

The main combustible impurity in methane-air mixtures is ethane. At some deep mines its concentration in mine gas reaches up to 5 vol.%. Most significantly, the change in explosive properties of the mixture is affected by propane, the content of which in some mixtures is up to 1 vol.%. When controlling the explosion hazard of mine workings and gas analyzers in the area close to unacceptable concentrations of methane, such as 1 or 2.0 vol.%, the presence of higher homologues of methane in the gas-air mixture at the considered compositions of combustible gases does not exceed 0.1 vol.% and practically does not affect the operation of explosion hazard control equipment. When controlling the explosion hazard of gas mixtures in degassing pipelines and controlling concentrations in the area of the upper limit of unacceptable methane concentrations, the content of higher homologues of methane may exceed 1 vol.%. Taking into account the fact that the higher methane homologues are characterized by a lower flammability temperature than methane, significantly differ from the latter in thermal conductivity and other physical properties, underestimation of their presence can lead to significant errors in the operation of gas analyzers, and in some cases to failures [14].

As a rule, degassing pipelines receive gas saturated with water vapor up to 20 g/m<sup>3</sup>. There may also be solid and liquid particles of noncombustible substances (dust, dripping moisture, rust, etc.) in the place of sensor installation [15]. The gas mixture flow velocity in pipelines up to vacuum pumps in some cases reaches 30 m/s. In the pipelines connecting the vacuum pumps outlet with consumers the velocity of methane-air mixture does not exceed 20 m/s. The highest flow velocity, up to 50 m/s, is observed at the mixture discharge into the atmosphere.

### 1.3. Analyze existing methods of methane content control

The known methods of explosion hazard control of gas mixtures are based on the difference in physical and chemical properties of explosive gases and other uncontrolled components of the mine atmosphere [16]. The common property of all combustible gases that distinguishes them from air and other gases present in the mine atmosphere is their ability to be oxidized by air oxygen (Table 1.1).

Table 1.1

Physicochemical properties of gases

Name values	Units of measurement	Values for gases					
		Air	CH <sub>4</sub>	C <sub>2</sub> H <sub>6</sub>	H <sub>2</sub>	CO	CO <sub>2</sub>
Density	kg/m <sup>3</sup>	1.293	0.717	1.357	0.0899	1.25	1.977
Specific heat of combustion	J/Kmol	–	892·10 <sup>6</sup>	1562·10 <sup>6</sup>	287·10 <sup>6</sup>	283·10 <sup>6</sup>	–
Diffusion coefficient	m <sup>2</sup> /s	–	19.6·10 <sup>-6</sup>	11.6·10 <sup>-6</sup>	66·10 <sup>-6</sup>	19.2·10 <sup>-6</sup>	13.9·10 <sup>-6</sup>
Refractive index		1.000292	1.000441	1.000696	1.000138	1.000334	1.000450
Thermal conductivity	W/(m K)	2.4·10 <sup>-2</sup>	3.1·10 <sup>-2</sup>	1.8·10 <sup>-2</sup>	17.9·10 <sup>-2</sup>	2.35·10 <sup>-2</sup>	1.4·10 <sup>-2</sup>
heat capacity	KJ/(Kmol K)	29.15	39.82	51.9	28.76	28.47	45.2
Auto-ignition temperature	°C	–	645	472	510	610	–
Lower explosive limit	vol.%	–	5	3.2	4	12.5	–
Upper explosive limit	vol.%	–	15	12.5	75.2	74.2	–
Wavelengths at maximum absorption	micrometer	–	3.31; 7.7	–	25	2.37; 4.65	2.7; 4.2; 15

The specific heat of combustion and autoignition temperature of different combustible gases differ significantly. Thus, methane has the highest autoignition temperature, and the lowest autoignition temperature is characteristic of the higher homologues of methane. Methane and its homologues differ significantly from other combustible gases (carbon monoxide and hydrogen) in their calorific value.

As a diagnostic sign of explosion hazard of a gas mixture almost all existing means and systems of explosion hazard control in mine workings and equipment of coal mines use information of gas analyzers about the concentration of methane in the mixture. In general, this approach is reasonable, because, as can be seen from Table 1.1, the presence of other combustible gases in mixtures does not significantly affect the lower concentration limit of its explosion ability. However, a significant difference between the properties of some combustible components and the properties of methane can lead to additional errors of methane concentration measurement when using specific control methods. For example, when using control methods based on measuring the thermal conductivity of the mixture, the presence of ethane will lead to underestimation of the methane analyzers, while the lower concentration limit of the explosiveness of the mixture decreases and its explosive hazard increases. On the contrary, when using control methods based on measuring the refractive index of the mixture, the presence of ethane will lead to overestimation of methane analyzers. Obviously, in this case it characterizes explosive properties of the mixture more reliably than in the previous method. At the same time, the presence of hydrogen in the mixture leads to a significant decrease in its refractive index and to underestimation of the gas analyzers' readings when the explosion hazard level increases.

When gas analyzers work in mine workings when methane concentration does not exceed the lower limits of unacceptable methane concentrations established by the Safety Board, the noted additional errors usually do not exceed 1/3 of the basic error and they are usually neglected. However, when gas analyzers work in rich mixtures, for example, in degassing pipelines, as well as in case of fires, gasification of mine workings up to explosive and higher methane concentrations, the influence of these combustible impurities can lead to significant measurement errors and incorrect assessment of the explosion hazard of the mixture.

Among the properties of methane that significantly distinguish it from air are its density, viscosity, thermal conductivity, heat capacity, light refractive index, sound propagation velocity, and diffusion properties. The diversity of distinctive properties of methane has also determined a significant number of existing methods of its concentration control.

Refractometric method was one of the first methods of controlling methane content in the mine atmosphere that became widespread. This method is based on the difference between the light refractive indexes of methane and air. The disadvantages of the refractometric method include the fact that such variable components of the mine atmosphere as carbon dioxide and water vapor have refractive indices of light that differ significantly from air, as well as the presence of optical elements that must be protected from pollution. To eliminate the influence of these components on the measurement results, it is necessary to pre-dry the analyzed air and absorb carbon dioxide, as well as to pre-clean the analyzed medium from dust or to protect optical elements from pollution. Taking this into account, the method is widely used in hand-held portable devices of episodic action – mine interferometers and much less often in stationary refractometric gas analyzers. In mine interferometers, the analyzed mixture is pre-passed through a filter and dryer, and the influence of carbon dioxide is eliminated by its preliminary absorption by a chemical lime absorber.

Another type of optical methods is the absorption method [17], which is based on selective absorption of radiant energy by gases in the infrared part of the spectrum. The wavelengths of maximum absorption characteristic of methane are 3.31 and 7.7  $\mu\text{m}$ . In this area the research was carried out in two directions, the first of which consisted in the development of dispersionless analyzers with selective optical-acoustic beam-receiver, and the second – in the use of narrowband or monochromatic radiation sources with a wavelength corresponding to the maximum absorption of methane and the use of broadband, non-selective optical receivers. In the first case for realization of the method it is necessary to use rather complicated optical-acoustic beam-receivers, which limits the possibility of wide application of this type of method. The second direction is more promising.

The advantages of the considered optical methods of methane content measurement include their low inertia, which makes it possible to create on its basis means for fast-acting gas protection. However, due to the need to protect optical elements from pollution, it is very difficult to realize this advantage of optical methods [18, 19].

When creating stationary means of automatic gas control systems and portable methane alarms, the most widespread in Ukraine and abroad is the thermocatalytic method. This method consists in flameless combustion of methane on the surface of the catalyst [16] and measuring the amount of heat released.

Thermocatalytic sensors of modern gas analyzers [16], as a rule, have two sensitive elements - catalytically active (working) and compensating (comparative). Usually, the elements are made in the form of miniature balls of  $\gamma$ -aluminum oxide inside of which a spiral of platinum wire is placed, which simultaneously performs the functions of a heating element and a resistance thermometer. In some cases, to reduce energy consumption, the inner layers of the elements are formed from  $\alpha$ -oxide, and the outer ones from  $\gamma$ -aluminum oxide [20]. A platinum-palladium catalyst is applied to the surface of the catalytically active element, while the compensating element remains clean. Solutions are known, when in order to equalize the radiation component of heat exchange of elements, as well as to reduce the activity of the comparative element, its surface is also treated with various compositions, such as  $\text{AgS}_2$  [21]. Most often the elements are placed in a common reaction chamber, which is formed inside a porous ceramic or metal-ceramic gas-exchange filter element and separated from each other by a heat-insulating screen. There are also known solutions, when in order to increase the reliability of explosion hazard control of multicomponent gas mixtures the working and compensating elements are placed under separate filter elements with different diffusion conductivity [22, 23], as well as solutions consisting in the use of a double diffusion filter [24, 25]. In the latter case, the external ceramic-metal filter element having high diffusive conductivity, first of all, performs protective functions in a highly dusty atmosphere, and the internal one, made in the form of a calibrated hole in an airtight cup, limits the diffusive flow to the sensitive elements and provides stability of the analyzers' characteristics.

The controlled medium enters the reaction chamber by molecular diffusion. On the working element methane is oxidized by air oxygen with the release of heat, which increases the temperature and resistance of the thermocouple, the incremental value of which is a measure of methane concentration. The comparative element serves to reduce the influence of changes in temperature, pressure and atmospheric composition on the

measurement results. Gas supply to the surface of the working element and removal of reaction products from it is conditioned by the presence of their concentration gradient between the surface of the element and the volume of the reaction chamber.

The platinum-palladium catalysts used in thermocatalytic sensors are deep oxidation catalysts. The reaction on the working element takes place according to the equation:



where:

$Q = 805.2$  kJ/mol is the amount of heat released during combustion of a mole of methane.

Depending on the temperature of the platinum-palladium catalyst, the heterogeneous methane oxidation reaction can occur in the kinetic or diffusion areas [26].

The oxidation reaction rate in the kinetic area is usually represented as a function of the volume-molar concentrations of methane and oxygen

$$\omega = kF_e f(C_{CH_4}, C_{O_2}), \quad (1.5)$$

where:

$\omega$  – reaction rate, mol/s;

$k$  – reaction rate constant, s<sup>-1</sup>;

$F_e$  – active surface of the catalyst, m<sup>2</sup>.

The value of  $k$  depends on the type of reacting substances and increases with increasing temperature

$$k = Z \cdot e^{-\frac{E}{RT}}, \quad (1.6)$$

where:

$Z$  – pre-exponential multiplier;

$E$  – activation energy, J/mol;

$R$  – universal gas constant, J/(mol·K);

$T$  – absolute temperature, K.

It can be seen from (1.6) that the oxidation reaction rate in the kinetic area depends on the catalyst temperature. Methane oxidation is accompanied by simultaneous adsorption of oxygen and methane by the catalyst surface [26]. Therefore, the reaction rate is affected not only by the methane concentration, but also by the oxygen concentration in the atmosphere, which makes it difficult to obtain a signal proportional to the methane content.

At temperatures above 360 °C, the process of methane oxidation on platinum-palladium catalysts proceeds in the diffusion area [27]. In this case, the rate of chemical reaction is determined by the rate of diffusion of the limiting component to the catalyst surface. At control of pre-explosive concentrations of methane and excess of oxygen in the analyzed mixture, all methane molecules reaching the active surface of the working element are oxidized and the amount of heat released per unit time on the working element is proportional to the concentration of methane in the reaction chamber and the lower heat of combustion of methane

$$R_m = Q_m \gamma_e C_m, \quad (1.7)$$

where:

$Q_m$  – lower heat of combustion of methane, J/m<sup>3</sup>;

$\gamma_e$  – effective diffusive conductivity of the element, m<sup>3</sup>/s;

$C_m$  – volume fraction of methane in the reaction chamber, %.

The effective diffusive conductivity of an element is generally determined by its geometric parameters, the efficiency of methane oxidation on the surface of the element and the parameters of methane mass transfer to its surface [27]

$$\gamma_e = 10^{-2} k_e \beta_m F_e, \quad (1.8)$$

where:

$k_e$  – methane oxidation efficiency factor;

$\beta_m$  – mass transfer coefficient, m/s;

$F_e$  – element surface area, m<sup>2</sup>.

The methane oxidation efficiency factor is introduced into expression (1.8) due to the fact that not the entire surface area of the element is catalytically active. In the ideal case  $k_e = 1$ , and for real conditions it is somewhat less than one.

The mass transfer coefficient depends on the diffusion properties of the gas and can generally be represented as

$$\beta_m = D_m / \delta_D, \quad (1.9)$$

where:

$D_m$  – molecular diffusion coefficient of methane in air, m<sup>2</sup>/s;

$\delta_D$  – thickness of the diffusion boundary layer, m.

The molecular diffusion coefficient of methane is determined at the average boundary layer temperature  $t_t$  by the Sutherland formula:

$$D_m = D_{m0} \left( \frac{t_t + 273}{273} \right)^{1.75}, \quad (1.10)$$

where:

$D_{m0}$  – molecular diffusion coefficient of methane in air at 0 °C, m<sup>2</sup>/s.

$$t_t = \frac{(t_e + t_g)}{2}, \quad (1.11)$$

where:

$t_e$  – thermocouple surface temperature, °C;

$t_g$  – gas temperature inside the reaction chamber outside the boundary layer, °C.

The expression for determining the thickness of the diffusion boundary layer at the element of a spherical shape with diameter  $d$ , has the form [27]:

$$\delta_D = d / (2 + 111d^{0.75}). \quad (1.12)$$

Analysis of the above expressions shows that at constant gas and element temperature, the power released on the working element due to methane oxidation is determined by the properties of the catalyst, and element design and is proportional to the product of the methane concentration in the chamber, the lower heat of combustion of methane and its diffusion coefficient. Taking this into account, expression (1.7) can be presented in the form of [28]:

$$R_m = K_d Q_m D_m C_m, \quad (1.13)$$

where:

$K_d$  – coefficient taking into account the design features of the sensor and properties of the catalyst, m.

The power released on the work cell as a result of methane oxidation leads to an increase in its temperature relative to the comparison cell

$$\Delta t = t_w - t_c = \frac{K_d Q_m D_m C_m}{K}, \quad (1.14)$$

where:

$t_w$  and  $t_c$  are respectively the temperature of the working and comparative elements, °C;  
 $K$  – thermal conductivity of the element, W/°C.

As can be seen from the equation (1.10), the increase in the heating temperature of the working element leads to an increase in the molecular diffusion coefficient of methane and, according to (1.13), to an increase in the power released on this element as a result of methane oxidation. However, at the same time, the thermal conductivity of the element also increases, which finally prevents the growth of the value of  $\Delta t$  at increasing the temperature of the working element.

The concentration of methane in the reaction chamber is related to the concentration of methane in the surrounding atmosphere  $C_{ma}$  by the relation [16]:

$$C_m = C_{ma} \frac{\gamma_f}{\gamma_e + \gamma_f}, \quad (1.15)$$

where:

$\gamma_f$  – diffusive conductivity of the filter element, m<sup>3</sup>/s.

Change of power supply parameters of the thermocatalytic sensor leads to change of effective diffusion conductivity of the element and, accordingly, to change of methane concentration in the reaction chamber. Thus, at constant value of  $\gamma_f$  the increase of heating temperature of the working element leads to the growth of effective diffusive conductivity of the element and, consequently, to the decrease of methane concentration in the chamber.

These features of methane oxidation on the working element determine the extreme nature of the dependence of the output signal of the thermocatalytic sensor on the preheating temperature of the sensing elements, which is related to the value of the current flowing through the thermocouple. The nature of the dependence of the bridge output voltage on the magnitude of the current through the thermocouples is shown in Fig. 1.2 (curve 1) [29].

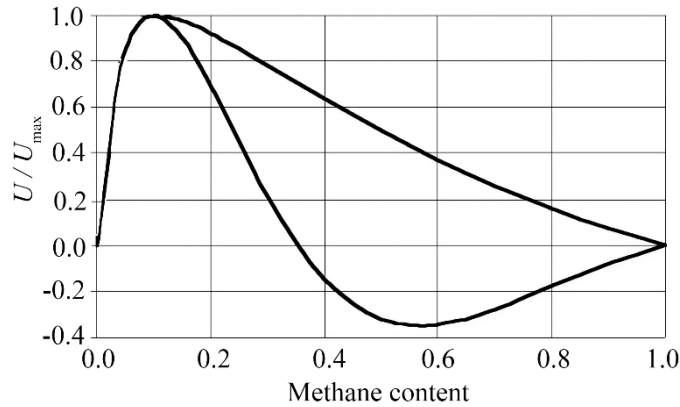


Fig. 1.2. Normalized characteristics of thermogroup at different diffusion limitations:  
 1 – without additional filter; 2 – in the presence of additional filter with calibrated hole  
 $d = 0.85$  mm;  $l = 0.6$  mm.

As a result of methane oxidation on the operating element, its temperature rises between 20 and 30 °C per 1 vol.% of methane. Without taking measures to limit the heating temperature of this element at high methane concentrations, this can lead to temperature overloads and changes in the characteristics of the sensing elements. In addition, such a temperature increase causes nonlinearity of the analyzer output characteristic at methane concentrations above 3-5 vol.% [27]. To exclude these phenomena, special modes of power supply of the measuring bridge are used, for example, with voltage stabilization on the working element [30], or methane diffusion to the working element is limited by introducing an additional gas diffusion filter. In the latter case, the constant sensitivity of the sensors is simultaneously ensured over a wide range of changes in

the thermogroup supply parameters (curve 2, Fig. 1.2).

Theoretically, at low methane concentrations, when the limiting agent in the gas mixture is fuel, the output voltage of a measuring bridge with a thermocatalytic sensor depends linearly on the methane concentration [16]:

$$U_{out} = \frac{R_{e_0} I_e \beta_e Q_m \gamma_e C_m}{2K}, \quad (1.16)$$

where:

$R_{e_0}$  – resistance of the element at 0 °C;

$\beta_e$  – temperature coefficient of resistance of the element, 1/°C;

$I_e$  – current flowing through the elements, A.

At high methane concentrations, when air oxygen becomes the limiting component, the bridge output voltage decreases down to zero at 100 vol.% methane [16]:

$$U_{out} = 0.0525 \frac{R_{e_0} I_e \beta_e Q_m \gamma_e}{K} (1 - C_m). \quad (1.17)$$

At the same time, experimental studies of thermocatalytic sensors show significant differences between real and theoretical characteristics. Thus, in the area of explosive methane concentrations, dips in the output characteristic are observed [31], at high methane concentrations, a significant hysteresis of readings and inversion of the output signal are observed [31, 32], and the characteristics of thermocatalytic sensors can change significantly during their operation in mine conditions [33, 34]. These phenomena are largely explained by changes in the catalytic activity of thermocouples during operation due to the accumulation on their surface during operation of products of thermal destruction of hydrocarbons [35] and oxidation on the comparative element of higher homologues of methane, hydrogen, and carbon monoxide, which may be present in mine gas.

At low concentrations of methane and excess of oxygen in the controlled gas mixture, it is assumed that each combustible component diffuses to the surface of the working element independently, at a rate determined by its diffusion coefficient. The heat effect from each combustible component is also independent, and the total heat release on the working element from the reaction of oxidation of combustible components  $P_\Sigma$  is equal to the sum of heat effects from all components [16]:

$$P_\Sigma = \sum_{i=1}^n Q_{h_i} C_{k_i} \gamma_{e_i},$$

where:

$Q_{h_i}$ ,  $C_{k_i}$ ,  $\gamma_{e_i}$  – lower heat of combustion, concentration in the reaction chamber and effective diffusion conductivity of the element relative to the  $i$ -th combustible component.

At preheating temperature of sensing elements over 360 °C higher homologues of methane, hydrogen and carbon oxide are intensively oxidized not only on the working element, but also on the comparative element. The bridge output voltage with thermocatalytic sensor in this case is determined by the difference of heat generation on the working and comparative element and practically depends only on the concentration of methane, which is not oxidized on the comparative element. At pre-explosive concentrations of methane in the mine atmosphere the content of these impurities is insignificant and does not significantly affect the explosive properties of the mixture. Therefore, the fact that these components are usually not taken into account when controlling the explosion hazard of gas mixtures in mine workings using the thermocatalytic method is acceptable.

As mentioned earlier, at high concentrations of methane the content of higher homologues of methane and other combustible impurities can be up to 5 vol.% and more. In this case, oxygen becomes an agent limiting the rate of reaction on the working element. Methane and its combustible impurities are simultaneously oxidized on the surface of the working element. The presence of impurities in this case reduces the oxygen

content in the gas mixture and reduces heat generation on the working element.

In this case, the comparative element is inactive with respect to methane, but is able to oxidize combustible gases with lower autoignition temperature. Depending on the composition of the gas mixture, the process of oxidation of these impurities can proceed both with an excess of oxygen and with an excess of fuel. Oxidation of impurities on the comparative element, on the one hand, leads to additional heating of this element, and on the other hand, reduces the oxygen content in the reaction chamber, which in turn leads to a decrease in heat generation on the working element. In this case, expression (1.17) becomes unacceptable for describing the output signal of the measuring bridge with a thermocatalytic sensor. Depending on the composition of the combustible mixture in the area of high methane concentrations, the output signal can vary within a very wide range and does not unambiguously determine the explosive properties of mixtures. This is also evidenced by various results obtained during experimental studies of thermocatalytic sensors in the area of high methane concentrations. Possible scatter of values of output signals of thermocatalytic methane sensors, borrowed from [32], shown in Fig. 1.3.

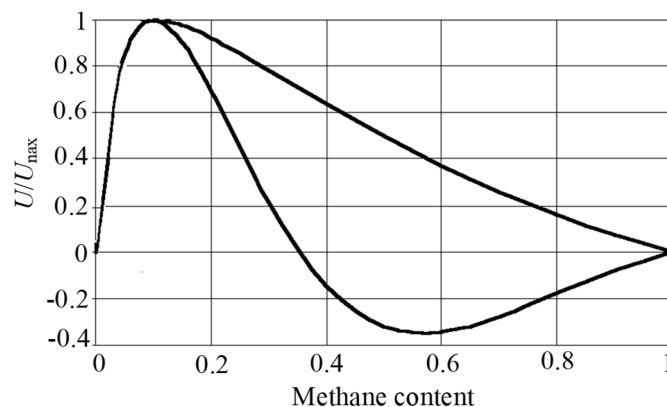


Fig. 1.3. Field of output signal values of thermocatalytic methane sensors [32]

The specified scatter of output signals of thermocatalytic methane sensors in the area of high concentrations predetermines that until recently they are used to measure low concentrations of methane, usually up to 5 vol.% and less, and in addition, there are problems with ensuring the unambiguity of the protection means in the area of high concentrations.

To exclude the considered phenomena causing ambiguity of methane content control in the area of high concentrations, solutions consisting in the use of different thermal modes of sensitive elements of thermocatalytic methane sensors [36] and separate control of diffuse flows of the controlled medium to the sensitive elements of a two-chamber thermocatalytic sensor [29, 36] have been proposed.

In the first case, the preheating temperature of the working element is selected 400 °C, and the temperature of the comparative element is below 300 °C. In this case, the low temperature of the comparative element excludes the possibility of oxidation on it of combustible components characterized by low ignition temperature and the jams at high methane concentrations. Another variant of the solution suggests creating sensors with two chambers. In this case there is an ability of separate control of the diffusion conductivity value of filters at simultaneous preservation of electrothermal analogy of elements. Diffusive conductivity of the filter of the sensor chamber, in which the working element is installed, is chosen commensurate with the effective diffusive conductivity of the working element, and the diffusive conductivity of the filter of the sensor chamber, in which the comparative element is installed, is taken to be several orders of magnitude less than that of the first chamber. In the presence in the gas mixtures of components capable of oxidizing on the comparative element at the preheating temperature of the elements, due to the small diffusive conductivity of the filter of the sensor chamber in which the comparative element is installed, the amount of heat generated on the comparative element is insignificant. In addition, at such arrangement of elements, the reaction on the comparative element does not affect the oxygen content in the chamber with the working element. All this significantly increases the stability of methane analyzers characteristics in the area of high concentrations, but the issue of using the proposed solutions in the creation of wide-range universal means of control requires further justification and research.

Disadvantages of the thermocatalytic method should also include a somewhat greater (in comparison with optical and ultrasonic methods) inertia of control means based on the thermocatalytic method. The question of increasing the rapidity of explosion hazard control means is very relevant for mines in danger of sudden emissions, as well as for mine workings, in which due to the presence of powerful sources of gas emission, rapid gasification of the atmosphere is possible (at opening of fumaroles, methane bursting from the soil of the workings, etc.). This issue is also essential in the development of gas protection equipment for downhole machines and mine electric locomotives. Despite some disadvantages inherent in the thermocatalytic method it is one of the most widespread and recognized methods of control, which finds the widest application in the control of explosion hazard of mine workings of coal mines.

One of the first methods of methane concentration control, which found wide application in the development of means of methane control in degassing pipelines is the thermoconductometric method based on the measurement of thermal conductivity of the mixture [37]. The thermal conductivity of methane differs significantly from the thermal conductivity of other components of the mine atmosphere (see Table 1.1). When justifying the thermoconductometric method, it is usually considered that the thermal conductivity of a mixture of gases has additive properties and unambiguously depends on the concentration of gas components. Thermal conductivity of binary methane-air mixture is determined by the expression:

$$\lambda_{tc} = C_m \lambda_m + (1 - C_m) \lambda_a, \quad (1.18)$$

where:

$\lambda_{tc}$ ,  $\lambda_m$ ,  $\lambda_a$  – heat conductivity coefficients of the gas mixture, methane and air, respectively, W/m·K.

The above expression is not strict even for mixtures of nonpolar gases, such as methane and air. More strict for such mixtures is the Brokaw formula, which for a two-component mixture has the form [38]:

$$\lambda'_{tc} = 0.5 \left[ C_m \lambda_m + (1 - C_m) \lambda_a + \frac{\lambda_m \lambda_a}{\lambda_a C_m + (1 - C_m)} \right]. \quad (1.19)$$

The greatest deviation of the true thermal conductivity of the gas mixture from the thermal conductivity calculated by the linear dependence (1.18) is observed at the methane content of 50 vol.%, which in this case is 0.8%.

Even more significant deviation of the true thermal conductivity from the thermal conductivity calculated by linear dependence (1.18) is observed for mixtures whose components differ significantly in molecular weight, for example, for hydrogen-air mixture, or polarity of molecules, for example, contain water vapor. When calculating the thermal conductivity of mixtures of water vapor with air, it is recommended to use the formulas proposed by Lindsey and Bromel [38]:

$$\lambda_{tc} = \frac{\lambda_a}{1 + A_a \frac{C_v}{C_a}} + \frac{\lambda_n}{1 + A_a \frac{C_a}{C_v}}, \quad (1.20)$$

where:

$$A_a = \frac{1}{4} \left[ 1 + \left( \frac{\mu_a}{\mu_v} \left( \frac{M_v}{M_a} \right)^{0.75} \frac{1 + \frac{S_a}{T_b}}{1 + \frac{S_v}{T_b}} \right)^{0.5} \right]^2 \frac{1 + \frac{S_{am}}{T_b}}{1 + \frac{S_a}{T_b}};$$

$$A_a = \frac{1}{4} \left[ 1 + \left( \frac{\mu_v}{\mu_a} \left( \frac{M_a}{M_v} \right)^{0.75} \frac{1 + \frac{S_v}{T_b}}{1 + \frac{S_a}{T_b}} \right)^{0.5} \right]^2 \frac{1 + \frac{S_{am}}{T_b}}{1 + \frac{S_v}{T_b}},$$

where:

$\mu_a$ ,  $\mu_v$  – viscosity of air and vapor, respectively, Pa·s;

$C_a, C_v$  – mole (volume) parts of air and vapor;  
 $M_a, M_v$  – molecular weight of air and vapor, respectively;  
 $S_a, S_v, S_{am}$  – Sutherland constants of air, vapor and mixture, K;  
 $S_{am} = 1.5T_b$  – for components;  
 $S_{am} = 0.735(S_a S_v)^{0.5}$  – for mixture of air with water vapor;  
 $T_b$  – boiling point of liquid.

When calculating the thermal conductivity of a multicomponent mixture of gases, Vasilieva's formula is used [39]:

$$\lambda_{tc} = \frac{\lambda_1}{1 + A_{12} \frac{C_2}{C_1} + A_{13} \frac{C_3}{C_1} + \dots} + \frac{\lambda_2}{1 + A_{21} \frac{C_1}{C_2} + A_{23} \frac{C_3}{C_2} + \dots} + \dots, \quad (1.21)$$

Among the mine air components affecting the measurement results by the thermoconductometric method, one should single out water vapor, hydrogen, carbon dioxide and ethane, the content of which can vary significantly. Water vapor and hydrogen lead to overestimation of readings of thermoconductometric methane analyzers, and carbon dioxide and ethane – to their underestimation. These components can have a particularly significant impact on the measurement results in case of fires, when the concentration of CO<sub>2</sub> in the mine air can reach tens of percent and the composition of the gas mixture in the degassing pipelines changes significantly. Therefore, when developing means of methane content control based on the thermoconductometric method, it is necessary to conduct research aimed at reducing the influence of these gases on the results of methane concentration measurement by thermoconductometric sensors.

Usually thermoconductometric methane sensors have a working chamber and a comparison chamber, in which there are analyzed and reference gas mixtures, and the determination of methane concentration is carried out by comparing the thermal conductivities of these mixtures. As sensing elements platinum thermistors of different design are used, which simultaneously perform the functions of heating elements and resistance thermometers. Heat exchange between the thermistor and the environment is carried out mainly by thermal conductivity of the gas medium. However, part of the heat is removed by radiation, conduction of current conducting ends and gas convection, as it is impossible to completely exclude heat transfer in thermoconductometer sensors due to these mechanisms.

Heat transfer due to radiation is determined by the Stefan-Boltzmann equation and is proportional to the fourth power of its absolute temperature:

$$P_a = \varepsilon_b C_0 F_t (T_b^4 - T_g^4), \quad (1.22)$$

where:

$\varepsilon_b$  – blackness coefficient of the body;

$C_0 = 5.67 \cdot 10^{-8}$  – Stefan-Boltzmann constant, W/(m<sup>2</sup>·K<sup>4</sup>);

$F_t$  – surface area of the body, m<sup>2</sup>;

$T_b$  and  $T_g$  – temperatures of the body and the gas surrounding the body, respectively, K.

Expression (1.22) is valid for the case of location of the heated body in an unbounded space. Realistically, in order to eliminate possible gas convection, the dimensions of the chambers in which the sensing elements are installed are comparable to the dimensions of the elements themselves. Therefore, the radiation heat exchange is influenced by the temperature and the degree of blackness of the inner surface of the chamber. Change of these parameters during operation, as well as the blackness factor of the elements leads to redistribution of heat fluxes in the working chamber and additional measurement errors. To reduce the influence of the radiation component of heat transfer on the operation of gas analyzers, the heating temperature of the working element is selected below 300 °C. Selection of a higher heating temperature is also hindered by possible oxidation of combustible gases on the surface of the working thermocouple, which leads to additional heating of the thermocouple and the occurrence of large measurement errors.

Convective heat transfer is caused by the presence of gas convection in the chamber. Its value is influenced by the temperature of elements, density, heat capacity and viscosity of gas, shape, size and location of sensing elements relative to the chamber walls. To reduce measurement errors caused by the presence of convective heat transfer, increase the diffusion resistance of the reaction chamber, reduce its size, place the thermocouples in the center or along the chamber axis, etc. However, convective heat transfer cannot be completely excluded, as a large diffusion resistance of the reaction chamber walls increases the inertia of measuring instruments, and minimizing the size of the working chamber makes thermoconductometric sensors sensitive to the displacement of the thermocouple during operation.

If the tightness of the comparison chamber is broken, the reference gas mixture, which is located in it, can undergo significant changes, which can lead to a failure of the gas analyzers' performance. The comparative thermistor of the thermoconductometric sensor installed in the sealed chamber eliminates the influence of only supply voltage and temperature changes on the output signal of the measuring bridge. Changes in other uncontrollable factors of the gas mixture are not compensated for.

There are known solutions when temperature sensors are introduced into thermoconductometric gas analyzers and only the working element is used, or two thermoelements, significantly differing in their thermal modes, are located in one chamber filled with the analyzed mixture [16]. In the latter case, the less heated element acts as a comparative element and provides temperature stability of the measuring bridge. The zero of the measuring bridge is set in air. When methane appears in the gas mixture, the temperature of the more heated working element changes significantly more than that of the comparative element.

It should be noted that thermal conductivity of gases practically does not depend on pressure and increases with increasing temperature according to the dependence of

$$\lambda = \lambda_0 (T / T_0)^n, \quad (1.23)$$

where:

$T$  – gas temperature, K;

$T_0 = 273$  K;

$\lambda_0$  – heat conductivity coefficient of gas at temperature 273 K, W/m·K;

$n$  – temperature coefficient of change of heat conductivity (for air  $n = 0.82$ , for methane  $n = 1.33$ ).

When the methane concentration increases due to different values of the temperature coefficient of air and methane, the thermal conductivity of the mixture for the working element increases significantly more than for the comparative element. This in turn contributes to the increase in sensitivity of the mentioned single-chamber sensors.

The disadvantages of these single-chamber thermoconductometric sensors include the need for individual selection of the parameters of resistors in the bridge branch with a comparative element to ensure its temperature stability. Therefore, this solution requires further theoretical development and experimental studies of single-chamber thermoconductometric sensors.

Taking into account the differences in the speed of sound propagation in air and methane, attempts were also made to create methane analyzers based on the ultrasonic method [40]. The advantage of this method is its low inertia, which makes it possible to create control devices for fast-acting gas protection systems. At the same time, the results of measurement by ultrasonic method are significantly affected by temperature, pressure, humidity, carbon dioxide and other gas impurities. In addition, when working in a highly dusty environment, it is necessary to take measures to protect the sources and receivers of radiation from pollution. The latter leads to complication of the design of meters and leads to an increase in its inertia. All this significantly narrows the possibilities of application of ultrasonic method to control the explosion hazard of mine workings. This method is recommended to be used for fast-acting gas protection systems when combining in one measuring device stable but relatively slow reacting to changes in the gas situation thermocatalytic and fast-acting ultrasonic means of control [16].

#### 1.4. Analysis of existing explosion hazard controls

Currently, the control of explosion hazard of gas mixtures in mine workings and degasification pipelines is reduced to the control of methane content. According to the safety rules in coal mines [9], the devices used to control the methane content are divided into:

- episodic portable devices;
- portable automatic devices;
- stationary automatic devices.

The type of instruments used to monitor methane content at a particular mine and their number depend on the methane gas category of the mine. At non-gas mines it is envisaged to use portable devices of episodic action. At mines of I and II category, except for the above devices episodic, it is mandatory to use portable automatic devices, and at mines of III category and above the use of all of the above means, and stationary automatic devices should provide automatic power failure at unacceptable methane concentration. All mines of category III and above under construction and reconstruction must be equipped with automatic remote control systems that provide collection, presentation and processing of information by means of computers.

A considerable number of publications have been devoted to the development of methane content control devices. Intensive work on development of methane content control devices was carried out in Ukraine, Japan, Germany, England, France, Poland and a number of other countries. The first devices of episodic action, which came to replace safety gasoline lamps, were mine interferometers. The appearance of small-sized semiconductor products in the beginning of the seventies of the last century stimulated the development of portable and stationary automatic devices – methane analyzers and alarms. Intensive work in this direction was carried out by institutes Giprougleavtomatizatsiya, IHD named after A.A. Skochinsky, MakNII, DGI and others. Production of the first stationary automatic devices – thermocatalytic methane analyzers AMT-2 and methane alarms “Miner’s Sputnik” was carried out by NPO “Krasny Metallist” in the mid-seventies. The analyzers provided continuous automatic control of methane as well as sound and light signal when inadmissible methane concentration appeared in the place of their installation. Stationary analyzers provided protective shutdown of electrical equipment at the site.

Abroad, in the seventies and eighties, active work on the development of methane control devices was carried out in Japan (firms “Riken Keiki Fine Instrument” and “Hokkaido Toka Fine Technique”), Germany (firms “Dreger”, GfG), the USA (firms “Industrial scientific corporation” and “Bacharach”), France (firm “Oldam”) and other countries [16]. The most famous models of gas analyzers created by these firms include Exylarm CP CH<sub>4</sub>, G 3014, GP-82 and others.

With a few exceptions, all automatic devices designed to monitor methane concentration in mine workings are based on the thermocatalytic method. Structurally, thermocatalytic sensors of automatic gas analyzers have recently undergone significant changes. In modern gas analyzers the sensors are usually made in the form of miniature pelistor thermocouples, which are placed in a reaction chamber separated from the controlled medium by a porous ceramic or metal-ceramic gas-exchange filter element [22]. The power consumption and mass-dimensional characteristics of sensors have been significantly reduced and improved, their design and technological parameters have been optimized, the measurement range has been extended, the reliability and temperature stability of analyzers have been increased, the issues of diagnosing the analyzers' condition, detecting unauthorized interference and ensuring unambiguous operation in the range of possible methane concentrations have been largely solved [23]. However, the issues of explosion hazard control in the simultaneous presence of methane, dust and combustible gases with low ignition temperature have not been solved so far. There are cases of analyzers malfunctioning at high methane concentrations. Existing thermocatalytic methane analyzers do not provide control over the whole range of possible methane concentrations and are used only for control of explosion hazard of gas mixtures in mine workings.

Recently, considerable attention has been paid to the development of explosion hazard control means for mixtures drained by mine degasification systems. On the one hand, this is due to safety requirements, and on the other hand, due to increased interest in the use of methane, which is melted by degasification systems, as an energy raw material. Automatic gas analyzers used to control the methane content in degasification pipelines are based on the thermoconductometric method [16]. The attempts to create methane analyzers for mine workings were also made on the basis of this method. However, this method is non-selective and,

therefore, later, when developing automatic portable and stationary methane analyzers designed to control the composition of the atmosphere in mine workings, preference was given to the thermocatalytic method, which is characterized by greater selectivity and sensitivity to the measured component.

Production of methane gas analyzers for control of degassing systems KAM-1 was mastered in the USSR in the 80s [16]. Nowadays conductometric gas analyzers are widely used for continuous measurement of methane concentration in gas mixtures sucked by degassing units. The domestic manufacturer of such devices is PJSC “Krasnyi Metallist”, which mastered the production of AKRD equipment with a thermoconductometric methane sensor DMD, designed to monitor the operation of degassing systems. The produced equipment has a number of disadvantages, the main of which is the presence of relatively large error of methane concentration measurement (the reduced error of measurement is 4%) and a significant impact on the measurement results of changes in pressure, temperature, humidity and gas composition of the controlled environment. The issues related to the assessment of the influence of these parameters of the gas mixture and unmeasured components on the error of gas analyzers have not been sufficiently studied so far.

Foreign companies have been producing thermoconductometric gas analyzers for monitoring high concentrations of methane since the 70s. An example of a modern model of such gas analyzers is a microprocessor-based methanometer MM-2A [41]. It contains a remote thermoconductometric sensor connected to the measuring unit by a cable up to 5 m long. It provides control of methane content in the range of 0-100 vol.% and has two control outputs for equipment shutdown in case of unacceptable methane concentration in the pipeline.

Despite the fact that modern models of gas analyzers for control of degassing systems have partially eliminated the influence of changes in a number of parameters on the measurement results, the issues of eliminating the influence of changes in pressure, humidity and gas composition of the controlled medium have not been properly solved. Practically all sensors of the produced analyzers are two-chambered and contain an isolated comparative element placed in a chamber with a reference gas medium. At long-term operation of such sensors the loss of sealing of such chamber is often observed, besides, such design of sensors complicates their construction and worsens dynamic characteristics of analyzers. This causes instability of “zero” of analyzers, relatively large error of measurement, the need for regulation and adjustment at the place of installation, regular maintenance and supervision of such gas analyzers.

These disadvantages can be partially eliminated by using the proposed single-chamber thermoconductometric sensor with unequal electrothermal parameters of sensing elements [16]. However, the issues of selecting the parameters of thermoelements, design and modes of operation of such a sensor have not been sufficiently substantiated to date.

An explosive situation in mine workings of coal mines occurs when methane and coal dust accumulate in them in such quantities that, when mixed with air, form an explosive concentration. Safety rules in coal mines [9] establish unacceptable concentrations of methane in mine workings and degasification pipelines, as well as parameters of methods and means of dust and explosion protection of mine workings, which are taken depending on the lower explosive limit of deposited coal dust [16]. The technical means developed to date to control the deposited dust by the principle of operation can be divided into the following groups:

- analytical scales;
- densitometric devices;
- radioisotope dust deposition meters;
- vibration resonance dust deposition meters;
- radio wave and optical meters.

The use of analytical scales involves determining the difference between the mass of clean and dusty substrate [16]. Due to the complexity of using the existing analytical scale designs in the mine, these devices have not found application.

Densitometric tools are based on the determination of the change in the optical density of the filter material depending on the amount of dust. In this method, dust is first collected on substrates, and then with the help of aspirators is applied to the filtering material, the optical density of which changes. With low accuracy, the devices require a large number of different manipulations and therefore are not used in practice [16].

The principle of operation of radioisotope dust deposit meters is based on the measurement of the change in the intensity of the  $\beta$ -particle flux reflected from a clean substrate and a dusty surface. There are known attempts to use it to control the deposited dust and to determine the ash content of dust after shaling of the workings (KPR-1 and KPR-1M), as well as to determine the content of inert dust in the mixture (“Inflabar” and KOR-1) [42]. Their disadvantages are the use of radioactive sources and the need to perform complex operations associated with the preparation of the deposition surface, calibration of the device and collection of dust on substrates, which limits the possibility of their use in the conditions of mining enterprises.

In vibration resonance sensors the dust mass deposited on the metal membrane or piezocrystal changes the resonance frequency of mechanical vibrations of the sensitive element. The working surface of the sensor is open to the settling dust, which predetermines poor protection from mechanical damage to the sensitive elements, wear of the material of the mechanical vibrating system during periodic removal of the settled dust, which leads to a significant error of measurements.

When using the radio wave method, the mechanical oscillating system [43] is replaced by an electromagnetic oscillating circuit, where the frequency of oscillations depends on the permittivity of the dust collecting substrate. In general, the radio wave method is similar to the vibration resonance method, but here the accuracy of readings is affected by humidity, dust composition and the presence of scratches and damage on the measuring substrate. Instruments based on this method are also not widespread

The common disadvantage of all the above methods of dust deposit control is the necessity of periodic removal of dust accumulated on the sensing elements. In addition, all of them imply installation of the sensor in any one point of the excavation. This place of excavation should most fully reflect the intensity of dust deposition in the excavation as a whole. In real conditions it is practically impossible to choose such a place. It is possible to increase the reliability of control by using several control points for one excavation, but this leads to the increase in the cost of the control system.

An indirect assessment of dust deposition is possible by the value of dust concentration in the air [43]. In this case, all dust entering the mine is controlled in the moving air flow, which helps to reduce the measurement error. The results of such control can serve as an information base for assessing the explosion hazard of the mine only under the condition of a high level of technological discipline and strict implementation of measures aimed at preventing coal dust explosions (e.g., binding or removal of deposited dust when the alarm about exceeding the permissible value of dust deposits is triggered). However, in case of low level of technological discipline, poor quality and untimely implementation of these measures, introduction of inaccurate information on their implementation in this case extremely dangerous situations may occur. Therefore, despite the possibility and all the advantages of determining the explosion hazard on the basis of information coming from air dust sensors [43], it is now necessary to search for solutions that allow to assess the real state of the mine. Moreover, this assessment should not depend on a subjective factor (e.g., input of information on the implementation of measures aimed at preventing coal dust explosions).

## **1.5. Conclusions**

The performed analysis of accidents caused by explosions of methane and coal dust, existing methods and means of control of explosion hazard in mine workings and equipment of coal mines, their operating conditions and modes of operation allows us to draw the following conclusions:

1. While the frequency of explosions of methane-air mixtures and dust at coal mines is relatively small, the consequences and damage caused by these phenomena are very significant and comparable to the consequences of the most common types of accidents such as fires, in addition, much more often than explosions, at coal mines there are emergencies associated with gasification of mine workings, which, in the presence of ignition sources, can develop into accidents with severe consequences.
2. The largest number of explosions occurs in preparatory and cleaning workings, as well as in the outgoing from the cleaning faces and panels of mines, which is associated with the stoppages of fans, defects in ventilation pipelines, failure of ventilation of workings, sudden release of methane into the workings caused by gas dynamic phenomena, formation of local methane accumulations and accumulation of methane in the mined-out spaces.

3. In case of failure of ventilation of mine workings, the maximum concentration of methane can reach tens of percent, and the time of gasification to the maximum concentration is tens of minutes, gasification of mine workings as a result of gas dynamic phenomena, proceeds much faster, and the maximum concentration of methane in a matter of seconds can reach 100 vol.%.
4. Combustible methane impurities contained in mine gas and fire gases propagating through mine workings can significantly change the composition of the atmosphere at the location where the gas analyzers are installed, which significantly affects the explosive properties of the gas mixture and the performance of the gas analyzers.
5. The existing thermocatalytic gas analyzers provide reliable control of the explosion hazard of the gas mixture only at pre-explosion concentrations of methane, and thermoconductometric gas analyzers, which are used to control degassing systems, have a large measurement error.

## References

- [1] Brukhanov A.M. (2004) *Scientific and technical basis for investigation and prevention of accidents at coal mines*. Donetsk: Nord-Press [in Russian]
- [2] Brukhanov A.M., Mnukhin A.G., Kolosyuk V.P. et al. (2004) *Investigation and prevention of accidents at coal mines*. Part I. Donetsk: Nord-press [in Russian]
- [3] Tkachuk S.P., Kolosyuk V.P., Ihno S.A. (2000) *Explosion and fire safety of mining equipment*. Kyiv: Osnova [in Russian]
- [4] Bryukhanov A.M., Mnukhin A.G., Busygin K.K. (2003) Analysis of circumstances of methane explosions at coal mines and development of measures to prevent them. *Ugol Ukrainy*, (4), 37-40. [in Russian]
- [5] *Guidelines for design of coal mines ventilation*. (1994) Kyiv: Osnova [in Russian]
- [6] Hrebenkin S.O., Yanko S.V., Brukhanov A.M., et al (2002) *Problems of development of steep and steeply sloping formations at great depths*. Donetsk: UkrNTEK [in Russian]
- [7] Bryukhanov A.M. (2007) Mathematical modeling of formation regularities of explosive environments during sudden coal and gas emissions in mines. *Geotechnical Mechanics: Intermed. sb. nauk. tr. IGTM NAS of Ukraine.*, (69), 121-128. [in Russian]
- [8] Bryukhanov A.M. (2007) Conditions of explosive environment formation after sudden coal and methane release. *Naukovy visnik UkrNDIPB of Ukraine*, 1(15), 23-27 [in Russian]
- [9] *Safety regulations in coal mines*. (2010) DNAOP 1.1.30-1.01-10. Kyiv: Osnova [in Ukrainian]
- [10] Holinko V.I., Smolanov S.M., Gryadshchiiy B.A. (2014) *Fundamental principles of mine rescue*. D.: Derzhavniy VNZ "NSU" [in Ukrainian]
- [11] *Guidelines for monitoring the composition of mine air, determining multi-gas content and establishing mine categories based on methane*. (2003). Collection of Instructions to the rules of safety in coal mines, (1). Kyiv [in Ukrainian]
- [12] *Technical specification for the mine methane relay MRSh.1* (2008) Konotop: Avtomatvuhlerudprom, 17 s. [in Ukrainian]
- [13] Horonovsky I.T., Nazarenko Y.P., Nekryach E.F. (1987) *Brief reference book on chemistry*. Kyiv: Naukova Dumka [in Russian]
- [14] Holinko V.I., Belonozhko A.V. (2007) Increase in reliability of explosion hazard control of multicomponent gas mixtures by thermocatalytic sensors. *Development of ore deposits: Scientific and Technical Collection*, (91), 242-245. [in Russian]
- [15] Demchenko V.B., Martovitsky A.V. (2004) *Analysis of methane capture parameters by regional degasification boreholes in mining zones* Geotechnichnichna mekhanika. Mizhvid. zb. nauk. pratsi. D.: ISTM NAS of Ukraine, (48), 108-115. [in Russian]

- [16] Holinko V.I., Kotlyarov A.K., Belonozhko V.V. (2004) *Control of explosion hazard in mine workings D.*: Nauka i Obrazovanie [in Russian]
- [17] Vovna, A.V.; Zori, A.A. (2013) Fast methane concentration meter in coal mines. *Visnyk Kremenchutsk. Natsionalnogo universytetu im. Mykhailo Ostrogradskiyi*, 6(83), 114-119. Kremenchuk [in Russian]
- [18] Vovna O.V., Zori A.A., Akhmedov R.M. (2017) Improving the accuracy of an optoelectronic methane concentration meter for coal mines. *Visnyk Natsionalnogo tekhnichnogo universytetu "KPI"*, "Power engineering and conversion technology", 4(1226), 19-24. Kharkiv: NTU "KPI" [in Ukrainian]
- [19] Vovna O.V., Zori A.A., Khlamov M.G. (2010) Dynamic error compensation method for infrared methane concentration meter for coal mines. *Visnyk Natsionalnogo tekhnichnogo universytetu "KPI"*, "Power engineering and conversion technology", (12), 65-70. Kharkiv: NTU "KPI" [in Ukrainian]
- [20] Bilonozhko V.V., Bilonozhko V.P., Holinko V.I., Kotlyarov A.K. et al. Pat. 61839A Ukraine, MK E21F17/16. *Sensitive element of mine gas analyzers and the method of its manufacturing*. Published 17.11.03 Bulletin No. 11. [in Ukrainian]
- [21] Bilonozhko V.V., Bilonozhko V.P., Holinko V.I., Kotlyarov A.K. Pat. 62857A Ukraine, MK G01N27/18. *Sensor of mine gas analysers and method of its manufacture* Published 15.12.03 Bulletin No. 12. [in Ukrainian]
- [22] Holinko V.I. Belonozhko A.V. (2006) Improvement of thermocatalytic method of control of methane content in mine atmosphere. *Girnycha Elektromekhanika ta Avtomatika*, (77), 81-87. [in Russian]
- [23] Holinko V.I., Belonozhko A.V. (2007) Increase in reliability of explosion hazard control of multicomponent gas mixtures by thermocatalytic sensors. *Development of ore deposits: Scientific and Technical Collection*, (91), 242-245. [in Russian]
- [24] Bilonozhko V.V., Bilonozhko V.P., Holinko V.I., Kotlyarov A.K. Pat. 61224A Ukraine, MK G01N25/22, E21F1/00. *A method for measuring the content of combustible gases in the mine atmosphere and a device for its implementation* Published 17.11.03 Bulletin No. 11. [in Ukrainian]
- [25] Holinko V.I. Belonozhko V.V. (2003) Methane oxidation process study in thermocatalytic sensors, *Naukovyi visnik NSU*, (7), 62-65. Dnipropetrovsk [in Russian]
- [26] Margolis Z.I. (1977) *Oxidation of hydrocarbons on heterogeneous catalysts*. M.: Khimiya, [in Russian]
- [27] Karpov E.F., Birenberg I.E., Basovsky B.I. (1984) *Automatic gas protection and mine atmosphere control*. M.: Nedra [in Russian]
- [28] Belonozhko, A.V.; Frundin, V.E. (2008) *Study of thermocatalytic methane sensor performance during emergency mine gasification: materialy mizhnarodnoyi naukovo-praktychnoyi konferentsiyi "School of underground development"* (pp. 225-229). D.: National Mining University [in Russian]
- [29] Holinko, V.I. Belonozhko, V.V. (2003) *Improvement of thermocatalytic method of methane content measurement and design of primary converters: materialy mizhnarodnoyi naukovo-praktychnoyi konferentsiyi "Forum Girnikiv"*17, Vol. 2, (pp. 325-331) [in Russian]
- [30] Holinko, V.I.; Romanenko, V.I.; Frundin, V.Yu. (2003) Justification of the bridge circuit in thermocatalytic gas analysers. *Collection of scientific articles of NSU* 17, vol. 2. (pp. 352-357) [in Russian]
- [31] Belonozhko, V.V.. Belonozhko, V.P.; Holinko, V.I. (2001) Experimental studies of thermocatalytic methane sensors to assess their unambiguity. *Hirnycha elektromekhanika ta avtomatyka*, (67), 122-130. [in Russian]
- [32] Medvedev V.N. (2006) *Mathematical model of output signal formation of thermocatalytic methane sensors. Ways and means of creating safe and healthy working conditions in coal mines*. Collection of scientific works of Mak NII, 18, 121-129. Makeevka [in Russian]
- [33] Belonozhko V.V. (2003) Study of temporal stability of thermocatalytic methane sensors. *Naukovyi visnik NSU*, (11), 76-79. Dnipropetrovsk [in Russian]

- [34] Holinko, V.I.; Belonozhko, A.V. (2006) Study of thermocatalytic methane sensors performance after their long-term operation. *Naukovy visnik NSU*, (10), 72-75 [in Russian]
- [35] Holinko, V.I.; Belonozhko, A.V. (2008) Study of hydrocarbon thermal degradation products accumulation on the surface of thermocouples. *Naukovy visnik NSU*, (7), 60-65 [in Russian]
- [36] Holinko, V.I.; Kotlyarov, A.K.; Belonozhko, A.V. (2008) *Development of methane control methods to ensure the performance of analysers in case of emergency gasification of mine workings: materialy mizhnarodnoyi naukovo-praktychnoyi konferentsiyi "Forum Girnikiv-2008"* (pp.33-43). D.: National Mining University [in Russian]
- [37] *SMP-NT system for monitoring mine atmosphere parameters*. (2001) Katowice: Center for Electrification and Automation of Mining Industry "EMAG" [in Russian]
- [38] Tsederberg, N.V. (1963) *Thermal conductivity of gases and liquids*. M.-L.: Gosenergoizdat [in Russian]
- [39] Bretschneider S. (1966) *Properties of gases and liquids*. M.-L.: Khimiya [in Russian]
- [40] Pavlenko V.A. (1965) *Gas analyzers* M.-L.: Mashinostroenie [in Russian]
- [41] *Operation, automation and monitoring in mines and underground* (2001) Poland, Tychy: "Karboavtomatika" [in Russian]
- [42] Kryvytsky M.D., Dehtyarev A.P., Evdokymova E.P. et al. (1988) *Determination by radioisotope method of the content of non-combustible substances in the process of mine workings shaling. Ways and technical means of ensuring safe and healthy working conditions at coal mines* (pp. 73-84). Makeevka: MakNII [in Russian]
- [43] Holinko V.I., Kolesnik V.E. (2001) *Ugol Ukrainy*, (6), 24-26. [in Russian]

## 2. Investigation of electrothermal processes in primary converters of methane analyzers

### 2.1. Theoretical analysis of heat transfer process in methane sensors

Despite the fact that quite a lot of work has been done on the research of the thermoconductometric method, the technical means produced on the basis of this method are characterized by a number of disadvantages consisting in a significant influence on the results of measuring pressure, temperature, humidity and gas composition of the controlled environment. Besides, the estimation of the influence of these factors based on the results of the given research often does not coincide with the real characteristics of analyzers. In our opinion, the reasons for this lie in the incomplete consideration of a number of factors affecting the heat transfer processes in thermal conductivity sensors.

Sensing elements of thermoconductometric sensors in early models of gas analyzers were most often made of platinum microwires in the form of a thread fixed along the axis of a cylindrical measuring chamber or glazed spirals in the form of a rod with a diameter of 1-2 mm and a length of about 20-25 mm [1]. Recently, in order to unify the design of sensors used in thermocatalytic and thermoconductometric gas analyzers, in the manufacture of thermoconductometric sensors, preference is given to elements in the form of a miniature ball (spiral of platinum microwire enclosed in a dielectric) located in the center of the measuring chamber of spherical shape (Fig. 2.1).

Thermocatalytic and thermoconductometric gas analyzers of all types are both resistance thermometers and heaters. The processes of heat removal to the environment from the sensing elements of thermoconductometric and thermocatalytic sensors are similar. However, there are some peculiarities due to the differences in the preheating temperature of the sensing elements. In addition, when analyzing the heat transfer of the working element of the thermocatalytic sensor, it is necessary to take into account the power released due to oxidation of combustible gases on it.

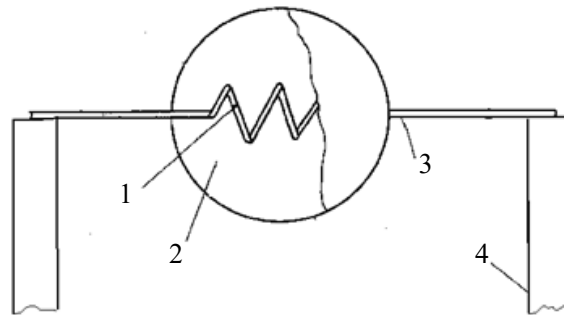


Fig. 2.1. Sensing element of a thermoconductometric sensor:  
1 – platinum microwire spiral; 2 – dielectric ball; 3 – current supply ends; 4 – stands

In the stationary mode, the power released in the element when the electric current  $P_{el}$  passes through it, is dissipated to the environment through the gas space inside the chamber and the structural elements:

$$P_{el} = P_{gm} + P_k + P_r + P_p, \quad (2.1)$$

where:

$P_{gm}$  – power dissipated due to heat conduction of the gas medium, W;

$P_k$  – power dissipated due to natural convection, W;

$P_r$  – power dissipated due to radiation, W;

$P_p$  – power dissipated through current carrying ends, W.

When analyzing the processes of heat transfer from the heated element to the chamber walls due to thermal conductivity of the gas medium and natural convection, usually the complex phenomenon of heat transfer is simplified and considered as an ordinary conductive heat transfer with an equivalent heat transfer coefficient [2]:

$$\lambda_{eq} = \varepsilon_k \lambda, \quad (2.2)$$

where:

- $\varepsilon_k$  – convection coefficient;
- $\lambda$  – gas thermal conductivity coefficient, W/(m·°C).

The value of the convection coefficient depends on the thickness of the gas layer, the element heating temperature and the properties of the gas medium. The value of the coefficient is usually calculated as

$$\varepsilon_k = f(G_r P_r), \quad (2.3)$$

where:

$G_r$  and  $P_r$  – are respectively the Grashof and Prandtl numbers calculated for the gas layer at the average temperature  $t_t = (t_e + t_k) / 2$ ;  $t_e$  and  $t_k$  – the temperature of the element and the chamber walls, °C.

The values of Grashof and Prandtl numbers are defined as:

$$G_r = g \delta^3 (t_e - t_k) / \nu_t^2 (t_t + 273); \quad P_r = \nu_t / \alpha_t, \quad (2.4)$$

where:

- $\delta$  – thickness of gas layer, m;
- $\nu_t$  – coefficient of kinematic viscosity of medium at temperature  $t_t$ , m<sup>2</sup>/s;
- $\alpha_t = \lambda_t / C_p \rho_t$  – coefficient of diffusivity at temperature  $t_t$ , m<sup>2</sup>/s;
- $C_p$  – heat capacity of gas mixture at constant pressure, J/(kg·°C);
- $\rho_t$  – density of gas mixture at temperature  $t_t$ , kg/m<sup>3</sup>.

If the product value  $G_r P_r < 1000$ , almost all heat is transferred by conduction and the value  $\varepsilon_k = 1$ . If, the value of  $10^3 < G_r P_r < 10^6$   $\varepsilon_k$  should be calculated by the formula:

$$\varepsilon_k = 0.105(G_r P_r)^{0.3}. \quad (2.5)$$

When designing thermal conductivity sensors, the convective component of heat transfer is sought to be as small as possible, because in the presence of convective heat transfer, the measurement results are significantly affected by atmospheric pressure. At the element temperature of 200 °C and the use of a spherical-shaped element, this is ensured when the thickness of the gas layer is 5 mm or less.

The power dissipated by heat conduction of the gas medium from the spherical thermocouple located inside the ball-shaped chamber through a layer of radius  $r$  according to Fourier's law is:

$$P_t = -\lambda 4\pi r^2 dt / dr, \quad (2.6)$$

where:

- $dt / dr$  – gradient of temperature change in the direction of the radius.

The gas thermal conductivity coefficient  $\lambda$  included in equation (2.6) is practically independent of the atmospheric pressure change and increases with temperature increase according to the dependence [1]:

$$\lambda = \lambda_0 (T / T_0)^n, \quad (2.7)$$

where:

- $T$  – gas temperature, K;
- $T_0$  – temperature equal to 273 K;
- $\lambda_0$  – heat conductivity coefficient of gas at temperature 273 K, W/m·K;
- $n$  – temperature coefficient of change of heat conductivity (for air  $n = 0.82$ , for methane  $n = 1.33$ ).

In a small temperature range with sufficient accuracy for practical purposes the complex step dependence is represented as a linear dependence:

$$\lambda = \lambda_0(1 + \beta_t t), \quad (2.8)$$

where:

$\beta_t$  – temperature coefficient of gas thermal conductivity, 1/°C.

Substituting the value of  $\lambda$  from equation (2.8) into equation (2.6) and dividing the variables, we obtain:

$$(1 + \beta_t t) dt = -\frac{P_t}{4\pi\lambda_0} \frac{dr}{r^2}. \quad (2.9)$$

The solution of equation (2.9):

$$t + \frac{1}{2}\beta_t t^2 = \frac{P_t}{4\pi\lambda_0} \frac{1}{r} + C. \quad (2.10)$$

The integration constant  $C$  is found from the condition that at  $r = r_k$ ,  $t = t_i$ , and taking into account that at  $r = r_e$ ,  $t = t_e$ , we finally obtain the expression for determining the power dissipated by heat conduction of the gas medium from the spherical thermocouple.

$$P_t = \frac{4\pi\lambda_0}{1/r_e - 1/r_k} \left( t_e - t_i + \frac{1}{2}\beta_t t_e^2 - \frac{1}{2}\beta_t t_i^2 \right). \quad (2.11)$$

In contrast to the known equations [3] describing the process of heat removal from the thermocouple through the value of thermal conductivity of the gas mixture at the average temperature in the chamber, on the basis of which the authors draw a conclusion about the linear dependence of power on the value of  $\Delta t = t_e - t_i$ , equation (2.11) explicitly shows the presence of a significant nonlinearity between the temperature of the element and the removed power. This is explained by the fact that the third summand in parentheses in the range of operating temperatures is comparable in its value to  $t_e$ . It should be noted that the known equations [3] can be reduced to the form (2.11) by substituting into them the value of  $\lambda_{medium}$ , which in turn depends on the temperature of the element and the chamber walls.

The power dissipated from the thermocouple due to radiation is generally determined by the Stefan-Boltzmann equation:

$$P_d = \varepsilon_e C_0 F_e (T_e^4 - T_i^4), \quad (2.12)$$

where:

$\varepsilon_e$  – blackness coefficient of the element;

$C_0 = 5.67 \cdot 10^{-8}$  – is the Stefan-Boltzmann constant, W/(m<sup>2</sup>·K<sup>4</sup>);

$F_e$  – surface area of the element, m<sup>2</sup>;

$T_e$  and  $T_i$  – temperatures of the body and the element and the surrounding gas medium, K.

Analysis of the numerical value of  $T_e^4 - T_i^4$  shows that in the range of variation of operating temperatures of elements and medium, as well as taking into account their mutual connection for the sensor, it can be approximated by the expression:

$$T_e^4 - T_i^4 = 1.12 \cdot 10^6 (t_e^2 - 0.5t_e t_i). \quad (2.13)$$

In this case, the relationship (2.12) can be represented as follows:

$$P_d = 6.35 \cdot 10^{-2} \varepsilon_e r_e (t_e^2 - 0.5t_e t_i). \quad (2.14)$$

From expression (2.14) we can see that the radiation component of heat exchange does not directly depend on the composition of the gas medium, however, if the mode of operation of the thermal conductivity sensor is chosen so that a change in the composition of the gas medium leads to a change in the temperature of thermoelements, it entails a significant change in the power dissipated through this channel. It should also be noted that the blackness coefficient of the element made in the form of a miniature dielectric ball is significantly greater than the blackness coefficient of the platinum filament. So for the element from  $\gamma$ -aluminum oxide in the range of operating temperatures the value of the coefficient reaches 0.8, and for the platinum filament it is about 0.1. This determines that the radiation component of heat exchange in thermoconductometric sensors with a spherical-shaped element is almost an order of magnitude greater than in sensors with a sensing element in the form of platinum filament and is comparable to the power removed from the element due to the thermal conductivity of the gas medium.

Analytically describing the process of heat dissipation from the thermocouple through the lead ends is very difficult for several reasons. Firstly, heat is dissipated from the lead ends by conduction and convection of the surrounding gas medium, by radiation from their surface and, directly through the lead ends, to the metal posts pressed into the dielectric base. Secondly, unlike a thermocouple, the temperature, and therefore the heat fluxes dissipated by the ends are not constant along their length. The ends of the leads adjacent to the thermocouple have a temperature close to the temperature of the thermocouple, and the opposite ends adjacent to the massive metal posts have a temperature close to the temperature of the surrounding gas medium. Thirdly, the temperature change along the length of the leads is nonlinear. In addition, the current-supplying ends connecting the thermocouple with the posts are made by the same platinum microwire as the spiral, and therefore, when the current flows, they are additionally heated.

Comparison of real values of surface area, temperature, and blackness coefficients of the element and the platinum microwire shows that the power dissipated from the current-supplying ends by radiation from the surface is almost 500 times less than the analogous heat flux from the thermocouple. Therefore, this component of heat transfer can be neglected without significant damage to accuracy. Besides, at small dimensions of the chamber and the previously mentioned thickness of the gas layer, the convective component of heat exchange of the current-supplying ends is insignificant and it can also be neglected when describing the process of heat removal from the thermocouple through the current-supplying ends. Thus, it is possible to consider that all the heat entering the current-supplying end in the zone of its contact with the element and released in it as a result of current flow, is dissipated into the environment by means of gas heat conduction and by means of heat conduction of the platinum filament on the metal posts.

The issues related to heat dissipation from a rod fixed at one end in a heated array are considered in [2]. Using the approach proposed in this paper, the authors [3] showed that there is a critical length of the current-supplying ends at which the amount of heat dissipated by means of thermal conductivity of the medium from the heated element remains practically unchanged. That is, when this length is reached, all of the heat entering the lead end from the heated element is dissipated in the surrounding gas medium, and the temperature of the lead filament practically approaches the ambient temperature. The expression for determining this length in the case of platinum microwire is as follows:

$$l_{br} = 64.5d_m, \quad (2.15)$$

where:

$d_m$  – diameter of platinum current carrying ends, m.

The expression (2.15) is obtained for air. With increasing thermal conductivity of the gas medium, the critical length will slightly decrease. Although the obtained expression is an approximation, it shows that in air at the real length of current carrying ends (for a wire of 20  $\mu\text{m}$  diameter  $l_{br} = 1.3$  mm) the heat coming from the heated element to the current carrying end is almost all dissipated due to the thermal conductivity of the medium. As the thermal conductivity of the gas medium increases, the critical length will slightly decrease, while the amount of heat that will be dissipated from the heated element into the lead end will remain unchanged. That is, when the length of the current supply ends is greater than  $l_{br}$ , this component of heat transfer is actually independent of the thermal conductivity of the gas medium. The power dissipated in this case by the two current carrying ends can be calculated by the expression:

$$P_{ic} = 3.45d_m(t_e - t_i). \quad (2.16)$$

When considering the process of heat removal from the element through the current-supplying ends and deriving dependence (2.15) and (2.16), the authors [3] did not take into account the fact that during current flow their additional heating occurs. The power released in the current-supplying end during current flow is as follows:

$$P_r = 4I_e^2 \frac{\rho l_t}{\pi d_m^2}, \quad (2.17)$$

where:

- $I_e$  – current through the element, A;
- $\rho$  – specific resistance of platinum, Ohm·m;
- $l_t$  – length of the lead end.

Taking into account the fact that the resistivity of platinum depends on temperature, and the temperature along the length of the current-supplying end varies nonlinearly, it is practically impossible to obtain the exact value of the released power and the distribution of its density along the length. At the same time, it can be estimated with a sufficient degree of accuracy by assuming the value of the resistivity of platinum to be constant, equal to the resistivity at the average temperature  $t_i$ . In this case expression (2.17) will have the form:

$$P_r = 4I_e^2 \frac{\rho_0 l_t}{\pi d_m^2} \left( 1 + \beta \frac{t_e + t_i}{2} \right), \quad (2.18)$$

where:

- $\rho$  – resistivity of platinum at 0 °C, Ohm·m;
- $\beta$  – temperature coefficient of thermal conductivity of platinum, 1/°C.

The power released in the lead ends during current flow leads to their heating and to redistribution of heat fluxes. Obviously, if the temperature of the lead ends at the point of connection with the thermocouple as a result of their heating by the current will be higher than the temperature of the element (the case is possible with large ball sizes), the heat will be transferred from the filament to the element, and not vice versa. Considering that the heat transfer from the platinum filament is no longer affected by the influence of the stands when the length of the current-supplying end is greater than border length  $l_{br}$ , we estimate the possible value of its temperature at the point of connection to the thermocouple without taking into account the heat flows caused by the presence of the latter. The equation describing the processes of heat exchange of the filament due to gas thermal conductivity, obtained by analogy with the heat removal from a spherical element, has the form:

$$P_t = \frac{2\pi\lambda_0 l_t}{\ln(2r_k / d_m)} \left( t_e - t_i + \frac{1}{2}\beta_t t_e^2 - \frac{1}{2}\beta_t t_i^2 \right). \quad (2.19)$$

Equating the right parts of equations (2.18) and (2.19), we obtain an expression; its solution with respect to  $t_e$  allows us to estimate the possible value of the filament temperature:

$$2I_e^2 \frac{\rho_0}{\pi d_m^2} \left( 1 + \beta \frac{t_e + t_i}{2} \right) = \frac{\pi\lambda_0}{\ln(2r_k / d_m)} \left( t_e - t_i + \frac{1}{2}\beta_t t_e^2 - \frac{1}{2}\beta_t t_i^2 \right). \quad (2.20)$$

Let's reduce the obtained equation:

$$t_e^2 + p t_e + g = 0, \quad (2.21)$$

where:

$$p = \frac{2}{\beta_t} - I_e^2 \frac{\rho_0 \beta \ln(2r_k / d_m)}{\pi^2 d_m^2 \beta_t \lambda_0}; \quad g = \frac{2t_i}{\beta_t} - t_i^2 - I_e^2 \frac{\rho_0 \ln(2r_k / d_m)}{\pi^2 d_m^2 \beta_t \lambda_0} (2 + \beta_t t_i).$$

The solution of equation (2.21):

$$t_e = -p/2 \pm \sqrt{(p/2)^2 - g}. \quad (2.22)$$

For a real thermoconductometric sensor at  $I_e = 100$  mA,  $t_i = 20$  °C,  $d_i = 20$  μm and  $g_k = 3$  mm, the temperature value of the platinum filament in air calculated by these dependencies is 148 °C. At the same time, the experimentally determined value of the temperature of the thermocouple in the form of a miniature ball at such a current value is within 180-205 °C. This means that in a real sensor a part of heat from the thermocouple will be transferred to the current supplying ends.

It should be noted that the temperature of the platinum filament was calculated without taking into account the heat fluxes from the thermocouple. At the same time, the current-supplying ends, and especially the part of them located closer to the thermocouple, are in a gas medium, the temperature of which is significantly higher than the body temperature. This leads to its additional heating, growth of specific resistance and increase of power generated in the current supplying ends. Thus, if we take in expression (18)  $t_i = 80$  °C, which approximately corresponds to the gas temperature at a distance of 1.2 mm from the chamber wall in the place of fixing the current-supplying end to the rack, then the calculated value of the platinum filament temperature will be 192 °C, i.e. close to the temperature of the thermocouple. At the length of current conducting ends equal to  $l_{br}$  border length the powers released in current conducting ends as a result of electric current flow and dissipated by current conducting ends due to their thermal conductivity are also close in value. So in this case, for the considered thermoconductometric sensor, the powers calculated on the basis of expressions (2.18) and (2.19) are 12.44 mW and 12.21 mW, respectively.

Taking into account the above, with sufficient accuracy for practical purposes, it can be considered that at the length of the conductive ends close to the critical length, the heat from the thermocouple to the conductive end is practically not transferred, and the heat generated in the conductive ends due to the flow of electric current is removed by the conductive ends due to their thermal conductivity to the racks. Accordingly, this part of the heat flux is practically independent of the gas thermal conductivity and is uninformative.

Taking into account expressions (2.11), (2.14) and (2.16), equation (2.1) will take the form

$$P_e = \frac{4\pi\lambda_0}{1/r_e - 1/r_k} \left( t_e - t_i + \frac{1}{2}\beta_t t_e^2 - \frac{1}{2}\beta_t t_i^2 \right) + 6.35 \cdot 10^{-2} \varepsilon_e r_e^2 (t_e^2 - 0.5t_e t_i) + 3.45d_m (t_e - t_i). \quad (2.23)$$

In turn, the power released during the passage of electric current, without taking into account the non-uniform temperature distribution along the length of the current-supplying ends, can be determined from the expression

$$P_e = I_e^2 R_e, \quad (2.24)$$

where:

$$R_e = R_0(1 + \beta t_e) - \text{resistance of the element at temperature } t_e, \text{ Ohm.}$$

Equating the right parts of (2.23) and (2.24) and expressing the temperature of the element through its resistance, we obtain an implicit expression for determining the resistance value of the element:

$$I_e^2 R_e = \frac{4\pi\lambda_0}{1/r_e - 1/r_k} \left( \frac{R_e - R_0}{\beta R_0} - t_i + \frac{1}{2}\beta_t \frac{(R_e - R_0)^2}{\beta^2 R_0^2} - \frac{1}{2}\beta_t t_i^2 \right) + 6.35 \cdot 10^{-2} \varepsilon_e r_e^2 \left( \frac{(R_e - R_0)^2}{\beta^2 R_0^2} - 0.5 \frac{R_e - R_0}{\beta R_0} t_i \right) + 3.45d_m \left( \frac{R_e - R_0}{\beta R_0} - t_i \right). \quad (2.25)$$

The obtained equation is solved analytically with respect to  $R_e$ , however, this solution is cumbersome and very difficult to analyze. At the same time, we can clearly see from equation (2.25) that there is no simple inversely proportional relationship between the temperature head (temperature difference between the element and the

medium) and the thermal conductivity of the gas medium, as assumed by the authors of [4] when deriving the dependence of the bridge output voltage on the thermal conductivity of the medium. Even if we neglect the radiation component of heat transfer and heat transfer through the current-supplying ends, as it is done by the authors of many works, the specified relationship is not observed. Let us show it on the example of a real thermoconductometer sensor.

At  $I_e = 100$  mA,  $t_t = 20$  °C,  $d_t = 20$  μm and  $g_k = 3$  mm, calculated by expressions (2.11), (2.14) and (2.16) the values of heat transfer components are equal to:  $P_t = 39.32$  mW,  $P_d = 6.44$  mW,  $P_r = 12.44$  mW. For a total power of 58.2 mW, the proportions of these components will respectively be: 67.5%; 11.1% и 21.4%. As can be seen, the second and third components total 33.5% and play quite a significant role in heat transfer. If we neglect these components of heat exchange as directly independent of the thermal conductivity of the medium, then, when determining the sensitivity of the analyzer, it is necessary to exclude from equation (2.25) the part of power dissipated due to these paths of heat exchange. In this case, equation (2.25) will take the form:

$$0.675I_e^2R_e = \frac{4\pi\lambda_0}{1/r_e - 1/r_k} \left( \frac{R_e - R_0}{\beta R_0} - t_t + \frac{1}{2}\beta_t \frac{(R_e - R_0)^2}{\beta^2 R_0^2} - \frac{1}{2}\beta_t t_t^2 \right). \quad (2.26)$$

Let's reduce the obtained equation:

$$R_e^2 + pR_e + g = 0,$$

where: 
$$p = 2R_0 \left( \frac{\beta}{\beta_t} - 1 \right) - 0.35I_e^2 \frac{\beta^2 R_0^2 (1/r_e - 1/r_k)}{2\pi\beta_t \lambda_0}; \quad g = \left( 1 - \frac{2\beta}{\beta_t} - \frac{2\beta^2 t_t}{\beta_t} - \beta^2 t_t^2 \right) R_0^2.$$

Then the solution of equation (2.26) has the form:

$$R_e = R_0 \left( 1 - \frac{\beta}{\beta_t} \right) + 0.35I_e^2 \frac{\beta^2 R_0^2 (1/r_e - 1/r_k)}{2\pi\beta_t \lambda_0} + \sqrt{\left( R_0 \left( 1 - \frac{\beta}{\beta_t} \right) + 0.35I_e^2 \frac{\beta^2 R_0^2 (1/r_e - 1/r_k)}{2\pi\beta_t \lambda_0} \right)^2 + \left( \frac{2\beta}{\beta_t} + \frac{2\beta^2 t_t}{\beta_t} + \beta^2 t_t^2 - 1 \right) R_0^2}. \quad (2.27)$$

The equation [4] allows to determine the resistance of a spherical-shaped thermocouple located in the center of a spherical chamber

$$R_e = \frac{4\pi\lambda_{tc}}{I_e^2 (1/r_e - 1/r_k)} (t_e - t_k), \quad (2.28)$$

where:

$\lambda_{tc}$  – thermal conductivity of the gas mixture calculated for the gas layer at the average temperature  $t_t = (t_e + t_k) / 2$ , W/(m·°C).

This expression includes the thermal conductivity of the gas mixture at the average temperature in the chamber, which is a function of the element temperature. In turn, the element temperature value is related to its resistance by the expression

$$t_e = \left( \frac{R_e}{R_0} - 1 \right) \frac{1}{\beta}. \quad (2.29)$$

Taking into account (2.8) and (2.29), the thermal conductivity in air and in methane, respectively, specified in expression (2.28) can be determined as follows:

$$\lambda_a = \lambda_{a_0} + 0.5\lambda_{a_0}\beta_a \left( \frac{R_e}{R_0\beta} - \frac{1}{\beta} + t_k \right); \quad (2.30)$$

$$\lambda_{br} = \lambda_{br_0} + 0.5\lambda_{br_0}\beta_{br} \left( \frac{R_e}{R_0\beta} - \frac{1}{\beta} + t_k \right), \quad (2.31)$$

where:

$\lambda_{a_0}$ ,  $\lambda_{br_0}$  – thermal conductivity coefficients of air and methane at 0 °C, W/(m·°C).

Only after substituting into (2.28) the value of the element temperature (2.29) and the corresponding thermal conductivity, according to (2.30) and (2.31), this equation can be solved explicitly with respect to the element resistance in air and methane.

The obtained expression, in contrast to the known (2.28), includes the thermal conductivity of the medium at zero temperature and the temperature coefficient of change of thermal conductivity, and also takes into account the processes of heat dissipation by radiation and conduction through the current conducting ends. Using the expression (2.27) the resistance and temperature of the thermocouple with the parameters  $R_0 = 3$  Ohm,  $d_t = 20$  microns,  $g_e = 0.5$  mm,  $g_k = 3$  mm at  $I_e = 100$  mA,  $t_g = 20$  °C in air and methane were calculated and compared with the experimentally measured values and the values calculated according to the known relationships. The obtained results are given in Table 2.1.

Table 2.1

Calculated and experimentally determined parameters of the thermocouple

Gas medium	Calculated and experimental parameters of the thermocouple					
	by expression (2.27)		by known expressions		experimental	
	$R_e$ , Ohm	$t_e$ , °C	$R_e$ , Ohm	$t_e$ , °C	$R_e$ , Ohm	$t_e$ , °C
Air	5.46	205.5	6.36	280.5	5.44	203.3
Methane	4.77	147.3	5.20	183.5	4.76	146.7

As can be seen from the table, the element parameters calculated by the obtained expressions and experimentally determined parameters practically coincide. At the same time, the parameters of the elements determined by the known dependences are strongly overestimated. Significantly overestimated in the latter case is also the relative change of element parameters at transition from air to methane, which is one of the reasons of discrepancy between theoretically calculated and real parameters of thermoconductometric gas analyzers.

## 2.2. Analysis of operation modes of bridge circuits in methane analyzers

Thermal conductometric sensors of methane are usually included in bridge circuits of gas analyzers. The peculiarities of sensor operation in such circuits are well covered in the References [5, 6, 7]. In existing thermoconductometric methane analyzers, bridge circuits with thermoconductometric sensors are usually powered with stable voltage (Fig. 2.2, a). However, in such circuits, the change of ambient temperature leads to the change of temperature modes of thermocouples, which causes a significant error in measurement of high methane concentrations due to the ambiguous temperature dependence of air and methane thermal conductivity [6]. It is possible to reduce this error by using inclusion circuits that ensure stable temperature mode of thermocouples when the temperature of the gas medium changes. In this respect, the circuits of sensor switching with voltage stabilization on one of the thermocouples are of interest [7]. Theoretical analysis of the operation of such circuits, performed for the case of using thermocatalytic methane sensors, showed that they have a number of significant advantages over traditional sensor inclusion circuits. Thermoconductometric sensors of methane, unlike thermocatalytic sensors, have much lower sensitivity and a different character of dependence of resistance of the working element on the concentration of the measured parameter. Therefore, to make a final conclusion about the most rational inclusion circuits of thermoconductometric sensors it is necessary to conduct additional studies of the peculiarities of operation of bridge measuring circuits of thermoconductometric gas analyzers.

For unbalanced bridge circuits, which are used in thermoconductometric methane analyzers, the output signal is directly proportional to the bridge supply voltage, and therefore, if the supply voltage is unstable, the measurement error will be proportional to its relative change. When measuring the methane content by a thermoconductometric sensor the zero content corresponds to the bridge balance, and when methane appears in the analyzed mixture the bridge becomes unbalanced. The working and sealed comparative elements of the thermoconductometric sensor try to be identical in resistance and geometric dimensions to ensure the stability of the analyzer's zero at changes in the temperature of the analyzed mixture and possible changes in the bridge power supply parameters. As a rule, the working and comparative thermocouples are included in one arm of the bridge and ballast resistors in the other arm. The output signal of the bridge is usually amplified by precision operational amplifiers with high input impedance. Therefore, it is assumed that the measuring diagonal of the bridge operates in no-load mode, and the internal resistance of the power supply is zero.

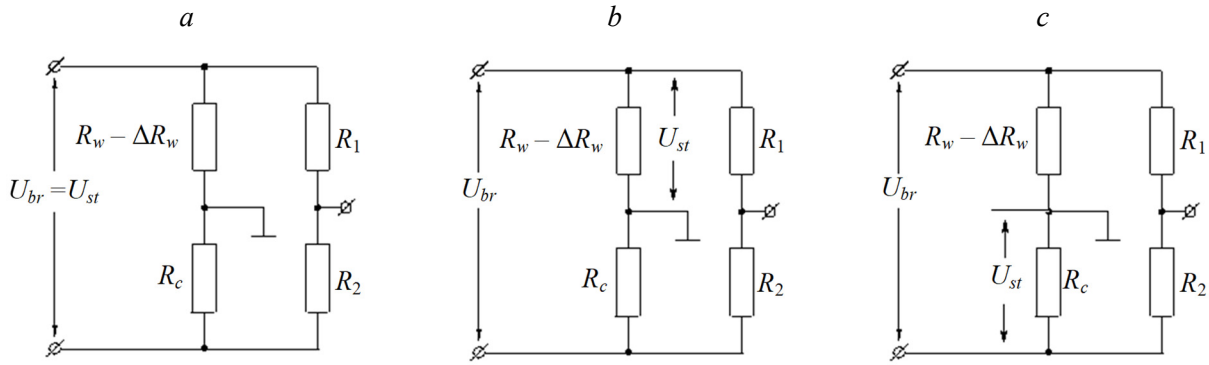


Fig. 2.2. Power circuits of unbalanced bridges

The equation of the output signal of the measuring bridge with a thermocatalytic sensor when it is powered by a stable voltage source is [1]:

$$U_{out}^a = \frac{U_{br} \cdot R_1 \cdot \Delta R_a}{(R_1 + R_2) \cdot (R_a + \Delta R_a + R_c)}, \quad (2.32)$$

where:

$U_{br}$  and  $U_{out}$  – supply voltage and output bridge voltage, respectively;

$R_a$  and  $R_c$  – resistance of active and comparative elements of the thermocatalytic sensor, respectively;

$\Delta R_a$  – increment of resistance of the active element of the thermocatalytic sensor due to catalytic reaction on it.

By analogy with (2.32) we write down the equation of the output signal of the bridge with a thermoconductometer sensor:

$$U_{out}^a = \frac{U_{br} \cdot R_1 \cdot \Delta R_w}{(R_1 + R_2) \cdot (R_w - \Delta R_w + R_c)}, \quad (2.33)$$

where:

$R_w$  and  $R_c$  – resistance of the working and comparative elements of the thermoconductometric sensor;

$\Delta R_w$  – decrease in resistance of the working element of the thermoconductometric sensor due to the growth of thermal conductivity of the mixture.

At zero methane concentration for a symmetrical bridge at the moment of bridge balance, the voltage across the sensor elements is equal to  $0.5 U_{br}$ . In this case, the bridge supply voltage at stabilization of the voltage on the working element (Fig. 2.2, b) at the growth of methane concentration increases in comparison with the moment of the bridge balance:

$$U_{br}^b = \frac{U_{br} \cdot (R_w - \Delta R_w + R_c)}{2 \cdot (R_w - \Delta R_w)}. \quad (2.34)$$

By stabilizing the voltage on the comparison element (Fig. 2.2, c), the bridge supply voltage decreases compared to balance momentum as the concentration of the measured component increases:

$$U_{br}^c = \frac{U_{br} \cdot (R_w - \Delta R_w + R_c)}{2 \cdot R_c}. \quad (2.35)$$

The output equation for variant “b”, obtained by substituting (2.34) into (2.33), is:

$$U_{out}^b = \frac{U_{br} \cdot R_1 \cdot \Delta R_w}{2 \cdot (R_w - \Delta R_w) \cdot (R_1 + R_2)}. \quad (2.36)$$

The equation of the output signal for variant “c”, will be:

$$U_{out}^c = \frac{U_{br} \cdot R_1 \cdot \Delta R_w}{2 \cdot R_c \cdot (R_1 + R_2)}. \quad (2.37)$$

Passing to the relative changes of resistance of the working element of the sensor  $\delta R_w = \Delta R_w / R_w$ , taking into account that the bridges are equal-armed, i.e.  $R_w = R_c$ , and  $R_1 = R_2$ , we finally obtain:

$$U_{out}^a = \frac{U_{br} \cdot \delta R_w}{4 - 2\delta R_w} = \frac{U_{br} \cdot \delta R_w}{4(1 - 0.5\delta R_w)}; \quad U_{out}^b = \frac{U_{br} \cdot \delta R_w}{4(1 - \delta R_w)}; \quad U_{out}^c = \frac{U_{br} \cdot \delta R_w}{4}. \quad (2.38)$$

Analysis of equations (2.38) shows that the greatest sensitivity of bridge measuring circuits when using thermoconductometric sensors is provided at stabilization of voltage on the working element. It should be noted that in contrast to thermoconductometric sensors, when using thermocatalytic sensors, the greatest sensitivity is provided at voltage stabilization on the comparative element [1]. This is explained by the different kinds of the element resistance value dependence on the methane content.

The lowest sensitivity of bridge circuits at application of thermoconductometric sensors is observed at stabilization of voltage on the comparative element. At the same time, the output signal of the bridge circuit only in this case linearly depends on the increment of resistance of the working element, and the error from the nonlinearity of the bridge circuit in variant “c” will be equal to zero. On the contrary, variant “b”, which provides the maximum sensitivity, is characterized by the greatest nonlinearity.

The relative degree of nonlinearity of the bridge output characteristic, calculated by us for the first two variants of the bridge power supply according to [1], is:

$$D_a = \frac{1}{2} \sigma R_a; \quad D_{a1} = \sigma R_a. \quad (2.39)$$

Thus, the non-uniformity of the bridge output signal according to variant “a” is equal to 0.5% for each percent change in resistance of the working element of the thermoconductometric sensor, and according to variant “b” twice as much as according to variant “a”.

Numerical analysis, performed taking into account real parameters of thermocouples and temperature modes of their operation, shows that in comparison with the typical inclusion circuit (variant “a”) the sensitivity of the bridge with thermoconductometric sensor at stabilization of voltage on the working element (variant “b”) increases by 5%, and in variant “c” decreases by 5%. At the same time, when the analyzers are adjusted for two points, for example, air and 100 vol.% of methane, without taking measures to linearize the scale, the error due to nonlinearity of the output characteristic of the bridge in the middle part of the range in variant “a” is up to 2.5%, and in variant “b” it reaches 5%.

Let us consider one more of the possible modes of operation of bridge circuits of thermoconductometric methane analyzers – powering the bridge from a stable current source  $I = const$ , which is recommended when using remote thermocatalytic sensors [1]. If the resistance of ballast resistors is much higher than the resistance of thermocouples, it can be considered that the voltage value on the bridge at the growth of methane concentration will be determined by the expression:

$$U_{br}^I = I_{br} \cdot (R_w - \Delta R_w + R_c). \quad (2.40)$$

Substituting (2.40) into (2.33) we obtain

$$U_{out}^I = \frac{I_{br} \cdot R_1 \cdot \Delta R_w}{(R_1 + R_2)}. \quad (2.41)$$

Turning to the relative changes in resistance of the working element for a symmetrical bridge, we obtain:

$$U_{out}^I = \frac{U_{br} \cdot \delta R_w}{4}. \quad (2.42)$$

Comparison of the obtained expression (2.42) with equations (2.38) allows us to conclude that the mode of operation with the bridge power supply from a stable current source is equivalent to the bridge operation at a stable voltage on the comparative element and is characterized by a slightly lower sensitivity of bridge circuits and linear dependence of the bridge output signal on the increment of the resistance of the working element, and therefore, the absence of error from the nonlinearity of the bridge circuit.

At the same time, it should be noted that the linear dependence of the bridge output signal on the increment of the resistance of the working element does not guarantee a linear dependence of this signal on the methane concentration. Obviously, this is provided only if the ratio of the change in resistance of the working element  $dR_w$  to the change in methane concentration is constant over the entire range of measured concentrations  $dC$ .

$$\frac{dR_w}{dC} = const. \quad (2.43)$$

Therefore, the final conclusion regarding the most expedient variant of the power supply circuit for the measuring bridge of the gas analyzer can be made only after establishing the functional relationship between the methane concentration and the resistance of the working element for different power supply circuit.

### 2.3. Selection of power supply mode for thermoconductometric sensors in methane analyzers

In existing thermoconductometric methane analyzers, bridge circuits with thermoconductometric sensors are usually powered with stable voltage (Fig. 2.2, a). At the same time, our analysis of operating modes of bridge measuring circuits in methane analyzers shows that other known circuits for supplying measuring bridges with thermoconductometric sensors, including those with voltage stabilization on one of the sensor thermocouples and with supplying the bridge from a stable current source have certain advantages over the typical inclusion circuit in terms of sensitivity and linearity of the measuring bridge. However, the analysis of the operation of these circuits is performed in Section 2 without taking into account the peculiarities of the thermoconductometric sensors themselves in multicomponent gas mixtures, which does not allow us to make an unambiguous choice of the most appropriate inclusion circuit. Therefore, it is necessary to substantiate the expedient inclusion circuit of thermoconductometric sensors of methane in bridge circuits taking into account the peculiarities of their operation in multicomponent gas mixtures.

Based on the expression (2.32), when powering the measuring bridge from a source of stable voltage (Fig. 2.2, a), taking into account that it is made equal-armed, i.e. in the air  $R_w = R_c$ , and  $R_1 = R_2$ , the output voltage of the bridge is related to the change in the resistance of the working element  $\Delta R$  dependence.

$$U_{out}^a = \frac{U_{br} \cdot \Delta R_w}{2(2R_c - \Delta R_w)}. \quad (2.44)$$

At stabilization of voltage on the working or comparative element of the thermoconductometric sensor (respectively Fig. 2.2 b, c) this dependence takes the following form

$$U_{out}^b = \frac{U_{br} \cdot \Delta R_w}{4(R_c - \Delta R_w)}; \quad (2.45)$$

$$U_{out}^c = \frac{U_{br} \cdot \Delta R_w}{4R_c}. \quad (2.46)$$

Expression (2.46) is also valid when the bridge with thermoconductometric sensor is powered by a stable current source  $I = const$ .

The relative degree of nonlinearity of the bridge output characteristic calculated for different variants of the bridge power supply is:

$$D_a = \frac{1}{2} \frac{\Delta R_w}{R_c}; \quad D_{a1} = \frac{\Delta R_w}{R_c}. \quad (2.47)$$

To determine the value of  $R_w$  and  $\Delta R_w$  we will use the dependence of the resistance value of the spherical thermistor located in the center of the spherical measuring chamber on the gas mixture (2.28), and the temperature of the platinum thermocouple will be calculated by expression (2.29). Taking the temperature of the chamber walls equal to the temperature of the analyzed gas mixture  $t_k = t_t$  taking into account (2.28) and (2.29) determine the resistance of the comparative and working thermocouples, which are located in the chambers filled with air and gas mixture.

$$R_c = \frac{b\lambda_a R_t}{b\lambda_a - R_0\beta}; \quad (2.48)$$

$$R_w = \frac{b\lambda_{tc} R_t}{b\lambda_{tc} - R_0\beta}, \quad (2.49)$$

where:  $b = \frac{4\pi}{I_e^2(1/r_e - 1/r_k)}$ ;

$\lambda_a$  – thermal conductivity of air at average temperature, W/(m·°C);

$R_t = R_0(1 + \beta t_t)$  – resistance of thermocouple at gas temperature, Ohm.

Let's define the value  $\Delta R_w$  as the difference of expressions (2.48) and (2.49)

$$\Delta R_w = \frac{b\lambda_a R_t}{b\lambda_a - R_0\beta} - \frac{b\lambda_{tc} R_t}{b\lambda_{tc} - R_0\beta} = \frac{bR_t R_0\beta(\lambda_{tc} - \lambda_a)}{(b\lambda_a - R_0\beta)(b\lambda_{tc} - R_0\beta)}. \quad (2.50)$$

In practical calculations, it can be assumed that the thermal conductivity of a mixture of nonpolar gases has additive properties and unambiguously depends on the concentration of gas components [8]. In this case, the thermal conductivity of a binary methane-air mixture can be determined from the dependence

$$\lambda_{tc} = C\lambda_{br} + (1 - C)\lambda_a, \quad (2.51)$$

where:

$C$  – methane content in the gas mixture in fractions of a unit.

Taking into account (2.48) – (2.51), the output voltage of the bridge at different power supply circuits will be:

$$U_{out}^a = \frac{U_{br}}{4} \frac{CR_0\beta(\lambda_{br} - \lambda_a)}{\lambda_a(b\lambda_a - R_0\beta) + C(\lambda_{br} - \lambda_a)(b\lambda_a - 0.5R_0\beta)}; \quad (2.52)$$

$$U_{out}^b = \frac{U_{br}}{4} \frac{CR_0\beta(\lambda_{br} - \lambda_a)}{\lambda_a(b\lambda_a - R_0\beta) + C(\lambda_{br} - \lambda_a)(b\lambda_a - R_0\beta)}; \quad (2.53)$$

$$U_{out}^c = \frac{U_{br}}{4} \frac{CR_0\beta(\lambda_{br} - \lambda_a)}{\lambda_a(b\lambda_a - R_0\beta) + Cb\lambda_a(\lambda_{br} - \lambda_a)}. \quad (2.54)$$

From expressions (2.52) – (2.54) it is evident that none of the considered power supply circuits provides linear dependence of the measuring bridge output signal on the methane concentration in the gas mixture. However, the degree of nonlinearity and sensitivity of the bridge measuring circuits differ significantly. For more clarity, below are the expressions describing the dependence of the bridge output voltage on methane concentration calculated for a specific thermoconductometric sensor included in the bridge circuit at the value of  $U_{br} = 1.1$  V;  $I_e = 0.1$  A;  $R_0 = 3$  Ohm;  $g_e = 0.6 \cdot 10^{-3}$  m;  $g_k = 5 \cdot 10^{-3}$  m;  $t_g = 20$  °C.

$$U_{out}^a = 0.425 \frac{C}{4.98 + 2.795C}; \quad (2.55)$$

$$U_{out}^b = 0.425 \frac{C}{4.98 + 2.015C}; \quad (2.56)$$

$$U_{out}^c = 0.425 \frac{C}{4.98 + 3.580C}. \quad (2.57)$$

Fig. 2.3 shows the dependences of the output signal of the measuring bridge on the volume fraction of methane in the gas mixture, constructed on the basis of expressions (2.55) – (2.57).

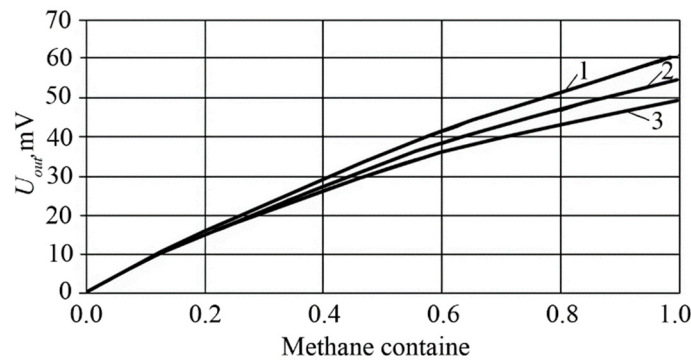


Fig. 2.3. Dependences of the measuring bridge output signal on the methane concentration in the gas mixture

The lower curve 3, obtained by expression (2.57), corresponds to the inclusion circuit with voltage stabilization on the comparative element or powering the bridge from a stable current source. In spite of the fact that these power supply circuits provide linearity of the bridge with respect to the change in the value of the working thermocouple resistance  $\Delta R_w$ , they are characterized by the greatest nonlinearity of the dependence of the bridge output signal on the methane concentration, which is caused by the nonlinear character of the dependence of the  $\Delta R_w$  value on the methane concentration. Besides, such inclusion circuits are characterized by lower sensitivity in comparison with other investigated inclusion circuits.

The average curve 2, obtained by expression (2.55), corresponds to the typical inclusion circuit with voltage stabilization on the bridge. It is characterized by slightly lower nonlinearity and higher sensitivity compared to the previous one.

The upper curve 1, obtained by expression (2.56), corresponds to the inclusion circuit with voltage stabilization on the working element. In spite of the fact that according to expression (2.53), this inclusion circuit is characterized by the largest nonlinearity of the bridge with respect to the change in the resistance value of the working thermocouple  $\Delta R_w$ , it provides less nonlinearity of the dependence of the bridge output signal on the methane concentration and higher sensitivity compared to the typical inclusion circuit.

Numerical analysis of the obtained dependences shows that without taking measures on scale linearization in thermoconductometric methane analyzers in case of application of the circuit with voltage stabilization on the working element, the reduced measurement error in the middle part of the measurement range reaches 8%, which is significantly lower than in case of the typical inclusion circuit. However, to ensure the required metrological characteristics of methane analyzers, even in this case it is necessary to linearize the output signal of the bridge.

In all the considered modes of its power supply, the nonlinear dependence of the bridge output signal on the methane concentration from the physical point of view is explained by the fact that in all cases, including at stabilization of the voltage on the working element, with increasing methane concentration there is a decrease in the temperature of the working element, and this, in turn, leads to a decrease in the sensitivity of the sensor. The ratio of change in resistance of the working element to change in methane concentration (2.43) decreases with increasing methane content in the gas mixture.

It is possible to provide constant sensitivity of the sensor by stabilizing the temperature of the working element, which is possible by maintaining a constant value of the resistance value of the working thermocouple

$$R_w = \frac{U_w}{I_e} = const. \quad (2.58)$$

This mode of operation of the bridge (Fig. 2.4) can be implemented by using a microprocessor.

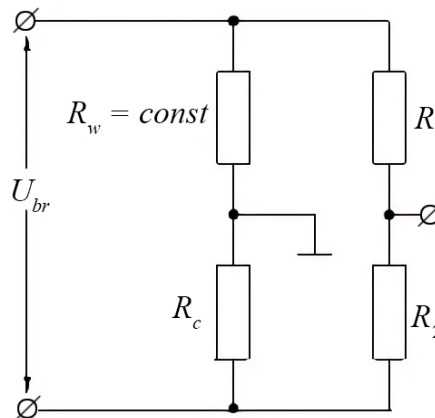


Fig. 2.4. The unbalanced bridge power supply circuit when stabilizing the temperature of the working element

The equation of the output signal of the bridge with a thermoconductometric sensor at stabilization of the temperature of the working element is:

$$U_{out}^s = \frac{U_{br}^s \cdot R_1 \cdot \Delta R_c}{(R_1 + R_2) \cdot (R_w + R_c + \Delta R_c)}. \quad (2.59)$$

At zero methane concentration for a symmetric bridge at the moment of bridge balance, the voltage across the sensor elements is equal to  $0.5 U_{br}$ . In this case, the bridge power supply voltage at stabilization of the working

element temperature and methane concentration growth increases compared to the moment of bridge balance

$$U_{br}^s = \frac{U_{br} \cdot (R_w + \Delta R_c + R_c)}{2R_w}. \quad (2.60)$$

The output equation for this variant, obtained by substituting (2.60) into equation (2.59), is:

$$U_{out}^s = \frac{U_{br} \cdot R_1 \cdot \Delta R_w}{2 \cdot R_w \cdot (R_1 + R_2)}. \quad (2.61)$$

Under the condition of symmetry of the bridge we have

$$U_{out}^s = \frac{U_{br} \cdot \Delta R_c}{4 \cdot R_w}. \quad (2.62)$$

In this expression, the value of  $R_w = const$ , and the value of  $\Delta R_c$  will be defined as the difference of resistance of the comparison element and in air

$$\Delta R_c = R_c - R_{c_0}, \quad (2.63)$$

where:

$R_{c_0}$  – resistances of the comparison element when the working element is in the air.

To determine the resistance of the comparative element, let us use dependences (2.28) and (2.29). By analogy with (2.48) and (2.49), when the working element is located in a mixture of gases and in this case we have

$$R_c = \frac{b\lambda_a R_t}{b\lambda_a - R_0\beta}. \quad (2.64)$$

$$R_w = \frac{b\lambda_{tc} R_t}{b\lambda_{tc} - R_0\beta}. \quad (2.65)$$

To determine the resistance of the comparative element when the working element is in the air with (2.65), we calculate the value of  $b$

$$b = \frac{R_w R_0 \beta}{\lambda_{tc} (R_w - R_t)}. \quad (2.66)$$

In this expression at constant temperature and the accepted gas operation mode  $R_w$ ,  $R_0$ ,  $R_t$  are constant values. In this case, let us present (2.66) in the form

$$b = \frac{a}{\lambda_{tc}}, \quad (2.67)$$

where:

$$a = \frac{R_w R_0 \beta}{R_w - R_t}. \quad (2.68)$$

Taking into account (2.67) the resistance of the comparative element when the working element is in air and in a mixture of gases are equal to

$$R_{c_0} = \frac{aR_t}{a - R_0\beta}. \quad (2.69)$$

$$R_c = \frac{a\lambda_a R_t}{a\lambda_a - R_0\beta\lambda_{rc}}. \quad (2.70)$$

Substituting the obtained values of resistances into (2.63) we have

$$\Delta R_c = \frac{aR_t R_0\beta(\lambda_{rc} - \lambda_a)}{(a\lambda_a - R_0\beta\lambda_{rc})(a - R_0\beta)}. \quad (2.71)$$

Substituting in (2.71)  $\lambda_{rc}$  its value from expression (2.51) and substituting the obtained expression into (2.72) we obtain

$$U_{out}^s = \frac{U_{br}}{4 \cdot R_w (a - R_0\beta)} \cdot \frac{aR_t R_0\beta C(\lambda_{br} - \lambda_a)}{a\lambda_a - R_0\beta C(\lambda_{br} - \lambda_a)}. \quad (2.72)$$

Comparison of the obtained expression (2.62) with expressions (2.52) – (2.54) shows that the nature of the bridge output signal dependence on the methane concentration in the gas mixture changes at stabilization of the working element temperature. The expression describing the dependence of the bridge output voltage on the methane concentration, calculated as in the previous case for a specific thermoconductometric sensor included in the bridge circuit at the same values of the power supply parameters, elements and gas medium is:

$$U_{out}^s = 0.425 \frac{C}{4.98 - 1.106C}. \quad (2.73)$$

Comparison of expression (2.63) with expressions (2.55) – (2.57) shows a significantly lower degree of nonlinearity and a different nature of dependence, since with increasing methane concentration the denominator in expression (2.63) decreases, and hence the sensitivity increases (Fig. 2.5).

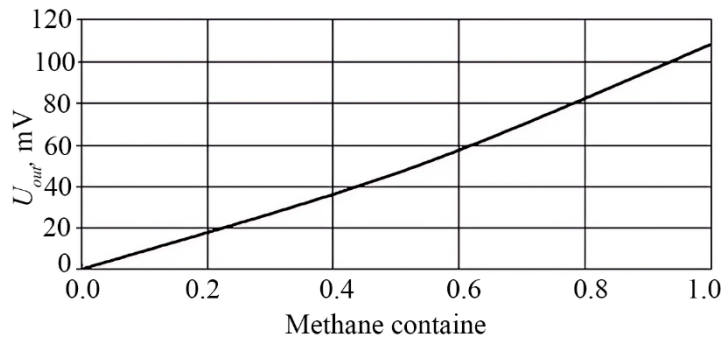


Fig. 2.5. Bridge output signal dependence on the methane content in the mixture at stabilization of the working element temperature

Numerical analysis of dependence (2.63) shows that without taking measures to linearize the scale when using the circuit with stabilization of resistance of the working element, the reduced error of measurement in the middle part of the measurement range reaches 4%, which is significantly lower than in the previously considered inclusion circuits. Besides, in this case the output voltage of the bridge at equal concentrations of methane is practically twice as high as at application of the previously considered variants of power supply. All this allows us to conclude the significant advantage of the bridge operation mode with stabilization of the working element resistance and recommend its application.

At the same time, it should be noted that both in the derivation of dependences (2.52) – (2.54) and dependence (2.72), assumptions were made that the thermal conductivity of a mixture of nonpolar gases has additive properties, and the thermal conductivity of the gas mixture calculated for the gas layer at the average gas

temperature in the chamber was assumed to be constant. In real conditions, even mixtures of nonpolar gases such as methane and air do not possess this property [5]. For a two-component mixture of such gases, the authors of [9] recommend to use Brokaw's formula for heat conductivity calculations, which has the following form

$$\lambda'_{tc} = 0.5 \left[ C_{br} \lambda_{br} + (1 - C_{br}) \lambda_a + \frac{\lambda_{br} \lambda_a}{\lambda_a C_{br} + \lambda_{br} (1 - C_{br})} \right]. \quad (2.74)$$

Fig. 2.6 shows the ratio of thermal conductivities calculated by expressions (2.51) and (2.74). The deviation of the true thermal conductivity of the gas mixture from the linear dependence at the methane volume content of 50% is about 1%.

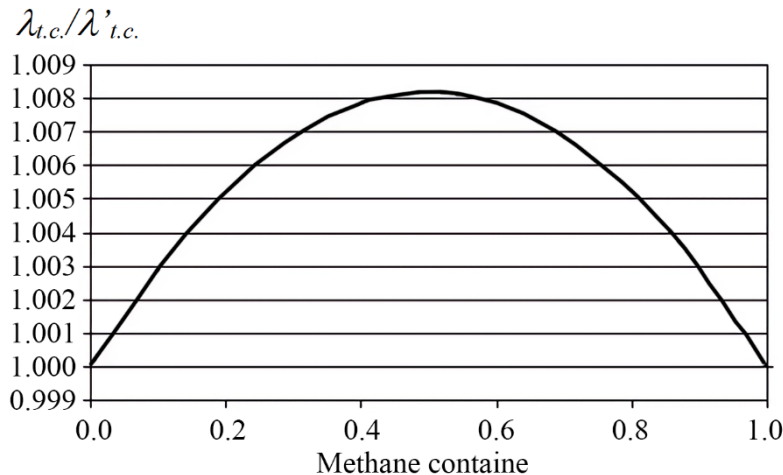


Fig. 2.6. Deviation of the true thermal conductivity of a gas mixture from a linear dependence for binary mixtures

As can be seen from Fig. 2.6, in the middle part of the concentration range, the true thermal conductivity of the gas mixture is practically higher than the one accepted in our calculations by 1%. This character of the dependence leads to an increase in the nonlinearity of the bridge output signal for the previously considered variants of the power supply and reduces the nonlinearity when using the circuit with stabilization of the resistance of the working element.

At stable temperature of the working element in case of increase of the volume fraction of methane in the gas mixture, the temperature of the comparative element and, consequently, the average temperature of air in the chamber with the comparative element increase. According to expression (2.7) it leads to some growth of heat conductivity of air in the comparison chamber. Under the accepted modes of operation of the thermoconductometer sensor, the average temperature of air in the chamber with a comparative element in the case of increasing the volume fraction of methane in the gas mixture from 0 to 100% increases by 30-40 °C, which leads to an increase in the thermal conductivity of air by 4-6%. In turn, the growth of thermal conductivity leads to some decrease in the temperature of the comparative element and, consequently, in the bridge output voltage relative to its value calculated by expression (2.72), which in our case reduces the nonlinearity of the bridge output voltage.

Thus, when applying the circuit with stabilization of the resistance of the working element, both factors that we did not take into account when deriving expression (2.72) lead to a decrease in the nonlinearity of the output voltage of the bridge, and the degree of influence of these factors is comparable to the magnitude of nonlinearity and practically eliminates it. However, to confirm the conclusion regarding the linearity of the output signal and other advantages of this variant of the bridge power supply, it is necessary to conduct its experimental studies.

## 2.4. Study of influence of gas medium parameters on temperature modes of thermocouples in bridge circuits of methane analyzers

Bridge circuits of thermocatalytic and thermoconductometric gas analyzers are most often powered by stable voltage sources. However, our analysis of other modes of operation of bridge circuits, for example, supply with stable current, with voltage stabilization on one of the thermocouples and with temperature stabilization of the working element, showed that these inclusion circuits have certain advantages over typical circuits. Thus, when supplying the measuring bridge with a stable voltage, changes in the parameters of the gas medium, for example, the ambient temperature, lead to changes in the temperature modes of thermoelements, which causes measurement error due to the ambiguous temperature dependence of the thermal conductivity of air and methane [1]. The issues related to the reduction of this error have not been sufficiently studied so far. Therefore, for the final choice of the sensor inclusion circuit it is necessary to carry out studies of the influence of the measured gas temperature change on the temperature modes of thermocouples operation at different inclusion circuits.

The temperature of the thermocouple in general depends on the ambient temperature, geometric and electrical parameters of the element, heat exchange conditions and the current flowing through the element. The theoretical dependence describing the dependence of the element temperature on these parameters is [1, 3].

$$t_e = t_t + b_e I_e^2, \quad (2.75)$$

where:

$b_e$  – thermoresistive coefficient that determines the relationship between the electrical, thermal and geometric characteristics of the element.

Both the resistance of the thermocouple and the heat transfer coefficient depend on temperature. For platinum thermistors this dependence is linear

$$R_e = R_{0e}(1 + t_e). \quad (2.76)$$

The total heat transfer coefficient of the element is the sum of the heat transfer coefficients of the element due to the thermal conductivity of the medium, convection, radiation and conductivity of the conductor ends. When designing transducer elements of thermoconductometric sensors, all components of heat transfer, except for the thermal conductivity of the surrounding gas medium, should influence the temperature of the element as little as possible. In this case, the temperature dependence of the heat transfer coefficient is related to the change in the coefficient of thermal conductivity of gases, which increases with temperature increasing according to the dependence (2.75).

When analyzing thermal processes, the nonlinear dependence (2.75) in a small range of operating temperatures, by analogy with the expression (2.76), is usually replaced with a sufficient degree of accuracy by a linear one

$$\lambda = \lambda_0(1 + \beta_t t_{ag}), \quad (2.77)$$

where:

$\beta_t$  – temperature coefficient of gas thermal conductivity, 1/°C;

$t_{ag}$  – average gas temperature in the chamber, °C.

The average gas temperature in the chamber is usually defined as

$$t_{ag} = \frac{t_e + t_t}{2}. \quad (2.78)$$

The thermoresistive coefficient determines the relationship between the electrical, thermal and geometric characteristics of the element

$$b_e = R_e / \alpha_e F_e, \quad (2.79)$$

where:

$\alpha_e$  – total heat transfer coefficient of the element,  $W/(m^2 \cdot ^\circ C)$ ;

$F_e$  – surface area of the element,  $m^2$ .

The nature of dependence of the thermoresistive coefficient of a thermocouple on temperature is determined by the ratio of the temperature coefficients of resistance and thermal conductivity of the gas. It is theoretically proved [3] and experimentally confirmed [1] that in air in the range of operating temperatures of elements the thermoresistive coefficient of platinum thermistors practically does not depend on their temperature and it can be considered constant.

The temperature coefficient of thermal conductivity of methane is actually twice as high as that of air, which causes a significant dependence of the thermoresistive coefficient of platinum thermistors on temperature at high concentrations of methane. This causes temperature instability of zero of thermoconductometric gas analyzers when changing the composition of the reference gas mixture in the comparison chamber due to the violation of its tightness and methane flow through micropores, and also, leads to a change in the sensitivity of the analyzer when changing the temperature modes of operation of thermocouples and the appearance of additional measurement error. In order to exclude this error and increase the temperature stability of zero, it is necessary to choose such a mode of operation of thermocouples in the measuring bridge, which ensures that the average gas temperature in the chamber remains constant.

Taking into account a rather simple kind of relationship between the element temperature and current flowing through the element (2.75), let us first analyze the effect of gas temperature change on the temperature mode of thermocouples in the case of the bridge supply from a stable current source  $I_{br} = const$  (Fig. 2.7).

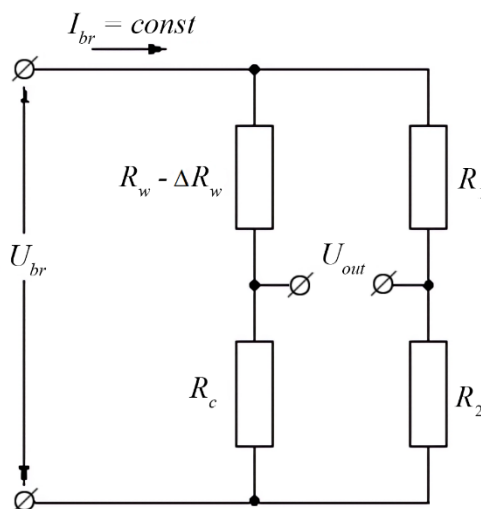


Fig. 2.7. Stable current bridge power supply circuit

Usually the resistance of ballast resistors  $R_1$  and  $R_2$  is chosen two orders of magnitude greater than the resistance of the working and comparative thermocouples  $R_w$  and  $R_c$ , and the change in the resistance of the working element in thermoconductometric methane analyzers at temperature changes of the analyzed medium does not exceed 10% of its initial value. Therefore, when the bridge is powered by a stable current source, the current flowing through the thermocouples can be considered as a constant value.

$$\Delta t_{ag} = \Delta t_t. \quad (2.80)$$

When operating methane content control devices in mine conditions, the possible range of gas temperature change is  $20 \pm 20$   $^\circ C$ . In this case, the possible value of change in the average gas temperature in the chamber is  $\Delta t_{ag} = \pm 20$   $^\circ C$ , which according to [5] causes a significant measurement error. In addition, when the bridge is powered by a constant current source, the change in the medium temperature leads to a change in the voltage

on the bridge, and when the medium temperature increases, and when it decreases so does the voltage. Similarly, the sensitivity of the bridge also changes. Thus, both factors causing instability of the analyzer sensitivity when the gas temperature changes (thermal conductivity of the medium and bridge supply voltage) act in a co-directional manner, which increases the measurement error.

Let us consider the most common case of supplying the bridge from a stable voltage source. The dependence of the voltage value on the thermocouple  $U_e$  of the thermocatalytic sensor on the current, obtained in [3], is

$$U_e = I_e R_{0e} (1 + \beta t_t) + \beta b_e R_{0e} I_e^3, \quad (2.81)$$

where:

- $I_e$  – current flowing through the thermocouple, A;
- $R_{0e}$  – resistance of the thermocouple at zero temperature, Ohm;
- $t_t$  – gas temperature, °C;
- $\beta$  – temperature coefficient of resistance of the element, 1/°C;
- $b_e$  – thermoresistive coefficient of the element, °C/A<sup>2</sup>.

Let us present equation (2.81) in the form

$$I_e^3 + p I_e + g = 0, \quad (2.82)$$

where:

$$p = \frac{1 + \beta t_t}{\beta b_e}; \quad g = \frac{U_e}{\beta b_e R_{0e}}.$$

Let's determine the discriminant of the equation (2.82)

$$\Delta = p^3 / 27 + g^2 / 4 = \frac{1}{4} \left( \frac{U_e}{\beta b_e R_{0e}} \right)^2 + \frac{1}{27} \left( \frac{1 + \beta t_t}{\beta b_e} \right)^3.$$

Since  $\Delta > 0$ , equation (2.81) has one real and two complex roots. The real root is defined as

$$I_e = \sqrt[3]{-g/2 + \sqrt{\Delta}} + \sqrt[3]{-g/2 - \sqrt{\Delta}}. \quad (2.83)$$

Finally, the expression for determining the current through the thermocouple will be as follows

$$I_e = \sqrt[3]{\frac{U_e}{2\beta b_e R_{0e}} + \sqrt{\frac{1}{4} \left( \frac{U_e}{\beta b_e R_{0e}} \right)^2 + \frac{1}{27} \left( \frac{1 + \beta t_t}{\beta b_e} \right)^3}} + \sqrt[3]{\frac{U_e}{2\beta b_e R_{0e}} - \sqrt{\frac{1}{4} \left( \frac{U_e}{\beta b_e R_{0e}} \right)^2 + \frac{1}{27} \left( \frac{1 + \beta t_t}{\beta b_e} \right)^3}}. \quad (2.84)$$

Substituting the above dependence of the current value on voltage into equation (2.75), we obtain an expression that allows us to determine the temperature of the element when the gas temperature changes for the case of supplying the bridge from a voltage source

$$t_e = t_t + b_e \left[ \sqrt[3]{\frac{U_e}{2\beta b_e R_{0e}} + \sqrt{\frac{1}{4} \left( \frac{U_e}{\beta b_e R_{0e}} \right)^2 + \frac{1}{27} \left( \frac{1 + \beta t_t}{\beta b_e} \right)^3}} + \sqrt[3]{\frac{U_e}{2\beta b_e R_{0e}} - \sqrt{\frac{1}{4} \left( \frac{U_e}{\beta b_e R_{0e}} \right)^2 + \frac{1}{27} \left( \frac{1 + \beta t_t}{\beta b_e} \right)^3}} \right]. \quad (2.85)$$

Expression (2.85) is rather difficult to analyze. However, it shows that in this case the temperature of the analyzed gas affects the element temperature less than in the previous case. The reason for this is that at constant voltage the increase in element resistance due to the growth of the medium temperature leads to a decrease in the current through the element. Taking into account the quadratic dependence of the power released on the element on the current value, this reduces the additional heating of the element. When the ambient temperature decreases, the resistance of the element decreases, the current increases and the additional heating of the element increases. In this case the autostabilization properties of the circuit are manifested.

Numerical analysis of expression (2.84), performed by substituting real values of quantities, shows that the change in the temperature of the element when the gas temperature changes is about three times less than in the previous case, and the change in the average gas temperature in the chamber is

$$\Delta t_{ag} \approx \frac{2}{3} \Delta t_t. \quad (2.86)$$

In [3], an approximate expression describing the element temperature change when the gas temperature and supply voltage change was obtained

$$t_e = \frac{1}{3} t_t - \frac{2}{3} \beta + \sqrt[3]{\frac{b_e U_e^2}{\beta^2 R_{0e}^2}}. \quad (2.87)$$

It also follows from expression (2.87) that at a constant value of voltage  $U_e$  on the element, the change in its temperature is practically 1/3 of the change in gas temperature, which confirms the validity of expression (2.86). From the position of temperature modes of elements, the circuits of bridge supply with voltage stabilization on the working or on the comparative thermocouple do not differ from the considered case of bridge supply from the source of stable voltage. Therefore, expression (2.86) is also valid for these power supply circuits.

If we choose the previously considered power supply mode of the measuring bridge of the thermoconductometric sensor with stabilization of the resistance value of the working element

$$R_e = U_e / I_e = \text{const}. \quad (2.88)$$

Since the platinum thermocouple resistance unambiguously depends on its temperature, its stabilization ensures the constancy of the temperature mode of the element  $t_e = \text{const}$  regardless of the environmental conditions. The change of the average gas temperature in the chamber among all considered variants will be minimal in this case and will amount to  $\Delta t_{ag} = 0.5 \Delta t_g$ . Besides, in this case the voltage on the bridge decreases when the gas temperature increases, and vice versa. That is, the factors causing instability of the analyzer sensitivity when the gas temperature changes act in different directions, which reduces the measurement error.

In the absence of methane, temperature stabilization of one of the elements automatically provides temperature stabilization of the other. When stabilizing the resistance of the working element of the thermoconductometric sensor, the increase in methane concentration leads to an increase in current, an increase in the temperature of the comparative element and voltage on the bridge. When stabilizing the resistance of the comparative element and increasing methane concentration, the current through the elements and voltage on the comparative

element remain constant, and the temperature of the working element decreases, the voltage value on this element and on the bridge as a whole decreases.

Obviously, the temperature stability of the elements in the absence of methane does not provide high stability of the bridge zero due to the change of the bridge voltage with the change of the gas medium temperature. However, when using the bridge balancing proposed in [10, 11], which ensures the identity of voltampere characteristics of thermocouples, this disadvantage is completely eliminated, and when the bridge operates in the mode of stabilizing the resistance of the working element, a significant increase in the quality of both the measuring bridge and metrological characteristics of thermoconductometer methane analyzers as a whole is provided.

## 2.5. Conclusions

The following conclusions can be drawn based on the completed research:

1. The known analytical dependences describing the process of heat removal from the thermocouple include the value of thermal conductivity of the gas mixture at the average temperature in the chamber, which itself is a function of the temperature of the element, which leads to significant errors in determining the temperature modes of operation of thermosensitive elements.

2. The obtained analytical dependences, unlike the known ones, include the thermal conductivity of the medium at zero temperature and the temperature coefficient of change of thermal conductivity, and also take into account the processes of heat dissipation by radiation and heat conduction through the current-supplying ends of thermocouples. This makes it possible to significantly increase the accuracy of calculation of thermocouple parameters and to determine the influence of various factors on metrological and operational characteristics of analyzers at the stage of sensor development.

3. One of the reasons for the unstable operation of existing thermoconductometric gas analyzers with an insulated comparative element is the change of gas composition in the comparative chamber due to the flow of gases from the surrounding mixture through micropores and cracks. Ambiguity of temperature dependence of thermal conductivity coefficients of air and methane, can lead to the appearance of significant temperature errors of thermoconductometric gas analyzers, so when selecting modes of operation of thermoconductometric sensors measuring bridges are necessary to ensure a more stable temperature mode of thermocouples when changing the temperature of the medium.

4 The analysis of operation of two-chamber symmetric thermoconductometric sensors when the measuring bridge is powered by stable voltage and current sources, as well as when the voltage on one of the sensitive elements is stable, has shown that the maximum sensitivity is provided when the voltage on the working element is stable (by 5% higher compared to the typical inclusion circuit – supplying the bridge with stable voltage). Sensitivity of bridge circuits with thermoconductometric sensors at stabilization of voltage on the comparative element or supplying the bridge from a stable current source is slightly lower in comparison with the typical inclusion circuit (by 5%). For all the considered variants of power supply the nonlinearity of dependence of the measuring bridge output signal on methane concentration is characteristic, and the minimum nonlinearity is observed at application of the circuit with voltage stabilization on the working element. Without taking measures to linearize the scale in thermoconductometric methane analyzers in case of application of such a circuit, the reduced measurement error in the middle part of the measurement range reaches 8%, which is significantly lower than in case of the typical inclusion circuit.

5. The most preferable among all considered modes of operation of the measuring bridge is the mode with stabilization of resistance of the working element. In contrast to the bridge power supply modes traditionally used in analyzers, it provides a significant increase in sensitivity and is characterized by almost linear dependence of the measuring bridge output signal on methane concentration. Stable temperature value of thermocouples in thermoconductometric methane sensors at changing parameters of the controlled gas medium is provided only when using the bridge operation mode with stabilization of element resistance.

6. The analysis of different bridge circuit operation modes of thermoconductometric methane analyzers has shown that among the considered inclusion circuits the highest sensitivity and the lowest nonlinear dependence of the bridge output voltage on methane concentration is provided by the inclusion circuit with voltage stabilization on the working element. Taking into account that such inclusion circuit provides the most stable

temperature mode of thermocouples in bridge circuits when the ambient temperature changes, it allows us to recommend it for use in methane analyzers instead of traditionally used inclusion circuits with voltage stabilization on the measuring bridge. To ensure high zero stability, it is necessary to carry out additional balancing of the bridge, excluding zero shift at voltage fluctuations on the bridge.

## References

- [1] Holinko V.I., Kotlyarov A.K., Belonozhko V.V. (2004) *Control of explosion hazard in mine workings* D.: Nauka i Obrazovanie [in Russian]
- [2] Mikheev M.A., Mikheeva I.M. (1977) *Fundamentals of heat transfer* M.: Energia [in Russian]
- [3] Karpov E.F., Birenberg I.E., Basovsky B.I. (1984) *Automatic gas protection and mine atmosphere control*. M.: Nedra [in Russian]
- [4] Pavlenko V.A. (1965) *Gas analyzers* M.-L.: Mashinostroenie [in Russian]
- [5] Holinko, V.I.; Kotlyarov, A.K.(2006) *Improving the accuracy of methane content control in coal mine degasification pipelines: materialy mizhnarodnoyi naukovo-praktychnoyi konferentsiyi "Forum Girnikiv"* (pp. 142-148) [in Russian]
- [6] Holinko, V.I.; Kotlyarov, A.K.(2006) Theoretical substantiation of thermoconductometric methane sensor parameters with non-isolated comparative element. *Collection of scientific articles of NSU*, 26, 60-67 [in Russian]
- [7] Holinko V.I., Kotlyarov A.K. (2006) Study of heat exchange process in thermoconductometric methane sensors / Ways and means of creating safe and healthy working conditions in coal mines. *Collection of scientific articles*, 18, 301-314. Makeevka-Donbass: MakNII [in Russian]
- [8] Kotlyarov, A.K. (2006) Substantiation of bridge circuits operation modes of thermoconductometric methane analysers. *Naukovy visnik NSU*, (11), 62-65 [in Russian]
- [9] Reid R.C., Sherwood T.K.(1964) *The properties of gases and liquids* M.: Gostopizdat [in Russian]
- [10] Holinko, V.I., Belonozhko V.V. (2003) Improving thermocatalytic means of methane content control. *Girnycha Elektromechanika ta automatika*, (70), 92-100 [in Russian]
- [11] Tabachenko, M., Saik, P., Lozynskyi, V., Falshtynskyi, V., ... Dychkovskyi, R. (2016). Features of setting up a complex, combined and zero-waste gasifier plant. *Mining of Mineral Deposits*, 10(3), 37-45. doi:10.15407/mining10.03.037

### 3. Theory development of control methods of methane content in gas mixtures

#### 3.1. Theoretical evaluation of methane analyzer errors from unmeasured components of mine atmosphere

Among the components of the mine atmosphere that have a significant impact on the readings of methane analyzers, first of all, water vapor and carbon dioxide, as well as hydrogen and carbon monoxide, which may be present in significant quantities in mine air under emergency conditions. All of the above gases, as well as water vapor, differ significantly in their thermophysical properties from those of air. Among such properties of gases, first of all, it concerns thermal conductivity, the change of which can lead to significant measurement errors of methane thermoconductometer analyzers.

In [1], the theoretical evaluation of the errors of the thermal conductivity sensor from unmeasured components for mine operating conditions was made on the basis that the thermal conductivity of the mixture obeys the additive law and the electrical properties of molecules and the influence of the difference in molecular weights of components were not taken into account. The phenomenon of thermal conductivity in a gas mixture is still insufficiently studied, and the known methods of calculation are imperfect. However, there is [2] a good convergence of the results of theoretical and experimental studies of the thermal conductivity of a gas mixture, and it was found that a significant deviation of thermal conductivity from the law of additivity is observed for mixtures whose components differ significantly in molecular weight (i.e., contain hydrogen or helium) or polarity (i.e., contain water vapor). To calculate the thermal conductivity of a gas mixture, based on the thermal conductivity of pure gases, let us use Vasilieva's formula [2]

$$\lambda_{tc} = \frac{\lambda_1}{1 + A_{12} \frac{x_2}{x_1} + A_{13} \frac{x_3}{x_1} + \dots} + \frac{\lambda_2}{1 + A_{21} \frac{x_1}{x_2} + A_{23} \frac{x_3}{x_2} + \dots} + \dots, \quad (3.1)$$

where:

- $\lambda_{tc}$  – thermal conductivity coefficient of the mixture, W/m·°C;
- $\lambda_1, \lambda_2, \dots$  – thermal conductivity coefficients of the mixture components, W/m·°C;
- $x_1, x_2, x_3, \dots$  – mole (volume) fractions of the mixture components;
- $A_{12}, A_{13}, A_{21}$  – coefficients depending on the nature of the gases forming the mixtures.

We determine the values of coefficients A using the Sutherland formula adjusted by Lindsay and Bromley:

$$A_{12} = \frac{1}{4} \left\{ 1 + \left[ \frac{\mu_1 \left( \frac{M_2}{M_1} \right)^{0.75} \frac{1 + \frac{C_1}{T}}{1 + \frac{C_2}{T}}}{1 + \frac{C_2}{T}} \right]^{0.5} \right\}^2 \frac{1 + \frac{C_{12}}{T}}{1 + \frac{C_2}{T}}, \quad (3.2)$$

where:

- $\mu_1, \mu_2$  – viscosity of pure gas components, m<sup>2</sup>/s;
- $M_1, M_2$  – molecular masses;
- $C_1, C_2$  – constants in the Sutherland equation (one can take  $C \approx 1.5 T_b$ , where  $T_b$  – boiling point, K);
- $C_{12} = f \sqrt{C_1 C_2}$ , and both gases are either both polar or non-polar and  $f = 0.733$ , if one of the gases consists of non-polar molecules and the second consists of highly polar ones.

Substituting the reference data from [2] into equations (3.1) and (3.2), we determine the values of heat transfer coefficients of the following mixtures: methane – air, air – water vapor, methane – air – water vapor, methane – air – carbon dioxide at the sensor filament temperatures of 60, 120, 210, 320 and 400 °C. Calculation results are given in Tables 3.1 – 3.4. During the calculation, the average temperature of the mixture in the sensor chamber was determined by the formula

$$t_{tc} = \frac{t_e + t_c}{2}, \quad (3.3)$$

where:

$t_e$  – temperature of the thermocouple, °C;

$t_c$  – temperature of the chamber walls, which we take as 20 °C.

Table 3.1

Results of calculation of the heat transfer coefficient of methane – air mixture

Volume fraction of mixture component	$x_1$ (CH <sub>4</sub> )	0.0	0.01	0.05	0.2	0.4	0.6	0.8	1.0
	$x_2$ (air)	1.0	0.99	0.95	0.8	0.6	0.4	0.2	0.0
Coefficient of thermal conductivity of the mixture $\lambda \cdot 10^3$ W/m·°C, at the temperature of the thermocouple, °C	60	26.90	26.998	27.387	28.826	30.698	32.517	34.282	36.00
	120	29.20	29.319	29.796	31.559	33.857	36.095	38.276	40.40
	210	32.65	32.807	33.431	35.745	38.766	41.714	44.591	47.40
	320	36.60	36.810	37.646	40.757	44.839	48.848	52.784	56.65
	400	39.40	39.652	40.667	44.437	49.389	54.257	59.044	63.75

Table 3.2

Results of calculation of heat transfer coefficient of the mixture: air – water vapor

Volume fraction of mixture component	$x_1$ (air)	0.97	0.94	0.9	0.7	0.6	0.4	0.0
	$x_2$ (water vapor)	0.03	0.06	0.1	0.3	0.4	0.6	1.0
Coefficient of thermal conductivity of the mixture $\lambda \cdot 10^3$ W/m·°C, at the temperature of the thermocouple, °C	60	26.991	27.057	27.108	26.794	26.320	24.840	20.10
	120	29.303	29.381	29.447	29.194	28.737	27.244	22.30
	210	32.838	32.917	33.018	33.018	32.647	31.265	26.25
	320	36.859	37.090	37.356	37.999	37.920	37.030	32.60
	400	39.822	40.214	40.690	42.312	42.678	42.587	39.40

Table 3.3

Results of calculation of the heat transfer coefficient of the mixture: methane – air – water vapor

Volume fraction of mixture component	$x_1$ (CH <sub>4</sub> )	0.01	0.05	0.1	0.2	0.4	0.8	0.9
	$x_2$ (air)	0.93	0.89	0.84	0.74	0.54	0.14	0.04
	$x_3$ (water vapor)	0.06	0.06	0.06	0.06	0.06	0.06	0.06
Coefficient of thermal conductivity of the mixture $\lambda \cdot 10^3$ W/m·°C, at the temperature of the thermocouple, °C	60	27.164	27.541	28.021	28.970	30.829	34.389	35.248
	120	29.499	29.974	30.563	31.729	34.016	38.414	39.478
	210	33.073	33.695	34.469	36.003	39.015	44.822	46.230
	320	37.299	38.136	39.180	41.244	45.323	53.315	55.200
	400	40.468	41.481	42.889	45.25	50.201	59.852	62.214

Table 3.4

Results of heat transfer coefficient calculation of the mixture: methane – air – carbon dioxide

Volume fraction of mixture component	$x_1$ (CH <sub>4</sub> )	0.01	0,05	0.1	0.2	0.4	0.8	0.9
	$x_2$ (air)	0.97	0.93	0.88	0.78	0.58	0.18	0.08
	$x_3$ (CO <sub>2</sub> )	0.02	0.02	0.02	0.02	0.02	0.02'	0.02
Coefficient of thermal conductivity of the mixture $\lambda \cdot 10^3$ W/m·°C, at the temperature of the thermocouple, °C	60	26.769	27.155	27.627	28.583	30.439	33.997	34.854
	120	29.094	29.565	30.153	31.315	33.595	37.981	39.042
	210	32.584	33.204	33.972	35.501	38.499	44.283	45.686
	320	36.605	37.436	38.470	40.525	44.579	52.470	54.399
	400	39.465	40.472	41.725	44.216	49.135	58.728	61.076

Analysis of the data of Tables 3.1 and 3.4 shows that with increasing temperature of the sensor filament, the thermal conductivity coefficients of methane – air and methane – air – water vapor mixtures do not become

commensurable. On the contrary, the difference in the thermal conductivity coefficients increases, with the thermal conductivity coefficient of the methane – air – water vapor mixture being greater than the thermal conductivity coefficient of the methane – air mixture. To select a rational operation temperature mode of the thermoconductometric sensor, providing the minimum measurement error, we will quantitatively assess the influence of water vapor and carbon dioxide on the output signal of the bridge with a thermoconductometric methane sensor.

The value of the output signal of the unbalanced bridge with a thermoconductometric methane sensor depends on the power supply mode of the bridge, parameters and temperature mode of the sensor, temperature and thermal conductivity of the mixture, temperature coefficients of resistance of thermocouples and thermal conductivity of gases, as well as other factors. Let us evaluate the influence of these gases on the output signal of the bridge for the case of voltage stabilization on the working element of the sensor. In this case, the expression for determining the output signal for the given variant of the bridge power supply will be determined by substituting into equation (2.45) the values of the corresponding voltage values from expressions (2.48) and (2.50). After conversion we obtain

$$U_{out}^b = \frac{U_{br} \cdot R_0 \beta}{4(b\lambda_a - R_0 \beta)} \cdot \frac{\lambda_{tc} - \lambda_a}{\lambda_{tc}}. \quad (3.4)$$

Let us represent expression (3.4) in the form

$$U_{out}^b = K \cdot \frac{\lambda_{tc} - \lambda_a}{\lambda_{tc}}, \quad (3.5)$$

where:

$K$  – coefficient depending on the sensor's design, characteristics of the thermocouple and power supply;  
 $\lambda_a, \lambda_{tc}$  – thermal conductivity of air and analyzed mixture at the temperature determined by the formula (3.3).

The relative error of a thermal conductivity sensor can be summarized:

$$\delta U_{out} = \frac{U_{out} - U_{out_0}}{U_{out_0}} \cdot 100\%, \quad (3.6)$$

where:

$U_{out}$  – output signal of the methane sensor taking into account the influencing factor;  
 $U_{out_0}$  – output signal of the sensor in the methane – air mixture.

Relative and reduced measurement errors of the thermal conductivity sensor taking into account equations (3.5) and (3.6), respectively, will be:

$$\delta U_{out} = \frac{\lambda_a (\lambda_{tc2} - \lambda_{tc1})}{\lambda_{tc2} (\lambda_{tc1} - \lambda_a)} \cdot 100\%; \quad (3.7)$$

$$\delta U_{ap} = \frac{\lambda_a \lambda_{CH_4} (\lambda_{tc2} - \lambda_{tc1})}{\lambda_{tc1} \lambda_{tc2} (\lambda_{CH_4} - \lambda_a)} \cdot 100\%, \quad (3.8)$$

where:

$\lambda_a, \lambda_{tc1}, \lambda_{tc2}, \lambda_{CH_4}$  – thermal conductivity coefficients of air, methane – air mixture, methane – air – unmeasured component and methane, respectively.

Substituting the data from Tables 3.1 – 3.4 into equation (3.8) we see that the theoretical relative error of methane measurement by the thermal conductivity sensor at the maximum volume fraction of water vapor

equal to 6% (based on the operating conditions of mine gas analyzers) is in the range from 0.86 to 3.86%, and the error increases with increasing sensor filament temperature. At the volume fraction of CO<sub>2</sub> in the analyzed mixture equal to 2% the relative error of methane measurement is from 1.14 to 3.37% and decreases with increasing temperature of the sensor filament. The calculation results are summarized in Tables 3.5 and 3.6.

Table 3.5

Theoretical error of measurement from water vapors at their volume fraction of 6%

Element temperature, °C	Measurement error at methane volume fraction, %							
	0.01	0.02	0.05	0.2	0.4	0.6	0.8	0.9
60	2.41	2.25	2.16	1.83	1.47	1.18	0.96	0.86
120	2.2	2.17	2.09	1.79	1.45	1.20	0.99	0.90
210	2.57	2.55	2.46	2.10	1.72	1.44	1.21	1.11
320	3.68	3.64	3.54	2.99	2.46	2.06	1.80	1.62

Table 3.6

Theoretical error of measurement from carbon dioxide at its volume fraction of 2 %

Element temperature, °C	Measurement error at methane volume fraction, %							
	0.01	0.02	0.05	0.2	0.4	0.6	0.8	0.9
60	-3.37	-3.34	-3.32	-3.15	-2.95	-2.78	-2.61	-2.55
120	-2.78	-2.77	-2.75	-2.60	-2.43	-2.26	-2.14	-2.08
210	-2.19	-2.17	-2.15	-2.02	-1.83	-1.75	-1.64	-1.61
320	-1.57	-1.57	-1.54	-1.45	-1.35	-1.26	-1.17	-1.14

Analysis of the data in Tables 3.5 and 3.6 shows that it is impossible to exclude the influence of water vapor and carbon dioxide by selecting the temperature of sensitive elements of the thermoconductometric sensor, as proposed in [3], but it is possible to establish a rational thermal mode of operation of the sensor, providing a minimum measurement error from the presence of water vapor and carbon dioxide in the analyzed mixture.

The results of studies of explosive properties of methane – air mixtures show that with increasing moisture content of a methane – air mixture, the lower concentration threshold of its explosivity for methane increases, and the upper threshold decreases [4]. The upper explosivity threshold at the maximum possible for the conditions of operation of gas analyzers at volume fraction of water vapor 6% decreases by 1.5% vol. of methane compared to the explosivity threshold of dry mixtures. The lower explosive threshold under the same conditions is increased by 0.75% vol. of methane.

Comparison of the obtained data on the change of the upper explosivity threshold of methane – air mixture and data on the influence of water vapor on the output signal of thermoconductometric sensors shows that in the area of the upper threshold with the growth of mixture humidity its thermal conductivity and the analyzer output signal increase, while the value of the upper explosivity threshold decreases. As seen, due to the presence of measurement error caused by the influence of moisture on the thermal conductivity of the mixture, at the maximum volume fraction of water vapor of 6% and triggering the protection on the upper concentration limit, the actual volume fraction of methane in the mixture will be about 23%. At the same time, at this moisture content, the explosive threshold decreases by 1.5% vol. and the safety margin provided for by the normative documents [5] remains practically unchanged.

Consequently, from the point of view of ensuring the safety of the process of disposal of methane - air mixtures captured by mine degasification systems, methane content measurement error due to changes in the moisture content of the mixture can be ignored when controlling the explosive hazard of mixtures by thermoconductometric gas analyzers. Excluding this error component allows to reduce the main measurement error of the upper explosivity threshold of methane – air mixture and subsequently to revise the requirements of regulatory documents [5] regarding the reduction of the upper value of the unacceptable volume fraction of methane in gas mixtures during disposal while maintaining the existing safety reserve.

As can be seen from Table 3.6, thermoconductometric methane sensors that operate at the temperature of sensitive elements up to 120 °C have a large measurement error from carbon dioxide. Increasing the temperature of the sensitive elements above 300 °C, as experimental studies have shown, is undesirable, since oxidation of methane is observed on them. For this reason, as well as to ensure the cost-effectiveness of the sensor, the temperature of the sensitive elements of the thermoconductometric sensor should be taken in the range of 210-250 °C.

Let us evaluate the influence of carbon monoxide and hydrogen on the output signal of the thermal conductivity sensor, which may appear in the mine atmosphere under emergency conditions. The thermal conductivity coefficients of carbon monoxide and air are insignificantly different from each other. Therefore, the reduced measurement error of the thermal conductivity sensor, determined by the formula (3.8), at the volume fraction of carbon monoxide 1% in the analyzed methane – air mixture is 0.1%, which is insignificant.

The thermal conductivity coefficients of hydrogen and air differ significantly from each other. Calculations of the thermal conductivity of a mixture of gases containing hydrogen, carried out according to Brokaw's formula, and determination of the measurement error at a hydrogen volume fraction of 1% in a methane – air mixture, showed that the output signal of the thermal conductivity sensor at a hydrogen volume fraction of 1% is 7-8 times greater than at the same volume fraction of methane.

It follows that the maximum possible volume fraction of hydrogen 1% in the gas mixture, due to the presence of measurement error caused by its effect of hydrogen on the thermal conductivity of the mixture, when the protection is triggered by the upper concentration limit, the actual volume fraction of methane in the mixture will be about 18%. In turn, at such a volume fraction of hydrogen, the upper explosivity threshold of the mixture changes insignificantly, which at first glance, leads to a decrease in the safety margin stipulated by regulatory documents [5].

At the same time, the appearance of hydrogen in the mine atmosphere is observed only under emergency conditions, when combustion proceeds under oxygen deficiency, which significantly reduces the explosive properties of mixtures and the upper concentration limit of explosivity for methane. In addition, in these conditions in the gas mixture carbon dioxide is always present, the volume fraction of which in the presence of hydrogen in the mixtures is not less than 10%. The volume fraction of carbon dioxide 10% leads to a significant decrease in thermal conductivity of the mixture. Based on Table 3.6, when the protection is triggered by the upper concentration limit and the volume fraction of carbon dioxide is 10%, the actual volume fraction of methane in the mixture will be about 35%, which fully compensates for the reduction in the safety margin due to the presence of hydrogen.

It follows from the above that the effect of hydrogen on the means of explosion hazard control of gas mixtures in degassing pipelines can be disregarded. The presence of carbon dioxide in the gas mixtures leads to an increase in the safety reserve provided for by regulatory documents [5], which is undesirable when using co-opted gas mixtures as fuel, because it leads to an increase in the volume of forced discharge of substandard mixtures through candles into the atmosphere and deterioration of economic indicators of equipment operation. Therefore, in order to reduce losses at control of explosion hazard of gas mixtures in degassing systems it is advisable to control the volume fraction of carbon dioxide in mixtures used for energy purposes and to adjust the readings of methane analyzers depending on the content of CO<sub>2</sub> in the utilized mixture.

### **3.2. Justification of the thermoconductometric method of control using different thermal modes of sensing elements**

Both domestic and foreign conductometric methane analyzers have two chambers with identical thermocouples, working and comparison chambers. The analyzed gas mixture enters the working chamber due to free or forced convection, while the comparison chamber is hermetically sealed and filled with reference gas. Such design of analyzers provides sufficient stability of zero of measuring bridge at change of ambient temperature and power supply parameters, however, does not eliminate the influence of humidity, pressure, carbon dioxide content and other components on measurement results, and also causes relatively long duration of transient processes at change of temperature of analyzed mixture. Besides, when operating the analyzers, there are difficulties in ensuring the tightness of the comparison chamber, which leads to zero shift of the measuring bridge. This causes instability of “zero” of analyzers, relatively large error of measurement, the need for regulation and adjustment at the place of installation, regular maintenance and supervision of such gas analyzers.

These disadvantages can be partially eliminated by using the proposed single-chamber thermoconductometric sensor with unequal electrothermal parameters of sensing elements [6]. However, the issues of selecting the parameters of thermoelements, design and modes of operation of such a sensor have not been sufficiently justified to date.

In general, the difference in thermal modes of the sensing elements can be achieved by various methods, such as making the elements with different resistance or different sizes, shunting one of the elements, etc. Let's consider a variant of a single-chamber sensor with sensing elements having approximately the same resistance, but differing significantly in their sizes. This is ensured, for example, by the use of platinum microwires of different diameters for manufacturing the spirals of pelistor-type thermocouples. Taking into account the fact that at operating temperature the less heated element will have a significantly lower resistance for symmetrization of the bridge in series with it, it is advisable to introduce an additional resistance  $R_{add}$ . The circuit of such a bridge is shown in Fig. 3.1.

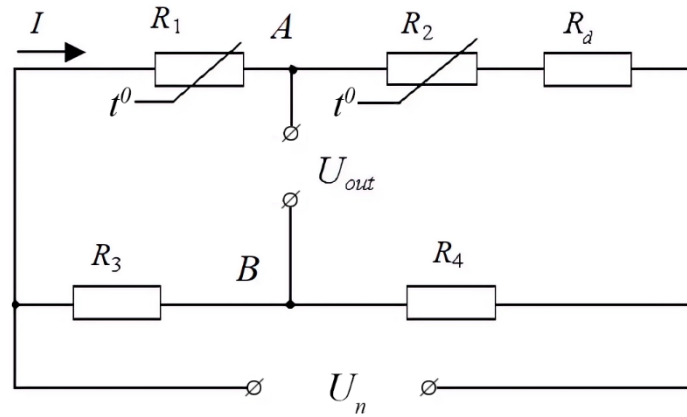


Fig. 3.1. Bridge circuit with thermocouples of significantly different sizes:  $R_1, R_2$  – thermocouples;  $R_{add}$  – additional resistor;  $R_3, R_4$  – ballast resistors

Based on the theoretical dependence of the voltage value on the thermocouple on the current value (2.71), the voltage value on the thermocouple of the sensor  $R_1$  with a higher initial heating temperature will be

$$U_1 = IR_{01}(1 + \beta t_t) + \beta b_1 R_{01} I^3. \quad (3.9)$$

Accordingly, the voltage on the second bridge arm with additional resistance

$$U_2 = IR_{02}(1 + \beta t_t) + \beta b_2 R_{02} I^3 + IR_d. \quad (3.10)$$

In [1] it was theoretically proved that in air in a wide temperature range the thermoresistive coefficient of platinum thermistors is a constant value. This was confirmed by subsequent experimental studies [7]. In this case, if the resistance value of the additional and ballast resistors is independent of the temperature, the condition of zero conservation of a symmetrical balanced bridge from changes in the ambient temperature will be

$$\frac{dU_1}{dt_t} = \frac{dU_2}{dt_t}. \quad (3.11)$$

Having differentiated the right parts of equations (3.9) and (3.10), we obtain the condition of independence of zero of the balanced bridge from temperature change when the measuring bridge is powered by a stable current source

$$R_{01} = R_{02}. \quad (3.12)$$

It follows from the last expression that to ensure temperature stability of the bridge of the thermoconductometric sensor with unequal electrothermal parameters of the sensing elements it is necessary

to use platinum thermistors with the same initial resistance.

As a rule, the measuring bridges of thermoconductometer analyzers are powered by a stable voltage or current source. However, slight variations of the supply voltage are not excluded in case of significant fluctuations of the supply voltage, temperature and other reasons. The condition of zero conservation of a symmetrical balanced bridge (with  $R_3 = R_4$ ) under possible changes of current through thermocouples is

$$\frac{dU_1}{dI} = \frac{dU_2}{dI}. \quad (3.13)$$

Taking into account the equality of initial resistances of thermocouples, we replace  $R_{01}$  and  $R_{02}$  by  $R_0$  and differentiate the right parts of equations (3.9) and (3.10) by current to obtain

$$3\beta b_1 R_0 I^2 = 3\beta b_2 R_0 I^2 + R_d. \quad (3.14)$$

From the expression (3.14) we find the value of additional resistance, at which the stability of zero of the balanced bridge is provided at change of current through thermistors

$$R_d = 3\beta R_0 I^2 (b_1 - b_2). \quad (3.15)$$

Substituting into equation (3.16) the value of  $b_e$  from (3.15), we obtain

$$R_d = 3\beta R_0 I^2 \left( \frac{R_1}{\alpha_1 F_1} - \frac{R_2}{\alpha_2 F_2} \right), \quad (3.16)$$

where:

$R_1, R_2$  and  $\alpha_1, \alpha_2$  – resistance and total heat transfer coefficient of the first and second thermocouples at their initial heating temperature Ohm and  $W/(m^2 \cdot ^\circ C)$ ;

$F_1, F_2$  – surface area of the first and second element respectively,  $m^2$ .

Based on the obtained expressions, the additional resistance value was calculated for different variants of execution of sensitive elements of the thermoconductometric sensor. So, at application for manufacturing of spirals of working and comparative thermocouples of platinum microwire with diameter 30 microns and 50 microns respectively, at the ratio  $F_1 = 0.2F_2$ , initial resistance of elements  $R_0 = 30$  m and current through thermocouples 100 mA the calculated value of additional resistance is  $R_d = 1.80$  m. For the limiting case, at  $F_1 \ll F_2$ , the value of additional resistance is  $R_d = 3.60$  m.

The value of the total heat transfer coefficients of thermocouples at the temperature of their initial heating was determined based on the values of thermoresistive coefficients calculated from the results of experimentally measured values of electrical parameters of the elements according to the expression

$$b_e = \frac{U_e - I_e R_{0e} (1 + \beta t_t)}{\beta R_{0e} I_e^3}. \quad (3.17)$$

The introduction of additional resistors of the calculated value into the measuring bridge predetermines its asymmetry, which increases with the ambiguity of the thermocouple parameters. In this case, when setting the zero of the bridge by changing the value of ballast resistors and the inequality of the values of resistances  $R_3$  and  $R_4$ , the condition (3.13) is not valid. This indicates that when choosing an additional resistance according to expression (3.17), the balanced asymmetrical bridge does not provide stability of zero at small possible changes of power supply parameters. Let us show this clearly. Fig. 3.2 shows the voltampere characteristics of the bridge arms with the calculated additional resistance for the case  $F_1 = 0.2F_2$ , as well as the dependence of the voltage difference on the specified bridge arms on the current value.

It is obvious that condition (3.13) is fulfilled at the value of current through thermocouples, where characteristics 1 and 2 have the same slope. This corresponds to points *b* and *c* in Fig. 3.2. At the same time it is possible to balance the bridge at symmetry of the ballast branch of the bridge only at the value of the current through the thermocouples corresponding to point *a*, i.e. the point of intersection of curves 1 and 2. The steepness of the difference characteristic 3 at such a value of current (at point *e*) reaches a significant value, and this entails instability of zero-readings of the balanced bridge at possible changes in the bridge power supply parameters, for example, at changes in voltage losses in the electrical conductors connecting the remote sensor with the measuring transducer.

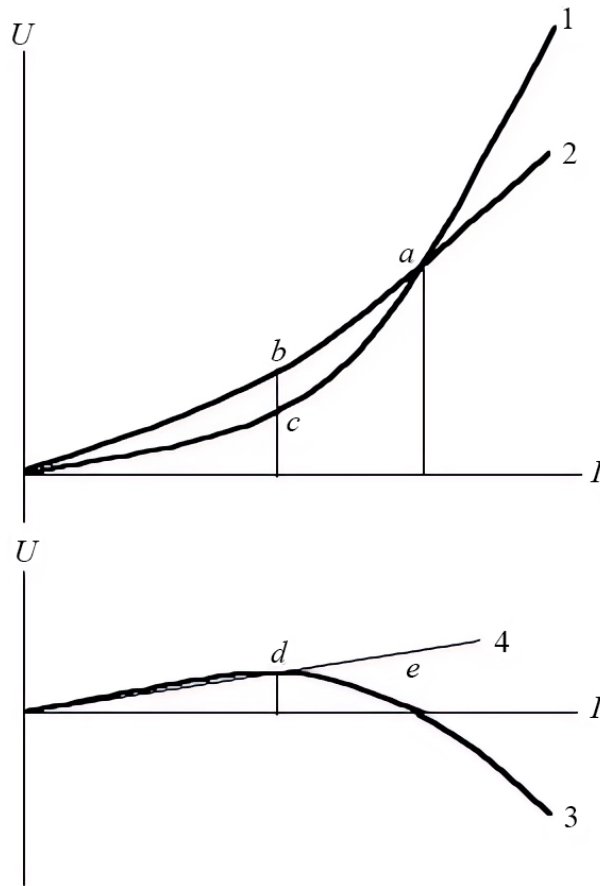


Fig. 3.2. Voltampere characteristics of bridge elements: 1 – thermocouple  $R_1$ ; 2 – bridge arm with  $R_2$  and additional resistance  $R_{add}$ ; 3 – difference curve  $\Delta U_e = U_1 - U_2$ ; 4 – difference curve of the asymmetrical bridge arm with ballast resistors

If the asymmetrical balanced bridge is chosen, then at the inequality of resistance of ballast resistors  $R_3 < R_4$  the difference curve of the arm with ballast resistors 4 appears, the slope angle that depends on the degree of asymmetry of the bridge. In this case, the selection of the ballast resistors value, considering the bridge balance at the point *e*, corresponding to the inflection point of the difference characteristic 3, does not provide high stability of zero-readings of the balanced bridge at possible changes of its power supply parameters. In this case, in order to increase the stability of the bridge zero, it is necessary to shift the operating point to the area of smaller currents, where the value of the slope angle of curves 3 and 4 is not very different. However, in this case the sensitivity of the analyzer is very low and therefore this mode of its operation is unacceptable. To ensure the stability of the analyzer zero at possible changes of the thermocouple power supply parameters and selection of the power supply mode corresponding to point *e*, it is possible to use for compensation of the difference voltage of the bridge with a symmetrical ballast branch precision sources of the reference voltage, the value of which corresponds to the voltage at point *A* (see Fig. 3.1) at the selected power supply mode of the thermocouples.

The second option is the use of an unbalanced measuring bridge with a symmetrical ballast branch, the mode of operation of which is selected from the condition of ensuring the same steepness of characteristics of the working branch of the bridge 1 and 2, which corresponds to point *e* on the difference characteristic 3. The zero

methane concentration will correspond to the voltage at point e of the difference characteristic 3. Such a mode can be realized using modern precision sources of reference voltage and microprocessors for processing the output signal of the measuring bridge. The final choice requires experimental studies and also depends on the convenience of the analyzer adjustment in the process of manufacturing, operation and the possibility of software implementation of the adjustment process automatically.

As shown in [7], it is practically impossible to achieve absolute identity of thermoelements and in case of using sensors with symmetric elements. Fig. 3.3 shows the nature of dependence of the bridge output voltage with identical thermoelements, balanced at  $U_{comp}$ , on the supply voltage in the zone close to  $U_{comp}$ . In case of non-identity of any parameter of thermistors, for example their resistances, the change of conditions under which the zero of the bridge was established, for example the supply voltage of the bridge, always leads to the appearance of voltage at its output, and the polarity of this voltage is ambiguous. The thermocouple inclusion circuit and the method of bridge balancing, proposed in [7], allows us to significantly reduce the zero drift.

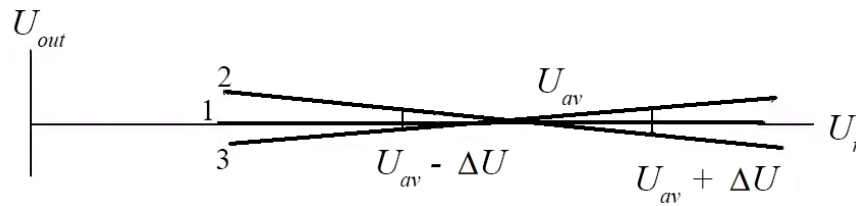


Fig. 3.3. Dependence of the bridge output voltage balanced at  $U_{av}$ , on the supply voltage:  
1 – ideal; 2 – at  $R_k > R_w$ ; 3 – at  $R_w > R_k$

In our case, when using a non-isolated comparative element and using a balanced asymmetrical bridge, the nature of dependence of the output voltage of the bridge balanced at  $U_{comp}$ , on the supply voltage is unambiguous but does not change its quality. Therefore, the solutions providing the increase of zero stability, which are proposed can be used in the development of analyzers with a non-isolated comparative element.

As a result, we can conclude that the use of a single-chamber thermoconductometric sensor with unequal electrothermal parameters of sensing elements for measuring methane concentration in degassing pipelines allows to simplify the design of the analyzer sensor, to exclude long transient processes arising from changes in the temperature of the gas mixture, eliminates the disadvantages of two-chamber analyzers associated with leakage violations of the comparison chamber. In order to ensure stability of the measuring bridge zero at changing ambient temperature, it is necessary to choose platinum thermocouples with the same initial resistance when designing analyzer sensors. At the same time the balanced measuring bridge of a single-chamber thermoconductometric sensor with unequal electrothermal parameters of sensitive elements does not allow high stability of zero-readings of the analyzer at possible changes of bridge power supply parameters. Therefore, it is more reasonable to use an unbalanced measuring bridge with a symmetrical ballast branch, the operating mode of which is selected from the condition of ensuring the same steepness of the voltampere characteristics of the elements of the working branch of the bridge and the introduction of a precision source of reference voltage to eliminate the zero offset.

For the final choice of parameters of thermoelements and modes of operation of the measuring bridge it is necessary to carry out studies of various variants of execution of a single-chamber thermoconductometric sensor with unequal electrothermal parameters of sensitive elements under different modes of power supply of bridge measuring circuits. Let's consider the conditions of providing thermal compensation of the bridge when it is powered by a stable voltage source. In the absence of additional heating from the electric current source, the dependence of platinum thermistor resistance on temperature is usually represented in the form of

$$R_e = R_{0e}(1 + \beta t_t). \quad (3.18)$$

In the presence of additional heating from the electric voltage source, expression (3.18) takes the form

$$R_e = R_{0e}(1 + \beta t_e). \quad (3.19)$$

The temperature of the thermocouple in general depends on the ambient temperature, geometric and electrical parameters of the element, heat exchange conditions and the current flowing through the element. The

theoretical dependence of the element temperature  $t_e$  on the above parameters is [1].

$$t_e = t_t + b_e I_e^2. \quad (3.20)$$

Taking into account the expressions (3.18) and the value of the thermoresistive coefficient, as well as the dependence of the current on the voltage, the expression (3.20) can be presented:

$$\frac{R_e}{R_{0e}\beta} - \frac{1}{\beta} = t_t + \frac{U_e^2}{\alpha_e F_e R_e}. \quad (3.21)$$

The solution of the equation (3.21) with respect to the resistance value has the form

$$R_e = \frac{R_{0e}}{2} \left( 1 + \beta t_t + \sqrt{(1 + \beta t_t)^2 + \frac{4U_e^2 \beta}{\alpha_e F_e R_{0e}}} \right). \quad (3.22)$$

Having differentiated (3.22) by  $t_t$ , we obtain

$$\frac{\partial R_e}{\partial t_t} = \frac{R_{0e}\beta}{2} + \frac{R_{0e}\beta(1 + \beta t_t) / 2}{\sqrt{(1 + \beta t_t)^2 + \frac{4U_e^2 \beta}{\alpha_e F_e R_{0e}}}}. \quad (3.23)$$

At  $U_e = 0$  the expression (3.22) will take the value, which can be obtained by differentiation of expression (3.18)

$$\frac{\partial R_e}{\partial t_t} = R_{0e}\beta. \quad (3.24)$$

As the voltage applied to the element and the element heating temperature from the external source increases, the second summand in the right part of expression (3.23) tends to zero, and in this case we have

$$\frac{\partial R_e}{\partial t_t} = \frac{R_{0e}\beta}{2}. \quad (3.25)$$

Thus, when powering the measuring bridge with unequal electrothermal parameters of the elements from a stable voltage source, a change in the medium temperature by the value  $\Delta t_t$  will lead to a change in the resistance of the less heated comparative element by a larger value than that of the working one. It means that unlike the mode of powering the measuring bridge with a stable current when powering with a stable voltage, the equality of the initial resistance of the working and comparative elements (3.12) does not ensure the temperature stability of the bridge. Such stability can be ensured by including a resistor with a lower heating temperature in parallel to the comparative thermocouple and selecting its value. Taking into account the fact that the voltage value on the comparative element in this case will be significantly less than the voltage value on the working element, for symmetry of the bridge it is advisable to introduce an additional resistance in the branch with the comparative element.

The circuit of the measuring bridge with a single-chamber thermoconductometric sensor, the thermocouples of which have the same initial resistance, but differ significantly in size, is shown in Fig. 3.4.

It is possible to obtain an analytical expression for determining the value of the shunt resistor, at which the temperature stability of the bridge is ensured, but it does not make sense, because for the calculation it is necessary to know the value of the area of thermoelements and heat transfer coefficients of elements, the exact value of which is practically impossible to determine. Therefore, the value of the shunt resistor at this variant of power supply can be selected only experimentally, by searching for the value of the shunt resistance that provides the minimum zero shift of the bridge at temperature changes in the required range [8].

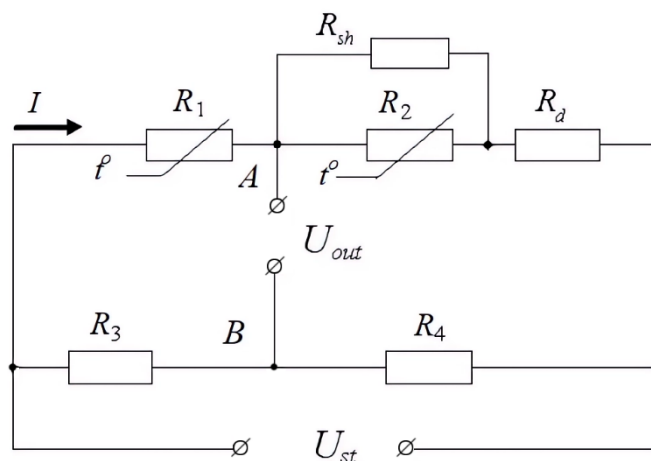


Fig. 3.4. Bridge circuit with a single-chamber thermoconductometer sensor:  
 $R_1, R_2$  – thermocouples;  $R_{add}$  – additional resistor;  $R_{sh}$  – shunt resistor;  $R_3, R_4$  – ballast resistors

Mastering the production of highly stable and economical voltage stabilizers in integrated design, high-quality operational amplifiers, comparators and microprocessors allows to implement various modes of power supply and processing of the output signal of thermoconductometric sensors, including: with voltage stabilization on one of the thermoelements, stabilization of the power spent on heating the element and stabilization of the element temperature. As we have shown in the previous section, the application of sensors with isolated comparative element in the latter case provides the highest sensitivity and practically linear dependence of the measuring bridge output signal on methane concentration. Taking this into account, as well as the ambiguity of dependence of air and methane thermal conductivity on the medium temperature, from the point of view of minimizing the measurement error, the operation mode of a single-chamber thermoconductometer sensor with stabilization of the working element temperature is of interest.

When using thermoconductometric sensors with a non-isolated comparative element, other conditions being equal, the maximum sensitivity of the bridge circuit is provided at the temperature of the comparative element equal to the ambient temperature [8]. This mode of the element operation is possible when the comparative element is mounted directly on the measuring chamber body. Since for exclusion of convective heat exchange in thermoconductometric sensors the dimensions of the chamber are chosen very small, and the range of ambient temperature change in mine conditions does not exceed  $\pm 15$  °C, such location of the comparative element allows stabilizing the temperature of the measuring chamber surface. In this case, the parameters of the working element will depend only on the characteristics of the power source and the properties of the gas medium.

In the stationary mode, the power released in the working element during the passage of electric current  $P_{el}$  through it is dissipated to the environment through the gas space inside the chamber and structural elements due to the heat conduction of the gas medium, natural convection, radiation and through the current-supplying ends. Taking into account the expressions (2.23) and (2.24), the equation describing the heat transfer process for a thermocouple of spherical shape will take the form:

$$I_e^2 R_e = \frac{4\pi\lambda_0}{1/r_e - 1/r_k} \left( t_e - t_i + \frac{1}{2} \beta_t t_e^2 - \frac{1}{2} \beta_t t_i^2 \right) + \quad (3.26)$$

$$+ 6.35 \cdot 10^{-2} \varepsilon_e r_e^2 (t_e^2 - 0.5 t_e t_i) + 3.45 d_m (t_e - t_i).$$

The second and third summands in the right part of equation (3.26) represent the power dissipated by radiation and through the current conducting ends. At constant temperature of the element and chamber walls, these components of heat transfer are constant and do not depend on the gas thermal conductivity. Under similar conditions, the first summand in the right part of equation (3.26), directly proportional to the gas thermal conductivity, and the value of this heat transfer component in real sensors usually exceeds 2/3 of the total dissipated power [9]. In this case, substituting into equation (3.26) the value  $R_e$  from (4.24), we obtain

$$I_e^2 R_0 = (1 + \beta t_e) = \lambda_0 b + a, \quad (3.27)$$

where:

$b$  – and  $a$  are constant values at the selected sensor mode of operation, which are respectively equal:

$$a = 6.35 \cdot 10^{-2} \varepsilon_e r_e^2 (t_e^2 - 0.5 t_e t_i) + 3.45 d_m (t_e - t_i); \quad (3.28)$$

$$b = \frac{4\pi\lambda_0}{1/r_e - 1/r_k} \left( t_e - t_i + \frac{1}{2} \beta_i t_e^2 - \frac{1}{2} \beta_i t_i^2 \right). \quad (3.29)$$

Assuming that the thermal conductivity of a binary methane – air mixture has additive properties and uniquely depends on the concentration of gas components, we present

$$\lambda_0 = \lambda_{a0} + C(\lambda_{br0} - \lambda_{a0}), \quad (3.30)$$

where:

$\lambda_{br0}$ ,  $\lambda_{a0}$  – heat conductivity coefficients of methane and air at 0 °C, W/m.

Taking into account expressions (3.29) and (3.30) we obtain

$$I_e^2 R_e = b\lambda_{a0} + Cb(\lambda_{br0} - \lambda_{a0}) + a. \quad (3.31)$$

From where:

$$I_e^2 = \frac{b\lambda_{a0} + a}{R_e} + C \frac{b(\lambda_{br0} - \lambda_{a0})}{R_e}. \quad (3.32)$$

The minimum value of current through the element  $I_{e0}$  corresponds to zero concentration of methane in the mixture. From equation (3.32) for this case we have

$$I_{e0}^2 = \frac{b\lambda_{a0} + a}{R_e}. \quad (3.33)$$

Taking into account the last expression and equation (3.32) we can write

$$I_e^2 - I_{e0}^2 = C \frac{b(\lambda_{br0} - \lambda_{a0})}{R_e}. \quad (3.34)$$

Denoting the current increment in the presence of methane as  $\Delta I = I_e - I_{e0}$ , we obtain an expression relating methane concentration and current increment

$$C = (2I_{e0}\Delta I + \Delta I^2)b_1, \quad (3.35)$$

where:

$$b_1 = \frac{R_e}{b(\lambda_{br0} - \lambda_{a0})}. \quad (3.36)$$

At stabilization of the working element temperature the coefficient  $b_1$  is a constant value. In this case, it follows from equation (3.36) that at the accepted operating mode of the thermoconductometer sensor the current increment  $\Delta I$  is unambiguously related to the methane concentration.

In real thermoconductometric sensors the current increment  $\Delta I$  at change of methane concentration depending on the selected temperature mode is from  $0.1 I_{e0}$  to  $0.2 I_{e0}$ . At such a value  $\Delta I$  the presence of a quadratic

component in the left part of expression (3.36) causes a noticeable nonlinearity of the dependence of current increment on methane concentration (Fig. 3.5).

In methane analyzers with digital indication, in order to eliminate the measurement error caused by this nonlinearity, the use of measuring transducers on analog integrated circuits requires the introduction of additional nodes to ensure the linearity of the scale. In addition, when using analog circuits there are certain difficulties with maintaining a stable value of resistance of the working element. Taking this into account, it is preferable to use modern microprocessors when designing the analyzer. In this case, the thermocouple used to control and stabilize the temperature of the measuring chamber surface can simultaneously function as a heating element.

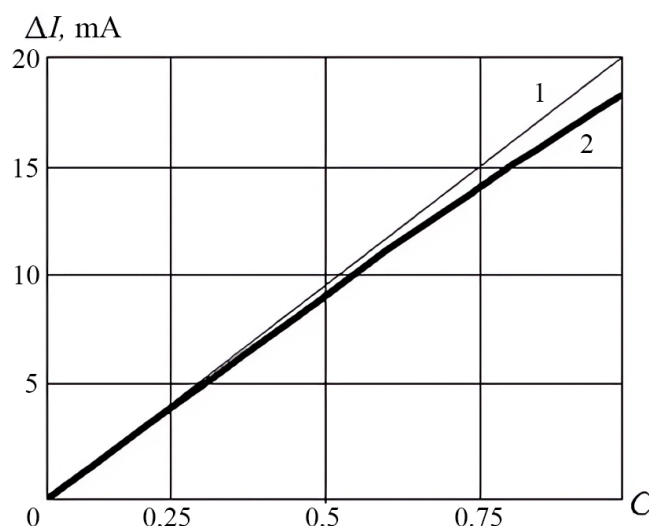


Fig. 3.5. Dependence of current increment on methane concentration: 1 – linear; 2 – calculated

When analog integrated circuits are used to design the analyzer, it is best to use separate elements for controlling the temperature of the measuring chamber surface and its heating. In case of supplying the thermocouple performing the functions of the measuring chamber temperature sensor from a current source, the chamber temperature constancy is relatively easily ensured by maintaining a stable voltage on the temperature sensor by controlling the heating element operation mode. In order to simplify circuit solutions due to the complexity of implementation of the measuring circuit providing maintenance of stable temperature of the working thermocouple on analog elements, in this case it is more appropriate to use the operation mode of the thermoconductometric sensor with voltage stabilization on the working element, by using which the temperature mode of the thermocouple in air and methane changes within minimum limits.

### 3.3. Justification of the control method using thermocatalytic methane sensor with unequal electrothermal parameters of sensing elements

Thermocatalytic sensors included in bridge measuring circuits [7], most often used in gas analysis, usually contain a gas-permeable working chamber, in which thermoelements of identical resistance and size are installed. This implementation of sensors allows stability of zero of the bridge circuit at change of power supply parameters, gas composition and temperature of the analyzed medium. At the same time our researches have shown that at the accepted temperature modes of thermocouples in emergency conditions, when the limiting agent is air oxygen and besides methane in the atmosphere of mine workings there are hydrogen, carbon oxide and higher homologues of methane, as a result of oxidation of these impurities on the comparative element there is a sharp decrease in the output signal (up to inversion) and the existing thermocatalytic sensors do not provide control of explosion hazard of the gas mixture. Besides, the choice of high thermocouples preheating temperature leads to accumulation rate increase of thermal destruction products of hydrocarbons on the comparative element, its activation and zero shift of the measuring bridge, and at low preheating temperature occurs working element carbonization and sensitivity of the sensor decreases.

One of the possible ways to resolve this contradiction can be the use of different thermal modes of sensitive elements in the thermocatalytic sensor. So, at a choice of temperature of a working element 400 °C, and

temperature of a comparative element below 300 °C excludes carbonization of both elements, provides stability of zero and sensitivity of the sensor and at the same time low temperature of a comparative element excludes possibility of oxidation on it of combustible components at emergency gasification of mine workings. At the same time at different thermal modes of the sensing elements their electrothermal analogy is violated, which can lead to a decrease in the stability of the measuring bridge. Therefore, such a solution should be sufficiently justified.

A similar problem was considered by the authors [8, 10], when theoretically justifying the parameters of a thermoconductometric methane sensor with a non-insulated comparative element. The difference of thermal modes of the sensitive elements of the single-chamber thermoconductometric sensor was provided in this case by manufacturing the spirals of pelistor-type thermocouples of platinum microwires of different diameters. Despite the similarity of these problems, the results obtained in [8, 10] can not be fully acceptable in the development of a thermocatalytic sensor, since the modes of operation of thermoelements in thermocatalytic and thermoconductometric sensors are significantly different, and the reaction of the sensitive element is opposite to the controlled component. This determines significant differences with respect to the recommended modes of power supply of measuring bridges that ensure zero stability and linearity of analyzer characteristics when using thermocatalytic and thermoconductometric sensors [8, 10].

It is possible to provide different thermal modes of sensing elements by various methods, for example, by making thermoelements with different resistance or different sizes, by shunting one of the elements, etc. Let us consider the simpler variant, which consists in shunting the comparative element of the existing commercially available symmetric thermocatalytic sensor (Fig. 3.6).

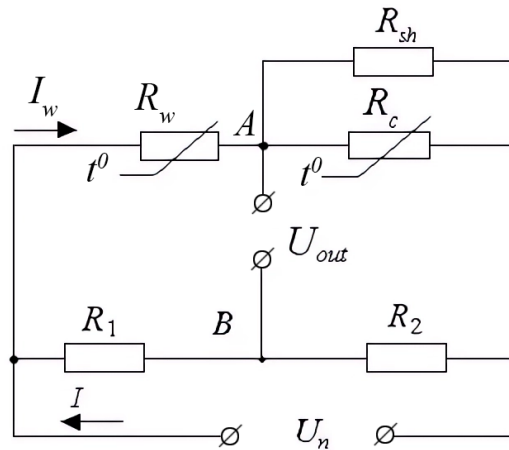


Fig. 3.6. Bridge circuit with thermocouples with significantly different thermal modes:  
 $R_w, R_{comp}$  – thermocouples;  $R_{sh}$  – shunt resistor;  $R_1, R_2$  – ballast resistors

Taking into account the fact that the less heated comparative element will have significantly lower resistance, the bridge shown in Fig. 3.1 is asymmetrical, if necessary to symmetrize the measuring bridge, additional resistance  $R_{add}$  is introduced into the bridge branch with the comparative element.

The balance conditions of an asymmetrical bridge circuit can be written

$$\frac{U_w}{U_c} = \frac{U_1}{U_2} = \frac{R_1}{R_2}. \quad (3.37)$$

In this case, if the resistance value of the shunt and ballast resistors is independent of the supply and gas medium parameters, the condition of zero conservation of the balanced bridge will be

$$\frac{\Delta U_w}{\Delta U_c} = \frac{U_w}{U_c}, \quad (3.38)$$

where:

$\Delta U_w, \Delta U_c$  – change of voltage on bridge elements at change of uncontrollable factors of gas

environment and power supply parameters.

The dependence of the voltage value on the thermocouple of the thermocatalytic sensor on the current, obtained in [7], is

$$U_e = I_e R_{0e} (1 + \beta t_t + \beta b_e I_e^2). \quad (3.39)$$

Taking into account the fact that in air in a wide temperature range the thermoresistive coefficient of platinum thermistors is a constant, for identical working and comparative elements of the thermogroup we write down

$$b = \frac{R_e}{\alpha_e F_e} = \frac{R_w}{\alpha_w F_w} = \frac{R_c}{\alpha_c F_c} = \text{const}. \quad (3.40)$$

Based on the expression (3.39) the voltage on the working thermocouple of the sensor  $R_w$  will be

$$U_w = I_w R_0 (1 + \beta t_t + \beta b I_w^2), \quad (3.41)$$

where:

$I_w$  – current through the working thermocouple, A.

Accordingly, the voltage on the comparative element

$$U_c = I_c R_0 (1 + \beta t_t + \beta b I_c^2), \quad (3.42)$$

where:

$I_c$  – current through the comparative thermocouple, A.

In turn, the voltage on the comparative element is equal to

$$U_c = R_{sh} (I_w - I_c), \quad (3.43)$$

Let's equate the right parts of equations (3.42) and (3.43) and present the obtained equation in the form of

$$I_c^3 + p I_c + g = 0, \quad (3.44)$$

where:

$$p = \frac{R_{sh} + R_0 (1 + \beta t_t)}{R_0 \beta b}; \quad g = -\frac{R_{sh} I_w}{R_0 \beta b}.$$

Let's determine the discriminant of the equation (3.44)

$$\Delta = \frac{p^3}{27} + \frac{g^2}{4} = \frac{1}{4} \left( \frac{R_{sh} I_w}{R_0 \beta b} \right)^2 + \frac{1}{27} \left( \frac{R_{sh} + R_0 (1 + \beta t_t)}{R_0 \beta b} \right)^3. \quad (3.45)$$

Since  $\Delta > 0$ , equation (3.44) has one real and two complex roots. The real root is defined according to the expression

$$I_c = \sqrt[3]{-g/2 + \sqrt{\Delta}} + \sqrt[3]{-g/2 - \sqrt{\Delta}}.$$

Then the expression for determining the current through the comparative element will have the form

$$I_c = \sqrt[3]{\frac{R_{sh}I_w}{R_0\beta b} + \sqrt{\frac{1}{4}\left(\frac{R_{sh}I_w}{R_0\beta b}\right)^2 + \frac{1}{27}\left(\frac{R_{sh} + R_0(1 + \beta t_t)}{R_0\beta b}\right)^3}} + \sqrt[3]{\frac{R_{sh}I_w}{2R_0\beta b} - \sqrt{\frac{1}{4}\left(\frac{R_{sh}I_w}{R_0\beta b}\right)^2 + \frac{1}{27}\left(\frac{R_{sh} + R_0(1 + \beta t_t)}{R_0\beta b}\right)^3}}. \quad (3.46)$$

Substituting the obtained current value into (3.43) we obtain the equation for determining the voltage on the comparative element

$$U_c = R_{sh}I_w - R_{sh}\sqrt[3]{\frac{R_{sh}I_w}{2R_0\beta b} + \sqrt{\frac{1}{4}\left(\frac{R_{sh}I_w}{R_0\beta b}\right)^2 + \frac{1}{27}\left(\frac{R_{sh} + R_0(1 + \beta t_t)}{R_0\beta b}\right)^3}} - R_{sh}\sqrt[3]{\frac{R_{sh}I_w}{2R_0\beta b} - \sqrt{\frac{1}{4}\left(\frac{R_{sh}I_w}{R_0\beta b}\right)^2 + \frac{1}{27}\left(\frac{R_{sh} + R_0(1 + \beta t_t)}{R_0\beta b}\right)^3}}. \quad (3.47)$$

When the measuring bridge is powered by a stable current source, all quantities included in the expressions are independent of the gas temperature. Therefore, by differentiating the right parts of equations (3.41) and (3.47) and taking their ratio we can obtain in explicit form the condition of independence of the zero of the balanced bridge from the temperature change (3.38) at the specified mode of supplying the measuring bridge. It should be noted that such analytical expression is very complicated and inconvenient for analysis, so the nature of gas temperature influence on zero stability we will find out by substituting real parameters of serial thermocatalytic sensors into equations (3.41) and (3.47) and finding numerical values of voltages on thermocouples and their increment at gas temperature change.

We will perform calculations at the following parameter values:  $I_w = 0.2$  A;  $R_0 = 2.0$  Ohm;  $R_{sh} = 20$  Ohm;  $\beta = 0.004$  1/°C;  $t_t = 25$  °C;  $b = 1 \cdot 10^4$  °C/A<sup>2</sup>.

Calculated values of voltages on thermocouples and their increments at change of gas temperature at the specified parameters are:  $U_w = 1.08$  V;  $U_c = 0.727$  V;  $\Delta U_w / \Delta t_t = 1.6$  mV/°C;  $\Delta U_c / \Delta t_t = 0.79$  mV/°C. The value of the ratio  $\Delta U_w / \Delta U_c = 2.02$ ;  $U_w / U_c = 1.49$ , therefore, the condition (3.38) is not fulfilled and the measuring bridge at shunting of the comparative element is thermally unbalanced. At symmetrization of the measuring bridge by introducing additional resistance into the bridge branch with the comparative element, the value of  $U_w / U_c = 1$ , and hence the thermal drift of the bridge will increase.

The performed experimental verification confirms the validity of this conclusion using serial thermocatalytic sensors and the specified shunt value. The temperature drift of the measuring bridge zero is from 0.4 to 0.6 mV/°C. Taking this into account, this variant of the solution can be realized only at additional introduction of a temperature sensor into the analyzer and correction of the analyzer's zero following the readings of this sensor. Taking into account the availability of miniature cheap temperature sensors in integrated design with insignificant power consumption and high metrological characteristics, such a solution is possible.

Another way to ensure that the thermal modes of the sensing elements of the single chamber thermoconductometric sensor differ, could be manufacturing a comparison element with a smaller value of the thermoresistive coefficient, which may be obtained by increasing its surface area or decreasing the resistance of the thermocouple.

Let us consider a variant of thermocatalytic sensor with sensing elements having the same resistance, in which the surface area of the comparative element is significantly larger than that of the working element. The circuit of the measuring bridge for such a case is shown in Fig. 3.7.

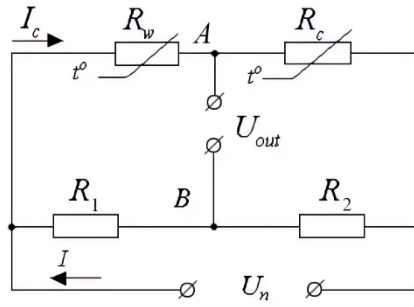


Fig. 3.7. Bridge circuit with thermocouples of different sizes:  
 $R_w, R_{comp}$  – thermocouples;  $R_1, R_2$  – ballast resistors

Based on the expression (3.39) the voltage on the working and comparative thermocouples at equality of their initial resistance will be

$$U_w = I_e R_0 (1 + \beta t_t + \beta b_w I_e^2), \quad (3.48)$$

$$U_c = I_e R_0 (1 + \beta t_t + \beta b_c I_e^2). \quad (3.49)$$

The voltage ratio on the elements for this case will be

$$\frac{U_w}{U_c} = \frac{1 + \beta t_t + \beta b_w I_e^2}{1 + \beta t_t + \beta b_c I_e^2}. \quad (3.50)$$

Setting the surface area of the comparative element 2 times larger than the sensitive element, we calculate the element voltages at the same values of parameters, provided that  $b_w = 1 \cdot 10^4 \text{ }^\circ\text{C}/\text{A}^2$ ;  $b_c = 0.5 \cdot 10^4 \text{ }^\circ\text{C}/\text{A}^2$ . The calculated values of the voltages are  $U_w = 1.08 \text{ V}$  and  $U_c = 0.762 \text{ V}$ , and the value of the ratio is  $U_w / U_c = 1.42$ . When the measuring bridge is powered by a stable current source, all values included in expressions (3.48) and (3.49) are independent of the gas temperature, in this case we obtain

$$\frac{dU_w}{dt_c} = \frac{dU_c}{dt_c} = I_e R_0 \beta. \quad (3.51)$$

The value of the voltage increment ratio will be  $\Delta U_w / \Delta U_c = 1$ . Therefore, the zero's condition of independence of the balanced bridge shown in Fig. 3.2, from the temperature change (3.38) at the specified mode of its power supply is also not fulfilled. Taking into account the fact that the ratio  $\Delta U_w / \Delta U_c = 1$ , to ensure the fulfillment of the condition (3.38) in such a bridge it is necessary to introduce an additional resistance to ensure the voltage symmetry (Fig. 3.8).

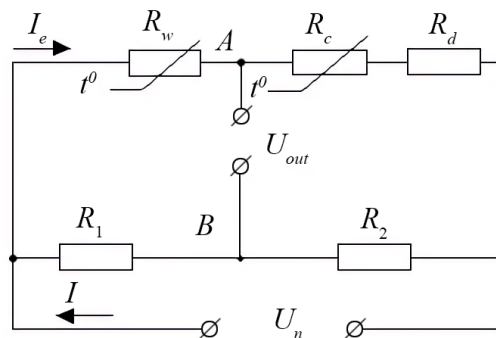


Fig. 3.8. Symmetrical bridge circuit with thermocouples of different sizes:  
 $R_w, R_{comp}$  – thermocouples;  $R_1, R_2$  – ballast resistors;  $R_{add}$  – additional resistance

In this case, the voltage on the bridge branch with the comparative element is

$$U_c = I_e R_0 (1 + \beta t_t + \beta b_c I_e^2) + I_e R_d. \quad (3.52)$$

The value of the additional resistance necessary for bridge symmetrization is determined from the condition of voltage equality on the bridge branches at the nominal mode of operation

$$R_0 (1 + \beta t_t + \beta b_c I_e^2) + R_d = R_0 (1 + \beta t_t + \beta b_w I_e^2). \quad (3.53)$$

Then the required value of the additional resistance is

$$R_d = R_0 \beta I_e^2 (b_w - b_c). \quad (3.54)$$

With the accepted parameters and power supply modes  $R_d = 1.6 \text{ Ohm}$ .

Thus, it is possible to ensure temperature stability of the thermocatalytic sensor bridge with unequal electrothermal parameters of the sensing elements by using thermistors with the same initial resistance and different surface area, provided that the measuring bridge is symmetrized and powered by a stable current source.

Another possible variant of a thermocatalytic sensor with unequal electrothermal parameters of sensing elements is a sensor with the same size of elements but with different resistance. When manufacturing thermocatalytic sensors of pelistor type, such variant can be easily implemented at insignificant increase of spiral pitch at winding of thermocouple elements and reduction of turn number. For this variant the voltage on elements is described by the equations

$$U_w = I_e R_{0w} (1 + \beta t_t + \beta b_w I_e^2); \quad (3.55)$$

$$U_c = I_e R_{0c} (1 + \beta t_t + \beta b_c I_e^2). \quad (3.56)$$

The voltage ratio on the elements in this case will be

$$\frac{U_w}{U_c} = \frac{R_{0w} (1 + \beta t_t + \beta b_w I_e^2)}{R_{0c} (1 + \beta t_t + \beta b_c I_e^2)}. \quad (3.57)$$

Setting the initial resistance of the comparison element  $R_{0c} = 0.8 R_{0w}$ , we calculate the voltages on the elements at the same parameter values, assuming that  $b_w = 1 \cdot 10^4 \text{ }^\circ\text{C/A}^2$ ;  $b_c = 0.8 \cdot 10^4 \text{ }^\circ\text{C/A}^2$ . The calculated voltages are  $U_w = 1.08 \text{ V}$  and  $U_c = 0.762 \text{ V}$ , and their ratio is  $U_w / U_c = 1.42$ . When the measuring bridge is powered by a stable current source, all values included in expressions (3.55) and (3.56) are independent of the gas temperature, in this case we obtain

$$\frac{dU_w}{dt_c} = I_e R_{0w} \beta; \quad \frac{dU_c}{dt_c} = I_e R_{0c} \beta. \quad (3.58)$$

The voltage increment ratios will be

$$\frac{\Delta U_w}{\Delta U_c} = \frac{R_{0w}}{R_{0c}}. \quad (3.59)$$

The calculated value of the ratio at the adopted parameters of the elements will be  $\Delta U_w / \Delta U_c = 1.25$ . Consequently, the zero's independence condition of the balanced bridge from the temperature change (3.38) at the specified power supply mode is not fulfilled. Taking into account that the ratio  $\Delta U_w / \Delta U_c$  is less than

the voltage ratio, it is necessary to introduce additional resistance to ensure the fulfillment of the condition (3.38) in such a bridge. The necessary value of the additional resistance is determined from the relation

$$\frac{U_w}{U_c} = \frac{R_{0w}(1 + \beta t_t + \beta b_w I_e^2)}{R_{0c}(1 + \beta t_t + \beta b_c I_e^2) + R_d} = \frac{R_{0w}}{R_{0c}}. \quad (3.60)$$

From where:

$$R_d = R_{0c} \beta I_e^2 (b_w - b_c). \quad (3.61)$$

With the accepted parameters and power supply modes  $R_d = 0.192$  Ohm.

As seen, it is possible to ensure the thermal stability of the bridge of the thermocatalytic sensor with unequal electrothermal parameters of the sensing elements when using thermistors with different initial resistance and the same surface area, provided that an additional resistor is introduced into the bridge arm with the comparative element. It should be noted that unlike the previous variant in this case the bridge remains asymmetrical, but the value of the additional resistor necessary to ensure the thermal stability of the bridge in this case is significantly smaller, which makes it possible to slightly reduce the power consumed by the sensor.

The mode of bridge power supply from a stable current source has a number of advantages, however, in this mode under conditions of gas overloads overheating of sensitive elements is possible, leading to changes in their parameters. In this case, the bridge power supply mode with voltage stabilization on the working element is preferable, which provides a stable temperature regime of the working element [15].

Let us evaluate the temperature stability of the bridge with unequal electrothermal parameters of the sensing elements, operating in the mode of stable voltage on the working element, when the resistance of the thermoelements is equal, but their surface area is different (Fig. 3.7). The voltage on the working and comparative thermoelements at equality of their initial resistance will be

$$U_w = I_e R_0 (1 + \beta t_t + \beta b_w I_e^2); \quad (3.62)$$

$$U_c = I_e R_0 (1 + \beta t_t + \beta b_c I_e^2). \quad (3.63)$$

From equation (3.62) we can obtain the dependence of the current through the thermocouples on the applied voltage. Let's represent equation (3.62) in the form of

$$I_e^3 + p I_e + g = 0, \quad (3.64)$$

where:

$$p = \frac{1 + \beta t_t}{\beta b_w}; \quad g = -\frac{U_w}{\beta b_w R_0}.$$

Let's define the discriminant of the equation (3.64)

$$\Delta = \frac{p^3}{27} + \frac{g^2}{4} = \frac{1}{4} \left( \frac{U_w}{\beta b_w R_0} \right)^2 + \frac{1}{27} \left( \frac{1 + \beta t_t}{\beta b_w} \right)^3.$$

Since  $\Delta > 0$ , equation (3.64) has one real and two complex roots. The real root is defined according to the expression

$$I_e = \sqrt[3]{-g/2 + \sqrt{\Delta}} + \sqrt[3]{-g/2 - \sqrt{\Delta}}.$$

Finally, the expression for determining the current through the thermocouple will be

$$I_e = \sqrt[3]{\frac{U_w}{2\beta b_w R_{0w}} + \sqrt{\frac{1}{4}\left(\frac{U_w}{\beta b_w R_{0w}}\right)^2 + \frac{1}{27}\left(\frac{1+\beta t_t}{\beta b_w}\right)^3}} + \sqrt[3]{\frac{U_w}{2\beta b_w R_{0w}} - \sqrt{\frac{1}{4}\left(\frac{U_w}{\beta b_w R_{0w}}\right)^2 + \frac{1}{27}\left(\frac{1+\beta t_t}{\beta b_w}\right)^3}}. \quad (3.65)$$

Using expression (3.65), let's calculate the value of current through thermocouples at  $t_t = 25^\circ\text{C}$  and its increment at temperature change at the given earlier parameters of the working element and stable voltage  $U_w = 1.08\text{ V}$ . The obtained calculated values are  $I_e = 0.20\text{ A}$ ,  $\Delta I_e / \Delta t_t = -0.137\text{ mA}/^\circ\text{C}$ .

According to (3.63), using the values of current and its increment, we calculate the voltage on the comparative element and its temperature changes. The obtained values are  $U_c = 0.76\text{ V}$ ;  $\Delta U_c / \Delta t_t = 0.617\text{ mV}/^\circ\text{C}$ . Taking into account the fact that at stabilization of voltage on the working element  $\Delta U_w / \Delta U_c = 0$ , as well as the different nature of dependence of current increment through thermocouples and voltage increment on the comparative element on temperature, the temperature stability of the bridge can be provided by introduction in the branch of the bridge with the comparative element of the additive resistance (similarly to Fig. 3.8), the value of which is  $R_d = 0.617/0.137 = 4.5\text{ Ohm}$ . The voltage on the arm of the bridge with a comparative element will be  $U_c = 0.76 + 4.5 \cdot 0.2 = 1.66\text{ V}$ , and therefore such a temperature-stabilized bridge is asymmetrical. In addition, compared to the current stable mode, in this case a larger added resistance is introduced into the bridge, which increases its power consumption.

Let us consider the second variant of the thermocatalytic sensor with the same dimensions of the elements, but with different element resistances. For this variant the voltages on the elements are described by equations (3.55) and (3.56). Similarly to the previous variant, the calculated values of current through thermoelements at  $t_t = 25^\circ\text{C}$  and its increment at temperature change with the previously given parameters of the working element and stable voltage  $U_w = 1.08\text{ V}$ , are  $I_e = 0.20\text{ A}$ ,  $\Delta I_e / \Delta t_t = -0.137\text{ mA}/^\circ\text{C}$ .

According to expression (3.56), using the values of current and its increment, we calculate the voltage on the comparative element and its temperature changes. The obtained values are  $U_c = 0.7616\text{ V}$ ;  $\Delta U_c / \Delta t_t = 0.175\text{ mV}/^\circ\text{C}$ . Taking into account that at stabilization of voltage on the working element  $\Delta U_w / \Delta t_t = 0$ , the obtained temperature change of voltage on the comparative element indicates that this sensor implementation at voltage stabilization on the working element is more thermostable. Taking into account the different character of dependence of current increment through thermocouples and voltage increment on the comparative element on temperature, temperature stability of the bridge can be increased similarly to the previous case by introducing an additional resistance into the bridge branch with the comparative element, the value of which is  $R_d = 0.175/0.137 = 1.28\text{ Ohm}$ . The voltage on the arm of the bridge with the comparative element without the additional resistance is less than on the working thermocouple, and with the additional resistance  $U_c = 0.7616 + 1.28 \cdot 0.2 = 1.022\text{ V}$ , and such a thermostabilized bridge is practically symmetrical.

Let us evaluate whether it is possible to balance the bridge without an additional resistor, for example, by changing the parameters of the comparison element. Taking into account the fact that at the selected power supply mode of the thermally balanced bridge the voltage on the comparative element remains constant with temperature change, let us equate the right parts of equation (3.20) found at temperature  $t_t$  and  $t_t + t_t + \Delta t_t$

$$I_e R_{0c} (1 + \beta t_t + \beta b_c I_e^2) = (I_e + \Delta I_e) R_{0c} \left[ 1 + \beta (t_t + \Delta t_t) + \beta b_c (I_e + \Delta I_e)^2 \right],$$

where:

$\Delta I_e$  – change in current through the elements when the temperature changes by  $\Delta t_t$ .

Hence the value of the thermoresistive coefficient, at which the thermal stability of the bridge is ensured, is

$$b_c = -\frac{1 + \beta(t_i + \Delta t_i)}{\beta(3I_e^2 + 3I_e\Delta I_e + \Delta I_e^2)}. \quad (3.66)$$

Since the expressions in the numerator and denominator of the dependence (3.66) are always greater than zero, the obtained value of the thermoresistive coefficient is a negative value. Consequently, it is impossible to thermally balance the bridge without introducing additional resistance in this case.

### 3.4. Development and justification of the control method using a two-chamber thermocatalytic methane sensor

The use of existing thermocatalytic gas analyzers for explosion hazard control of multicomponent gas mixtures is difficult due to the fact that higher homologues of methane, hydrogen, carbon monoxide and other explosive components of mixtures at the temperature of primary heating of elements necessary for methane oxidation are able to oxidize not only on the working, but also on the comparative element. In addition, our studies of thermocatalytic methane sensors after their long-term operation [16] have shown that there is a gradual accumulation of hydrocarbon thermal degradation products on the surface of the comparative element, and this leads to an increase in its catalytic activity. Oxidation of combustible components on the comparative element leads to an increase in its temperature and activity, the catalytic oxidation reaction on it can switch from the kinetic to the diffusion area, which causes a sharp decrease in the output signal of the measuring bridge and can lead to a failure of explosion protection equipment.

The solutions proposed in Section 3.3, aimed at the development of thermocatalytic sensors with different thermal modes of sensing elements, allow to eliminate the noted disadvantages of existing methane sensors, but with such sensor implementation the symmetry of measuring bridges is broken, which causes instability of their zero at change of power supply parameters. And this in turn imposes increased requirements to the stability of power supply sources of such sensors. Therefore, it is expedient to further improve the thermocatalytic control method, allowing to control the explosion hazard of multi-component gas mixtures arising from emergency gasification of mine workings.

The existing thermocatalytic sensors produced by domestic and foreign manufacturers are all single-chamber. Their use somewhat simplifies the design of analyzers and reduces the power consumed by element preheating. The latter was essential to ensure ignition safety of the equipment when using thermocouples made in the form of hollow cylinders with a spiral of platinum wire, which were characterized by significant power consumption. Modern analyzers use thermocouples with low power consumption, made in the form of a miniature ball of  $\gamma$ -aluminum oxide applied on a spiral of platinum microwire, and therefore the issues of power consumption are insignificant.

In a single-chamber sensor there is a mutual influence of thermocouples on each other, which leads to the appearance of dependence of the output signal on the spatial location of the sensor. To reduce this dependence, a thermal insulating screen is installed between the thermocouples. The presence of the screen increases the heat exchange between the elements and the sensor body and slightly reduces its sensitivity. In addition, in a single-chamber sensor it is difficult to select pairs of thermocouples with identical electrothermal characteristics and there is no possibility of separate control of gas diffusion flows to the elements.

At small concentration of combustible gas and oxidation reaction proceeding on the working element in the diffusion area, its flux  $Q$  to its surface of the thermocouple depends linearly on gas concentration in the reaction chamber and effective diffusive conductivity of the element [1], i.e.

$$Q = \gamma_w C_k, \quad (3.67)$$

where:

$\gamma_w = 10^{-2} K_e \beta_{br} F_e$  – effective diffusive conductivity of the working element,  $\text{m}^3/\text{s}$ ;

$C_k$  – gas concentration in the reaction chamber;

$K_e$  – gas oxidation efficiency coefficient;

$\beta_{br}$  – mass transfer coefficient,  $\text{m/s}$ .

In this case, the amount of heat released on the working element is proportional to the effective diffusive conductivity of the working element, the concentration of gas in the reaction chamber, and the lower heat of combustion:

$$P_w = Q_h \gamma_w C_k, \quad (3.68)$$

where:

$Q_h$  – lower heat of combustion of gas, J/m<sup>3</sup>.

The temperature of the working element is determined by the total power released on the element from the power source  $P_{эл}$  and methane oxidation, and can be written:

$$P_{эл} + P_w = K(t_w - t_l), \quad (3.69)$$

where:

$K$  – thermal conductivity of the element, W/°C;

$t_w$  – temperature of the working element, °C.

The temperature of the comparison element is determined by the power allocated to the element from the power source

$$P_{эл} = K(t_c - t_l), \quad (3.70)$$

where:

$t_c$  – temperature of the comparative element, °C;

Then, at equality of thermal conductivity of elements, taking into account expressions (3.68) – (3.70) the temperature difference between working and comparative elements, determining the output signal of the bridge circuit is equal to

$$\Delta t = t_{we} - t_{ce} = \frac{Q_h \gamma_w C_k}{K}. \quad (3.71)$$

Dependence of platinum thermocouple resistance  $R_e$  on temperature in the temperature range characteristic for thermocatalytic sensor operation is usually represented in a linear form

$$R_e = R_{e0}(1 + \beta_e t_e). \quad (3.72)$$

In this case, at equality of initial resistance of elements, the bridge output voltage with a single-chamber thermocatalytic sensor at low concentrations of combustible gas linearly depends on its concentration in the reaction chamber, i.e.

$$U_{out} = \frac{R_{e0} I_e \beta_e Q_m \gamma_w C_m}{2K}. \quad (3.73)$$

The concentration of gas in the reaction chamber is related to its concentration in the analyzed mixture

$$C_k = C_a \frac{\gamma_f}{\gamma_f + \gamma_w}, \quad (3.74)$$

where:

$\gamma_f, \gamma_w$  – diffusive conductivity of the filter and effective diffusive conductivity of the working element, m<sup>3</sup>/s;

$C_a$  – gas concentration in the analyzed mixture.

Taking into account expressions (3.37) and (3.38) we obtain

$$U_{out} = \frac{R_{e0} I_e \beta_e Q_h \gamma_w \gamma_f C_a}{2K(\gamma_f + \gamma_w)}. \quad (3.75)$$

When supplying to the thermocatalytic sensor a combustible gas, which at the temperature of initial heating of thermocouples (in thermocatalytic sensors of methane the temperature is higher than 360 °C) is intensively oxidized both on the working and comparative element, the concentration of such gas in the chamber will be determined by the expression

$$C_k = C_a \frac{\gamma_f}{\gamma_f + \gamma_w + \gamma_c}, \quad (3.76)$$

where:

$\gamma_c$  – effective diffusive conductivity of the comparative element, m<sup>3</sup>/s.

In addition, the temperature difference between the working and comparative elements, on which the bridge circuit output signal depends in the equation (3.71), will be determined not by the value of the effective diffusive conductivity of the working element, but by the difference of conductivities of the working and comparative elements. In this case equation (3.75) takes the following form:

$$U_{out} = \frac{R_{e0} I_e \beta_e Q_h \gamma_f (\gamma_{we} - \gamma_{ce}) C_a}{2K(\gamma_f + \gamma_{we} + \gamma_{ce})}. \quad (3.77)$$

As we can see, the presence of components in the mixture, which at the temperature of initial heating of thermocouples are intensively oxidized both on the working and comparative element, leads to a decrease in the output signal of the bridge circuit with a single-chamber thermocatalytic sensor and to a decrease in the reliability of explosion hazard control equipment.

At low concentrations of combustible components in multicomponent gas mixtures, the value of the output voltage of a measuring bridge with a single-chamber thermocatalytic sensor is usually determined as the sum of the output voltages from each component separately

$$U_{out} = \frac{R_{e0} I_e \beta_e}{2K} \sum_{i=1}^n Q_{ih} C_{ia} \frac{\gamma_{if} (\gamma_{iw} - \gamma_{ic})}{\gamma_{if} + \gamma_{iw} + \gamma_{ic}}. \quad (3.78)$$

However, at high concentrations of combustible gases, the presence of combustible components in the mixture, which are intensively oxidized on the comparative element, leads to additional heating and activation of this element, including with respect to methane. As a result of activation of the comparative element its effective diffusion conductivity with respect to all combustible components increases, and the value of the bridge output voltage significantly decreases, up to inversion of the bridge output voltage. Moreover, as shown by the results of experimental studies of single-chamber thermocatalytic sensors, shown in the section two, in the presence of components with low ignition temperature in the mixture of gases, as a result of activation of the comparative element, a significant decrease in the readings of methane analyzers are observed in the area up to explosive concentrations of gases. This may lead to malfunctioning of automatic gas protection equipment.

Let's consider whether there is a possibility to exclude the mentioned disadvantages of gas analyzers when thermocatalytic sensors are made as two-chamber sensors. In contrast to single-chamber sensors, when using two-chamber sensors, there is a possibility of separate control of the diffusion conductivity of filters while maintaining the electrothermal analogy of the elements. To ensure high sensitivity and small time constant of analyzers, the diffusion conductivity of the first chamber sensor filter, in which the working element is installed, should be commensurable with the effective diffusion conductivity of the working element [11]. The diffusive conductivity of the filter of the second sensor chamber in which the comparative element is installed does not affect the sensitivity and speed of the analyzer and can be chosen several orders of magnitude less

than that of the first chamber. Its minimum value is limited only by the conditions of providing compensation for changes in pressure and content of uncontrolled gas components of the mine atmosphere. For such a case we can write

$$\gamma_{wf} \gg \gamma_{cf}, \quad (3.79)$$

where:

$\gamma_{wf}, \gamma_{cf}$  – diffusive conductivities of filters of the sensor chambers with the working and comparative element,  $\text{m}^3/\text{s}$ .

If the condition (3.79) is fulfilled, the amount of heat released on the working element will be determined by the concentration of combustible components, their calorific value and the corresponding diffusion conductivities of the filter and the working element. With some approximation it is possible to consider that the value of this heat release is proportional to the total calorific value of the gas mixture and characterizes its explosive properties. The amount of heat released in this case on the comparative element from oxidation of combustible gases capable to oxidize on its surface at the element preheating temperature, practically does not depend on the catalytic activity of the element in relation to these gases, but is determined by the diffusive the sensor chamber conductivity filter with the comparative element. Taking into account expression (3.78), the value of heat release from oxidation of combustible gases on the comparative element in any case will be several orders of magnitude less than the value of heat release due to oxidation of these gases on the working element. Neglecting heat release on the comparative element, equation (3.75) for a multicomponent mixture can be presented as:

$$U_{out} = \frac{R_{e0} I_e \beta_e}{2K} \sum_{i=1}^n Q_{ih} \gamma_i C_{ia}, \quad (3.80)$$

where:

$\gamma_i = \gamma_{iw} \gamma_{if} / (\gamma_{if} + \gamma_{iw})$  – total diffusive conductivity of the filter and working element for the  $i$ -th combustible gas,  $\text{m}^3/\text{s}$ ;

$C_{ia}, Q_{ih}, \gamma_{iw}, \gamma_{if}$  – concentration in air, lower heat of combustion, effective diffusive conductivity of the element and diffusive conductivity of the filter for the  $i$ -th combustible gas, respectively.

The comparative element activity increase due to carbonization of its surface at long-term operation of the analyzer in this case practically does not cause additional heating of this element, since the amount of heat released from oxidation of any component on the comparative element is insignificant, when the condition (3.79) is fulfilled. This excludes cases of malfunctioning of thermocatalytic gas analyzers and failures of explosion protection means.

It should be noted that the considered two-chamber sensor can operate at elevated temperatures of element preheating, which increases the sensitivity of analyzers, eliminates the hysteresis of analyzer readings and prevents carbonization of the surface of the sensitive element. The advantages of such a sensor include the absence of mutual thermal influence of thermoelements on each other and, consequently, its insensitivity to spatial arrangement.

Thus, two-chambered thermocatalytic sensor implementation with diffusive conductivity of the chamber filter, where the comparative element with much smaller conductivity of the chamber filter with the working element is installed, allows to improve metrological and operational characteristics of gas analyzers, to exclude cases of their ambiguous malfunction after long-term operation and in the presence in gas mixtures of components capable to oxidize on the comparative element at preheating temperature.

### 3.5. Justification of the design and operating modes of two-chamber sensor thermocouples

Practical implementation of a two-chamber thermocatalytic sensor can be easily based on a thermogroup with a double diffusion filter described in [7]. Its construction is shown in Fig. 3.9. Such thermogroups are serially produced at PJSC “Krasnyi Metallist” and are used in gas control equipment.

The difference of this thermogroup from the known ones is that the metal-ceramic filter is made with slightly increased dimensions, and inside this filter there is a hollow cup with a calibrated hole. The diameter of the hole is made so that its diffusion conductivity is  $\gamma_{hole} \ll \gamma_f$ . In this case, the total diffusion resistance is determined by the resistance of the hole, and the external filter only performs the function of protection when operating in a polluted environment, and the pollution of this filter practically does not affect the total diffusion resistance. Besides, at providing high accuracy of manufacturing of the cup and the orifice, the constancy of diffusion resistance of all thermogroups and equality of output voltages of the measuring bridge are provided.

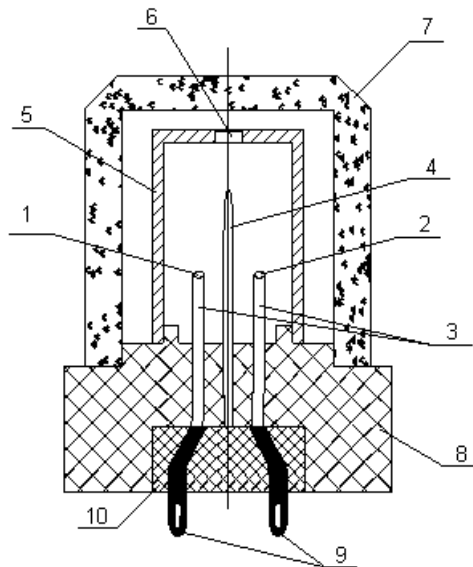


Fig. 3.9. Thermogroup with double diffusion filter: 1, 2 – working and compensating elements; 3 – holders; 4 – partition; 5 – beaker; 6 – calibrated hole; 7 – metal-ceramic filter; 8 – dielectric base; 9 – leads; 10 – compound

Based on the described thermogroup, several two-chamber sensor variants can be realized. The first variant consists in a separate arrangement of sensing elements (Fig. 3.10). In this case, the working and comparative thermoelements are placed in separate cups hermetically fixed on a dielectric base with two holders.

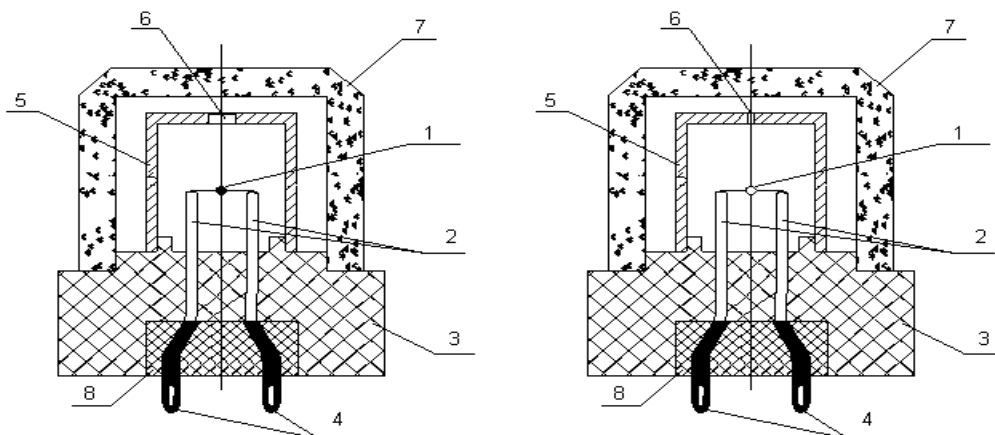


Fig. 3.10. Two-chamber thermocatalytic sensor with separate arrangement of sensitive elements: 1 – sensing elements; 2 – holders; 3 – dielectric base; 4 – leads; 5 – beaker; 6 – calibrated hole; 7 – metal-ceramic filter; 8 – compound

Beakers have calibrated holes of different diameters and are protected from the impact of polluted medium by separate metal-ceramic filters. The diameter of the calibrated holes is chosen so that the diffusion flux of the analyzed medium to the working element is significantly greater than the flux to the comparison element, i.e.  $d_w \gg d_c$ .

Separate arrangement of sensing elements allows to completely exclude their mutual thermal influence and, besides, makes it possible to make individual selection of thermoelements in pairs according to their voltampere characteristics [12]. The disadvantage of this sensor design is the impossibility of its application in existing commercially available gas analyzers without constructive changes in the latter. Therefore, as an alternative solution, it is reasonable to consider a variant of a two-chamber thermocatalytic sensor with the arrangement of sensing elements under one filter (Fig. 3.11). This two-chamber sensor differs from the known sensor with a double diffusion filter only by constructive execution of the beaker. The beaker has an insulating partition that divides the gas chambers into two parts isolated from each other. Access of the analyzed medium to the gas chambers is carried out through calibrated holes, the diameter of which is selected so that the diffusion flux to the working element is significantly greater than the flux to the comparison element, i.e.  $d_w \gg d_c$ .

This design of the two-chamber sensor allows its use in serial equipment instead of existing sensors without making any design changes. The presence of an insulating partition reduces the mutual thermal influence of elements on each other. At the same time, this version of the sensor does not allow individual selection of thermoelements in pairs according to their voltampere characteristics, and therefore, to reduce the zero drift caused by changes in uncontrolled parameters of the analyzed medium in this case it is advisable to perform additional thermal balancing of the elements, in accordance with the method described in [11].

The output characteristics of the proposed sensors depend on the selected temperature modes of the sensing elements and the value of gas diffusion resistances that determine the rate of supply of reacting components to these elements. The temperature modes of thermoelements in a two-chamber sensor do not differ from those in a single-chamber sensor, and when selecting these modes it is reasonable to be guided by the recommendations given in [7]. The rate of supply of reactive components to the sensing elements in the proposed two-chamber sensors is primarily determined by the sizes of the calibrated holes.

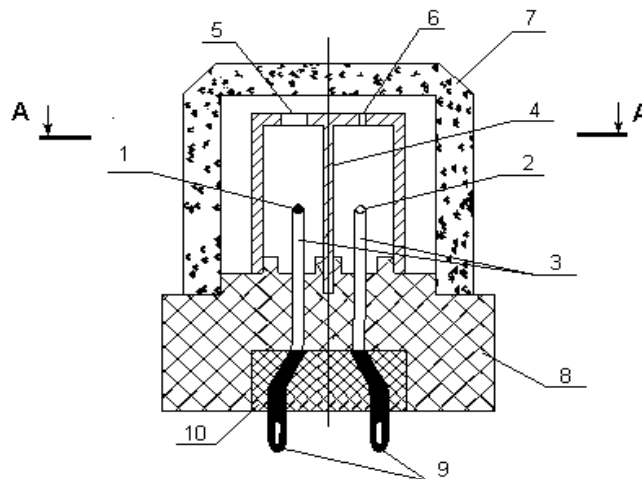


Fig. 3.11. Two-chamber thermocatalytic sensor with arrangement of sensitive elements under one metal-ceramic filter: 1, 2 – working and compensating elements; 3 – holders; 4 – beaker with insulating partition; 5, 6 – calibrated holes; 7 – metal-ceramic filter; 8 – dielectric base; 9 – leads; 10 – compound

The expressions for determining the bridge output voltage with a two-chamber thermocatalytic sensor (3.75) and (3.80) indicate a significant dependence of  $U_{out}$  on the activity of the catalyst, the magnitude of the supply current, the temperature of the medium, and other factors. The analysis of thermocatalytic sensors operation at different level of reacting components diffusion limitation into the reaction chamber, performed, shows that the greatest influence of the mentioned factors is observed at weak diffusion limitation, i.e. in the case when diffusion conductivity of the filter is greater or comparable to effective diffusion conductivity of the working

element. As  $\gamma_f$  decreases, so does the influence of the mentioned factors and the autostabilization properties of the sensor begin to appear. At significant limitation of diffusion of reacting components into the reaction chamber, for example, at application of a double diffusion filter with a small calibrated orifice, when  $\gamma_f \ll \gamma_e$ , the output voltage of the bridge is determined mainly by the size of the calibrated orifice and practically does not depend on ambient temperature, pressure, activity of the catalyst:

$$U_{out} = b_3 \beta Q_{mo} C_{ma} D_{mo} \frac{S}{l}, \quad (3.81)$$

where:

$b_3$  – coefficient, in the operating range of currents through thermogroup practically constant for this type of thermocouple, °C/A (for thermocouples of serial sensors made of platinum microwire with diameter  $d_{pr} = 30 \mu\text{m}$  at  $t_i = 30 \text{ °C}$ ,  $b_3 = 267 \text{ °C/A}$ ; at  $t_i = 70 \text{ °C}$ ,  $b_3 = 268,8 \text{ °C/A}$ );

$S$  – area of calibrated hole,  $\text{m}^2$ ;

$l$  – length of hole, m.

The independence of the measuring bridge output voltage from pressure when measuring gas volume concentration in this case is explained by the inverse nature of the relationship between  $D_{mass\ volume}$  and mass concentration  $C_{mass}$  from the pressure value. It is impossible to ensure the fulfillment of the condition  $\gamma_f \ll \gamma_e$ , because of a significant decrease in the output voltage, as in this case there are additional measurement errors due to instability of the measuring circuits of transducers and errors associated with changes in the spatial location of the sensor. It has been experimentally established [7] that when using serial sensors to ensure the measurement error of 0.2 vol.%, the diffusion conductivity of the hole should be  $\gamma_{hole} = (0.1 \div 0.25)\gamma_e$ . The value of the bridge output voltage in this case is  $(4 \div 10) \text{ mV/vol.}\%$ . At  $\gamma_{hole} > 0.2\gamma_e$ , the methane content in the reaction chamber is noticeably influenced by the activity of the working element, and this in turn can lead to a change in the diffusion flux of methane and the value of the bridge output voltage.

Taking into account the above, we set the value of diffusion conductivity of the chamber opening with the working thermocouple at the level  $\gamma_{hole} = 0.25\gamma_e$ , which, taking into account the typical value of effective diffusion conductivity of the element of serial sensors at nominal current [7] is  $\gamma_{hole} = 0.3 \cdot 10^{-7} \text{ m}^3/\text{s}$ .

Let us determine the hole parameters based on the first Fick's law, according to which in the stationary case

$$Q_{m_1} = -D_m \frac{dC_m}{dl} S, \quad (3.82)$$

where:

$D_m$  – diffusion coefficient of methane in air,  $\text{m}^2/\text{s}$ .

By accepting

$$\frac{dC_m}{dl} = \frac{C_{ma} - C_m}{l},$$

we have

$$Q_m = -D_m \frac{S}{l} (C_{ma} - C_m). \quad (3.83)$$

Thus

$$\gamma_f = D_m \frac{S}{l}. \quad (3.84)$$

Setting the thickness of the chamber wall at 1 mm, from (3.48) we obtain the area  $S = 15 \text{ mm}^2$ , which corresponds to a hole with diameter  $d = 4 \text{ mm}$ .

At the same thickness of the chamber wall with a comparative element we apply the diameter of the calibrated hole in the wall of this chamber  $d = 0.5 \text{ mm}$  to fulfill the condition (3.79).

### **3.6. Selection and justification of gas mixtures composition control methods for universal wide-range methane analyzers**

The well-known wide-range methane analyzers simultaneously used thermocatalytic and thermoconductometric measurement methods [13]. They included two bridge circuits for measuring low and high methane concentrations. The first circuit contained a catalytically active and a compensation element that were in contact with the monitored gas. The compensation element of the first bridge circuit was part of the second bridge circuit, wherein it acted as a sensing element. The second bridge circuit also contained an element shielded from the monitored gas, which is a compensating element in this bridge. The analyzers also included elements for switching the supply voltage of both bridge circuits depending on the concentration of the monitored gas.

As a result of sensors of low and high concentration of methane being constantly switched on, there are no transients associated with sensor heating in the equipment. Exclusion of transients associated with heating of sensing elements increases the reliability of the gas control system. However, the simultaneous use of two sensors complicates the design of analyzers, they have a relatively large power consumption, which limits the application of the above principle in portable devices for individual or group usage.

This disadvantage is eliminated in other designs by simultaneously using the comparative element of the thermocatalytic sensor in the thermal conductivity sensor and alternate switching on of the thermocatalytic sensor and the thermal conductivity sensor. In one of analyzer variants, when the combustible gas content increases above the specified level, the first bridge containing a catalytically active element is turned off and the second bridge that works on conductometric principle is switched on. In this case, the compensating element of the second bridge circuit, which is disconnected and cold in the initial state, begins to warm up, and measurement by the second bridge is possible only after the end of the transient process associated with the warming up of the compensating element. At this time the measurement of methane content does not take place, which reduces the reliability of gas control.

This disadvantage was eliminated in subsequent gas control equipment designs [14], where unlike the analyzer described earlier, in order to simplify the design and reduce power consumption, only the compensating sensitive element of the thermocatalytic sensor is used as a high concentration methane sensor. In this case, the information parameter is the voltage value on the comparative element when it is powered by a stable current source.

The use of a comparative element of a thermocatalytic sensor as a thermal conductivity sensor in a thermoconductometric sensor allows to reduce power consumption, the absence of a compensation element in a thermoconductometric sensor allows to reduce the duration of transient processes associated with its heating. However, both considered solutions have a number of common disadvantages that lead to failures in the analyzers operation and limit their application.

To find out the reasons for these failures, let us analyze the peculiarities of analyzers operation when using the comparative element of the thermocatalytic sensor as a thermal conductivity sensor. In this case we will consider two possible variants of the sensor operation at high methane concentrations, namely the variant when the catalytically active element of the thermocatalytic sensor is not turned off and the variant when the catalytically active element is turned off when the concentration threshold is reached.

Since at high methane concentrations the catalytically active element overheating is possible, leading to a malfunction, the first option is possible with a significant limitation of diffusion of the controlled medium into the reaction chamber, for example, when using sensors with a double diffusion filter [7], or when using an inclusion circuit with voltage stabilization on the working element [15]. In any case, due to the oxidation of methane on the catalytically active element, its concentration in the reaction chamber of single-chamber sensors will be significantly different from the concentration of methane in the analyzed medium. The

relationship between these values when methane enters the chamber by diffusion is usually represented in the form [7]

$$C_m = C_{mc} \frac{\gamma_f}{\gamma_f + \gamma_e}, \quad (3.85)$$

where:

$C_m$ ,  $C_{mc}$  – volume fraction of methane in the mixture and in the chamber, %.

Difference between the methane concentration in the mixture and in the chamber

$$\Delta C_m = C_{mc} \left( 1 - \frac{\gamma_f}{\gamma_f + \gamma_e} \right) \quad (3.86)$$

determines the value of methane flow into the chamber and, consequently, the amount of heat released on the working element, its temperature increase and the value of the output signal of the measuring bridge.

It should be noted that expressions (3.85) and (3.86) are valid for the case when the limiting agent in the mixture of gases determining the reaction rate is methane. When the volume fraction of methane exceeds 9%, air oxygen becomes the limiting component and the amount of heat released on the working element will be proportional to the oxygen flux  $Q_k$  to the surface of this element [7]. The value of  $\Delta C_m$  in this case will decrease from the maximum value at the volume fraction of methane 9% to zero at 100% methane in the mixture. Assuming that the value of  $\Delta C_m$  in this case decreases linearly, at a methane volume fraction above 9%, the expression for determining  $\Delta C_m$  will take the following form

$$\Delta C_m = \frac{9(100 - C_{mc})}{91} \cdot \left( 1 - \frac{\gamma_f}{\gamma_f + \gamma_e} \right). \quad (3.87)$$

In this case the volume fraction of methane in the chamber will be

$$C_m = C_{mc} - \frac{9(100 - C_{mc})}{91} \cdot \left( 1 - \frac{\gamma_f}{\gamma_f + \gamma_e} \right). \quad (3.88)$$

The methane flux into the chamber  $Q_m$ , oxidized on the working element is usually defined as [7]

$$Q_m = \Delta C_m \gamma_f. \quad (3.89)$$

Oxidation  $Q_m$  uses twice the amount of oxygen  $Q_k$ .

$$Q_k = 2Q_m. \quad (3.90)$$

In turn, the oxygen flux into the reaction chamber depends on the difference of oxygen concentrations in the mixture and in the chamber  $\Delta C_k$  and the diffusive conductivity of the oxygen filter  $\gamma_{fk}$

$$Q_k = \Delta C_k \gamma_{fk}, \quad (3.91)$$

From equations (3.89) – (3.90) follows

$$\Delta C_k = 2\Delta C_m \frac{\gamma_f}{\gamma_{fk}}. \quad (3.92)$$

Taking into account the linear dependence of the filter conductivity on the diffusion coefficients of gases [70], expression (3.92) can be represented in the form of

$$\Delta C_k = 2\Delta C_m \frac{D_m}{D_k}, \quad (3.93)$$

where:

$D_m, D_k$  – diffusion coefficients of methane and oxygen in air,  $m^2/s$ .

Thus, the oxygen supply to the chamber required for oxidation of methane stream  $Q_m$  is provided at the difference of oxygen concentrations in the mixture and in the chamber  $\Delta C_k$ , and, therefore, the volume fraction of oxygen in the chamber  $C_{kk}$  at the volume fraction of methane up to 9% will be as follows

$$C_{kk} = C_{kc} - \Delta C_k = C_{kc} - 2C_{mc} \left(1 - \frac{\gamma_f}{\gamma_f + \gamma_e}\right) \frac{D_m}{D_k}, \quad (3.94)$$

where:

$C_{kc}$  – volume fraction of oxygen in the mixture, %.

Correspondingly, in the range of higher methane concentrations

$$C_{kk} = C_{kc} - 2 \frac{9(100 - C_{mc})}{91} \cdot \left(1 - \frac{\gamma_f}{\gamma_f + \gamma_e}\right) \frac{D_m}{D_k}. \quad (3.95)$$

In turn, the oxygen content in the mine atmosphere decreases linearly with the methane supply. This relationship can be represented as

$$C_{kc} = 0.21(100 - C_{mc}). \quad (3.96)$$

In this case expressions (3.94) and (3.95) can be represented in the form

$$C_{kk} = 0.21(100 - C_{mc}) - 2C_{mc} \left(1 - \frac{\gamma_f}{\gamma_f + \gamma_e}\right) \frac{D_m}{D_k}; \quad (3.97)$$

$$C_{kk} = 0.21(100 - C_{mc}) \left(\frac{\gamma_f}{\gamma_f + \gamma_e}\right) \frac{D_m}{D_k}. \quad (3.98)$$

Oxidation of methane – air mixture on deep oxidation catalysts proceeds according to the known reaction



Oxidation products due to the difference of their concentrations in the chamber and in the mixture are removed from the reaction chamber by diffusion. Similarly (3.93) the difference of volume fraction of carbon dioxide  $\Delta C_{CO_2}$  and water vapor  $\Delta C_{wv}$  in the chamber and in the mixture will be as follows

$$\Delta C_{CO_2} = \Delta C_m \frac{D_m}{D_{CO_2}}, \quad (3.100)$$

$$\Delta C_{wv} = 2\Delta C_m \frac{D_m}{D_{wv}}, \quad (3.101)$$

where:

$D_{CO_2}, D_{wv}$  – diffusion coefficients of carbon dioxide and water vapor in air,  $m^2/s$ .

Taking into account the presence of carbon dioxide  $C_{CO_2C}$  and water vapor  $C_{wvc}$  in the analyzed mixture, their volume fractions in the chamber  $D_{CO_2K}$  and  $D_{wvk}$  will be equal.

$$C_{CO_2K} = C_{CO_2C} + \Delta C_m \frac{D_m}{D_{CO_2}}; \quad (3.102)$$

$$C_{wvk} = C_{wvc} + 2\Delta C_m \frac{D_m}{D_{wv}}. \quad (3.103)$$

Figs. 3.12 and 3.13 show the results of calculation of the difference between the volume fraction of methane in the analyzed mixture and the reaction chamber, changes in the volume fraction of methane, oxygen, carbon dioxide and water vapor in the reaction chamber depending on the methane content in the analyzed mixture. Calculations were performed using the expressions obtained by us at different ratio of filter diffusive conductivity and effective diffusive conductivity of the element. To simplify the analysis when determining the volume fraction of carbon dioxide and water vapor, their content in the analyzed mixture is conditionally assumed to be equal to zero.

As can be seen from Figs. 3.12 and 3.13, the composition of the gas mixture in the reaction chamber of the thermocatalytic sensor significantly differs from the composition of the analyzed mixture, and these differences increase with decreasing diffusive conductivity of the filter.

Let us consider how changes in the gas composition in the reaction chamber will affect the results of measurement by the thermal conductivity sensor, in the case  $\gamma_f = \gamma_e$  and the volume fraction of methane in the mixture of 5%, at which the wide-range analyzers usually switch from the thermocatalytic to the thermoconductometric measurement method. The composition of the analyzed gas mixture and the mixture in the reaction chamber determined for this case is given in Table 3.7. The results of thermal conductivity calculation of the gas mixture, in the case  $\gamma_f = \gamma_e$  and volume fraction of methane in the mixture of 5 %, performed using expressions (3.1) and (3.2) at different heating temperatures of the sensitive element of the thermal conductivity sensor are given in Table 3.8.

Table 3.7

Composition of the analyzed gas mixture and the mixture in the reaction chamber

Mixture name	Volume fraction of mixture components, %				
	CH <sub>4</sub>	O <sub>2</sub>	CO <sub>2</sub>	H <sub>2</sub> O	others
Analyzed mixture	5	20	0	0	75
The mixture in the reaction chamber of the thermocatalytic sensor at $\gamma_f = \gamma_e$	2.5	16.5	3.5	5.1	73.4

Table 3.8

Thermal conductivity of the analyzed mixture and the mixture in the reaction chamber

Mixture name	Thermal conductivity coefficient of the mixture $\lambda \cdot 10^3$ W/m·°C, at the temperature of the thermocouple, °C		
	400	320	210
Analyzed mixture	40.667	37.646	33.431
The mixture in the reaction chamber of the thermocatalytic sensor at $\gamma_f = \gamma_e$	40.362	37.119	32.729

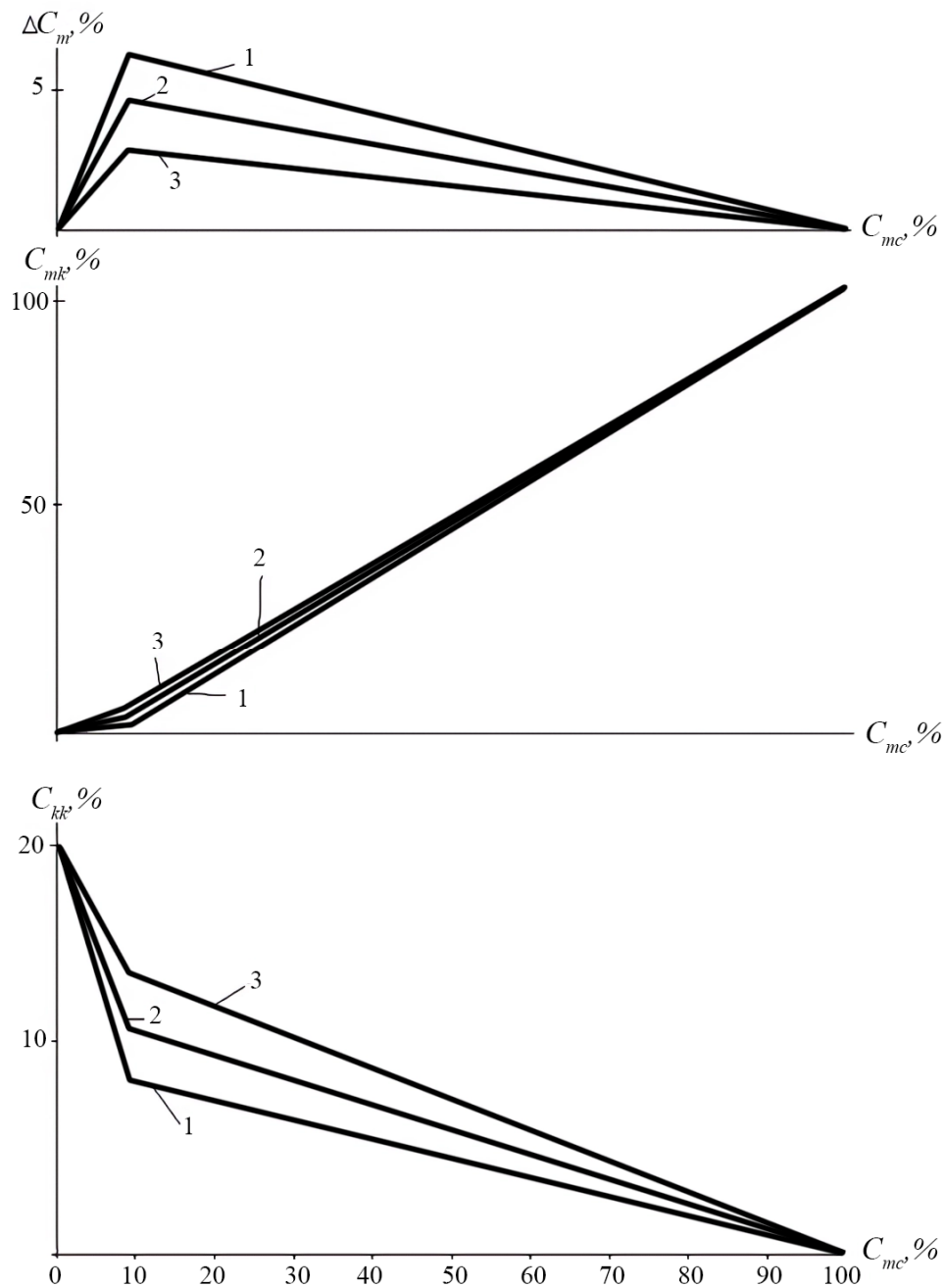


Fig. 3.12. Dependence of concentration pressure, methane and oxygen content in the reaction chamber of the thermocatalytic sensor on the volume fraction of methane in the mixture:  
 1 -  $\gamma_f = 0.5\gamma_e$ ; 2 -  $\gamma_f = \gamma_e$ ; 3 -  $\gamma_f = 2\gamma_e$

Based on the data of Table 3.8, the value of measurement error calculated by expression (3.8), due to the mismatch of the gas composition of the mixture in the reaction chamber of the analyzed mixture, at a volume fraction of methane 5% and heating temperature of thermocouples 400 °C is 0.7%. The maximum value of this error will be at a volume fraction of methane 9% and is 1.26%, which generally meets the requirements for explosion hazard control equipment. However, the experience of methane analyzers operation and their studies in laboratory conditions [16, 17] show that in the presence of high concentration of methane, its higher homologues, hydrogen and carbon oxide in the mine atmosphere and the temperature of preheating of the comparative element of the thermocatalytic sensor 400 °C their intensive oxidation on this element is observed, which leads to failures of the output characteristic of the measuring bridge. In addition, studies [17] have shown that at such a temperature of heating of the comparative element of the thermocatalytic sensor there is an accumulation of products of thermal destruction of hydrocarbons on its surface, which leads to changes in the heat exchange processes. All this practically excludes the possibility of using the comparative element of the thermocatalytic sensor as a thermal conductivity sensor at this thermal mode of its operation.

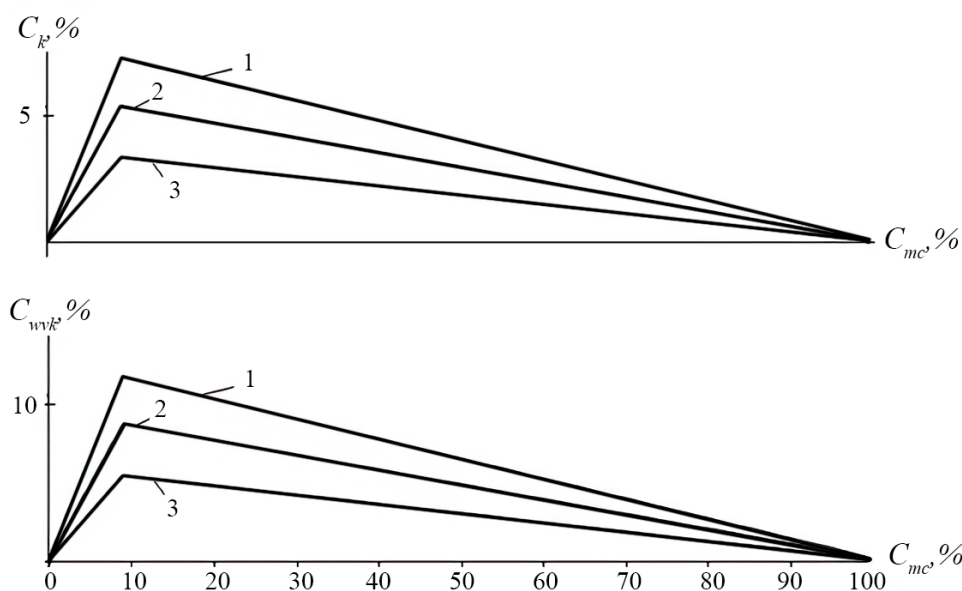


Fig. 3.13. Change in the content of carbon dioxide and water vapor in the reaction chamber of the thermocatalytic sensor at changing the volume fraction of methane in the analyzed mixture:

$$1 - \gamma_f = 0.5\gamma_e; 2 - \gamma_f = \gamma_e; 3 - \gamma_f = 2\gamma_e$$

To exclude the processes of carbonization of the comparative element and oxidation of combustible gases on it, we proposed a measurement method consisting in the use of different thermal modes of thermocouples in thermocatalytic sensors [18]. In this case, the value of the measurement error calculated by expression (3.8), caused by the mismatch of the gas composition of the mixture in the reaction chamber with the analyzed mixture, at the volume fraction of methane 5% and the heating temperature of the comparative thermocouple 320 °C and 210 °C, respectively, is 1.45% and 2.1%, and the maximum value of this error at the volume fraction of methane 9% is 2.61% and 3.78%, respectively. As can be seen, when using a thermocatalytic sensor operating at a lower heating temperature as a thermal conductivity sensor of the comparative thermocouple, the measurement error due to differences in gas composition increases significantly.

It should also be noted that at decreasing the gas diffusion conductivity of the filter, the gas composition in the chamber differs more from the composition of the analyzed mixture (see Fig. 3.12 and 3.13), which leads to an increase in the measurement error. At higher gas diffusion conductivity of the filter, the specified error decreases, but in this case, temperature overloads of the working element of the thermocatalytic sensor are possible, or (when powering from the bridge in the voltage stabilization mode on the working element) there is a significant hysteresis of readings [7].

The above disadvantages limit the possibility of using the comparative element of the thermocatalytic sensor as a thermal conductivity sensor. Therefore, in practice, when developing gas control equipment, when switching from the thermocatalytic method of control to the thermoconductometric one, the catalytic active element is either turned off or its temperature is reduced to the value at which methane combustion on it stops. For example, the serial produced analyzer Signal-9 uses a thermocatalytic sensor with different thermocouple temperature mode, and when switching to the thermal conductivity control mode (at volumetric methane content over 5%) the catalytically active element is shunted. To ensure a stable thermal mode of the comparative element of the thermocatalytic sensor, the mode of powering the measuring bridge with a stable current was chosen.

Let us consider the second variant of the sensor operation at high methane concentrations, when the catalytically active element is turned off when the concentration threshold is reached. The volume fraction of methane, oxygen and other gases in the reaction chamber at the moment of switching off the catalytically active element will be determined according to expressions (3.85), (3.97), (3.102) and (3.103).

After switching off the catalytically active element, the concentration of the gases in the chamber changes until the gas composition and the analyzed mixture is equalized. The rate of change of methane volume fraction in this case will be

$$\frac{dC_{mk}}{dt} = \frac{\gamma_f}{V_w} (C_{mc} - C_{mk}), \quad (3.104)$$

where:

$V_w$  – volume of the reaction chamber, m<sup>3</sup>.

Taking into account the initial conditions, the solution of the equation has the form

$$C_{mk} = C_{mc} - (C_{mc} - C_{mk0}) \exp\left(-\frac{\gamma_f}{V_w} t\right), \quad (3.105)$$

where:

$C_{mk0}$  – volume fraction of methane in the chamber at the moment of shutdown, %.

From expression (3.105) it is clear that the duration of the transient process is determined by the ratio of the diffusive conductivity of the filter to the volume of the reaction chamber. For example, the volume of the reaction chamber of thermocatalytic sensors used in commercially available methane analyzers AT1-1 and AT3-1 is about  $V_w = 4 \cdot 10^{-7}$  m<sup>3</sup>. The experimentally determined value of diffusive conductivity of the metal-ceramic filter of thermocatalytic sensors for these analyzers is  $\gamma_f = 10^{-7}$  m<sup>3</sup>/s [7]. At such values of diffusive conductivity of the filter and the volume of the reaction chamber the time constant is  $\tau = 4$  s and it can be considered that during the time  $3\tau$  the concentrations of methane in the reaction chamber and in the analyzed mixture are practically equalized.

Considering a slightly lower value of the diffusion coefficient of carbon dioxide compared to the diffusion coefficient of methane, the transient gas dynamic process lasts about 20 seconds after turning off the catalytically active element in the sensors. After this time the composition of the gas mixture in the chamber and in the environment can be considered identical.

Disabling or changing the operating mode of the catalytically active element of the sensor by shunting it leads to a decrease in the total heat release from the sensing elements and, accordingly, to a decrease in the average gas temperature in the chamber and the temperature of the comparative element. When analyzing the process of heat transfer from the heated element to the chamber walls [9], the average gas temperature is usually determined as

$$t_t = (t_e + t_k) / 2, \quad (3.106)$$

where:

$t_e$  and  $t_k$  – temperature of the element and the chamber walls, °C.

In turn, our studies of the gas medium parameters influence on the thermocouple temperature modes in methane analyzer bridge circuits [19] have shown that at a stable value of the current flowing through the sensitive elements, a change in the temperature of the chamber walls by the value  $\Delta t_k$  leads to an increase in the temperature of the element and the average gas temperature in the chamber by a similar value.

Heat generated by sensitive elements of the thermocatalytic sensor is removed from the reaction chamber to the environment due to the presence of temperature pressure  $\Delta t_d$  by means of heat conduction of air and sensor mounting elements, convection, heat conduction of current conductors and radiation. Thermal pressure

$$\Delta t_d = t_c - t_d \quad (3.107)$$

depends on the heat generation of the sensing elements and heat transfer conditions. The main forms of heat transfer from the sensor to the environment are conduction and convection. The process of heat transfer due to conduction of the gas medium and convection is usually simplified and considered as conductive heat transfer. In this case it can be written

$$P_e = \alpha_k F_k \Delta t_d + \alpha_f F_f \Delta t_d = (\alpha_k F_k + \alpha_f F_f) \Delta t_d, \quad (3.108)$$

where:

$\alpha_k, \alpha_f$  – heat transfer coefficients of mounting elements and filter, W/(m<sup>2</sup>·°C);

$F_k, F_f$  – contact area of sensor base with mounting elements and filter area, m<sup>2</sup>.

As can be seen from expression (3.108) the heat pressure in this case is linearly related to the power released in thermoelements, which in turn is determined by the power released during the passage of electric current and the power released on the active element due to methane oxidation. When the active element is turned off, this power and, consequently, the thermal pressure  $\Delta t_d$ , are reduced by more than two times.

Thermal pressure  $\Delta t_d$  in methane analyzers is within the range of 10-20 °C. In this case, when the active element is turned off, the value of  $\Delta t_k$  can be more than 10 °C and the temperature of the comparative element can decrease by the same value. It is obvious that in this case measurements by the thermal conductivity sensor are possible only after the end of the transient thermal process or when nodes and elements ensuring stable temperature of the reaction chamber are introduced into the analyzer.

Unlike transient gas dynamic processes in thermocatalytic and thermoconductometric gas analyzers, transient thermal processes are much slower. Thus, the warm-up time after turning on for different types of analyzers is standardized in the range from 10 to 60 minutes [19]. The duration of the transient thermal process in analyzers is determined by the mass and heat capacity of the structural elements of the sensor and the conditions of heat exchange. By analogy with (3.104), the equation describing the temperature change of the reaction chamber can be simplified as follows

$$\frac{dt_k}{dt} = \frac{\alpha_k F_k + \alpha_f F_f}{m_0 C_0 + m_f C_f} (t_c - t_k), \quad (3.109)$$

where:

$m_0, m_f$  – mass of the sensor and filter base, kg;

$C_0, C_f$  – heat capacity of the sensor and filter base material, J/(kg·K).

Taking into account the initial conditions, the solution of the equation has the form

$$t_k = t_{k0} + (t_c - t_{k0}) \left[ 1 - e^{-\left( \frac{\alpha_k F_k + \alpha_f F_f}{m_0 C_0 + m_f C_f} t \right)} \right], \quad (3.110)$$

where:

$t_{k0}$  – chamber temperature at the moment of element shutdown, °C.

The heat transfer coefficient of the filter depends on the value of forced air convection, which in turn depends on the air velocity in the mine workings and design features of the elements providing gas exchange between the sensor and the environment. The minimum value of  $\alpha_f$  will be in the absence of forced air convection. Its value in this case will be determined by the air thermal conductivity coefficient and the thickness of the gas layer between the filter and the analyzer body.

The heat transfer coefficient of the mounting elements when installing the sensor base into the sealing rubber ring will actually be determined by the thermal conductivity coefficient of the ring material  $\lambda_k$  and its thickness  $d_k$

$$\alpha_k = \lambda_k d_k. \quad (3.111)$$

The maximum value of the time constant calculated taking into account the real parameters of the analyzer “Signal-9” sensor in the absence of forced air convection is 123 seconds. Consequently, the transient process associated with the change of the temperature mode in the reaction chamber due to the shutdown of the catalytically active element lasts up to 6 minutes.

It is possible to exclude transient thermal and gas-dynamic processes at switching off or shunting of the catalytically active element in thermocatalytic sensors of gas analyzers at separate supply of the analyzed mixture to the sensor’s sensitive elements, i.e. placing sensitive elements under separate gas diffusion filters. In the proposed two-chamber thermocatalytic sensors [11], the gas diffusion resistance of the chamber filter with the comparative element was chosen several orders of magnitude higher than the resistance of the chamber filter with the working element in order to exclude failures in the analyzers’ operation at high methane concentrations caused by oxidation of combustible gases on the comparative element. In our case, when using the comparative element of the thermocatalytic sensor as a thermal conductivity sensor, the gas diffusion resistance of the chamber filters should be chosen the same, and to exclude the oxidation of combustible gases on the comparative element and its carbonization, our proposed measurement method should be used, which differs in the choice of thermal modes of thermocouples [18, 19].

It is possible to provide thermal modes of sensing elements in different ways, for example, by making thermoelements with different resistances or different sizes [18, 20]. Studies [21, 22] have shown that when using thermistors with the same initial resistance, but with different surface area and powering the measuring bridge from a stable current source, thermal stability of the bridge is ensured under the condition of its symmetry, which is implemented by including an additional resistance in the bridge branch with a comparative element. The bridge sensitivity and its power supply parameters in this case are similar to the specified parameters of the bridge with a serial thermocatalytic sensor.

Placement of sensing elements under separate filters allows to completely exclude transient temperature and gas-dynamic processes when the analyzer switches to the thermal conductivity measurement mode, and at the same time it ensures the identity of gas composition in the chamber with the comparative element of the thermocatalytic sensor and in the environment regardless of the operating modes of the catalytically active element. Besides, at significant limitation of analyzed medium supply to the reaction chamber with catalytically active element.

The heating temperature of the thermocatalytic sensor comparative element, which is used as a thermal conductivity sensor, should be chosen in the range of 240 °C – 250 °C. This makes it possible to exclude oxidation of higher homologues of methane, hydrogen and carbon oxide, which may be present in the mine gas, and also to prevent accumulation of products of thermal destruction of hydrocarbons on its surface [17, 23].

When the bridge with a thermocatalytic sensor is powered by a stable current source and its comparative element is used as a thermal conductivity sensor, the methane volume fraction is determined by the value of the voltage on this element. In turn, in such a power supply mode, the value of this voltage depends on both the thermal conductivity of the mixture and its temperature [20]. Therefore, in this case it is mandatory to have a temperature sensor in the analyzer and to correct the measurement results based on its readings.

At the same time, the placement of sensitive elements under separate filters and the use of different temperature modes of the elements allows to simultaneously use two measuring bridges for measuring low and high methane concentrations without changing the analyzer power supply parameters. The proposed bridge circuit of the general-purpose wide-range methane analyzer is shown in Fig. 3.14.

In the proposed bridge (Fig. 3.14), the output voltage of the thermocatalytic sensor  $U_{out1}$  is removed from the diagonal of the first bridge (point AB), one branch of which is formed by the working thermocatalytic sensor thermocouple and the comparative element, compensating element and additional resistors included in series, and the second branch by ballast resistors  $R_1$ ,  $R_2$ . The initial resistance of the comparative and compensating element in this case is as follows

$$R_{0c} = R_{0k} = 0.5R_{0w}. \quad (3.112)$$

The surface area  $F_c = F_w$ , and the area of the compensating element  $F_k \gg F_c$ .

The ballast resistors  $R_3$  and  $R_4$  are to be chosen several orders of magnitude higher than the resistance of thermocouples and can be ignored in the analysis. If the resistance value of additional and ballast resistors is independent of the supply and gas medium parameters, the condition of zero conservation of the balanced bridge will be

$$\frac{\Delta U_w}{\Delta U_{ck}} = \frac{U_w}{U_{ck}}, \quad (3.113)$$

where:

$U_w, \Delta U_w$  – voltage on the working element and its change with uncontrolled parameters, V;

$U_{ck}, \Delta U_{ck}$  – voltage on the bridge branch with the comparative and compensating elements and its change with uncontrolled parameters, V.

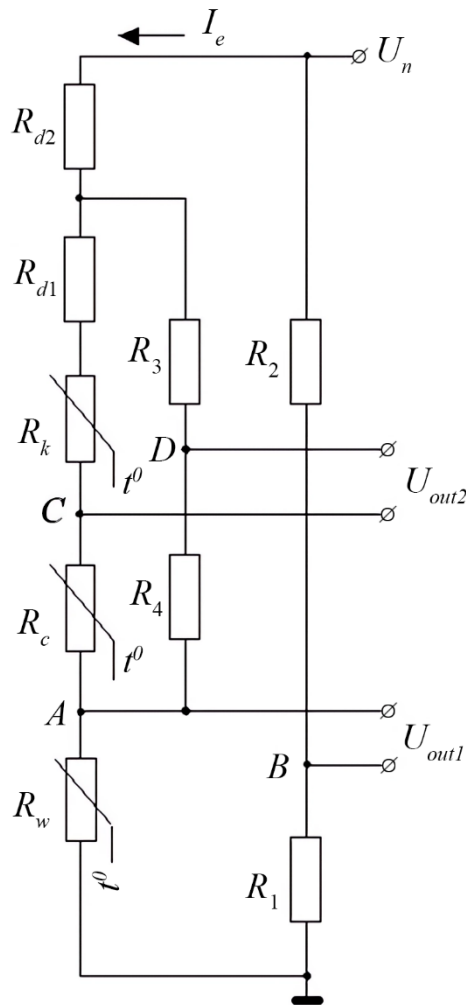


Fig. 3.14. Bridge circuit of the universal wide-range methane analyzer:  $R_w, R_{compar}$  – working and comparative thermocatalytic sensor thermocouples;  $R_{compen}$  – compensating thermocouple of the thermoconductometric sensor;  $R_{add1}, R_{add2}$  – additional resistors;  $R_1 - R_4$  – ballast resistors

Based on (3.9) the voltage on the working thermocouple will be

$$U_w = I_e R_{0w} (1 + \beta t_t) + \beta b_{0w} R_{0w} I_e^3. \quad (3.114)$$

Voltage on the second bridge arm will be

$$U_{ck} = I_e (R_{0c} + R_{0k}) (1 + \beta t_t) + \beta I_e^3 (b_c R_{0c} + b_k R_{0k}) + I_e (R_{d1} + R_{d2}). \quad (3.115)$$

At stable current, all values included in expressions (3.112) and (3.115) are independent of the gas temperature. In this case

$$\frac{dU_w}{dt_c} = I_e R_{0w} \beta; \quad (3.116)$$

$$\frac{dU_{ck}}{dt_c} = I_e \beta (R_{0c} + R_{0k}). \quad (3.117)$$

Based on expressions (3.116) and (3.117), when symmetrizing the bridge by selecting the additional resistance, in the case of gas medium temperature change, condition (3.113) is fulfilled if

$$R_{0c} + R_{0k} = R_{0w}. \quad (3.118)$$

Thus, at the chosen value of the initial resistance of the elements (3.112) and powering the bridge from a stable current source, the symmetric bridge with a thermocatalytic sensor is thermally stable.

The output voltage of the thermoconductometric sensor  $U_{out2}$  is removed from the diagonal of the second bridge (point CD). One branch of this bridge is formed by the comparative thermocouple of the thermocatalytic sensor, as well as by the compensation element and additional resistor  $R_{add1}$  in series, and the second branch by ballast resistors  $R_3$  and  $R_4$  (Fig. 3.14).

The voltage value on the comparison element, which in this bridge acts as a sensing element of the thermoconductometer sensor, will be

$$U_c = I_e R_{0c} (1 + \beta t_t) + \beta b_c R_{0c} I_e^3. \quad (3.119)$$

Voltage on the second arm of the bridge

$$U_k = I_e R_{0k} (1 + \beta t_t) + \beta b_k R_{0k} I_e^3 + I_e R_{d1}. \quad (3.120)$$

At stable current, all values included in expressions (3.119) and (3.120) are independent of the gas temperature. In this case

$$\frac{dU_c}{dt_c} = I_e R_{0c} \beta; \quad (3.121)$$

$$\frac{dU_k}{dt_c} = I_e R_{0k} \beta. \quad (3.122)$$

Proceeding from expressions (3.121) and (3.122), at symmetrization of the bridge by selection of additional resistance, selected initial resistance of elements (3.64) and powering the bridge from a stable current source, the symmetric measuring bridge with a thermoconductometric sensor is also thermally stable.

Using the obtained expressions (3.112), (3.113), (3.119), (3.120), as well as the dependences of temperature and resistance of thermocouples on their parameters and modes of operation, we calculate the additional resistances required for symmetrization of bridges and temperature modes of elements. Calculations will be performed at the following parameter values:  $I_e = 0.2$  A;  $R_{0w} = 2.0$  Ohm;  $R_{0c} = R_{0k} = 1.0$  Ohm;  $\beta = 0.004$  1/°C;  $t_t = 20$  °C;  $b_p = 1 \cdot 10^4$  °C/A<sup>2</sup>;  $b_c = 0.5 \cdot 10^4$  °C/A<sup>2</sup>;  $b_k = 0.05 \cdot 10^4$  °C/A<sup>2</sup>.

The calculated values of temperature conditions and additional resistances at the specified parameters are:  $t_w = 420$  °C;  $t_c = 220$  °C;  $t_k = 40$  °C;  $R_{d1} = 0.72$  Ohm;  $R_{d2} = 1.6$  Ohm.

Thus, when using the bridge shown in Fig. 3.8 with the specified parameters of the elements and powering it from a stable current source, the thermal stability of the analyzer and the possibility of measuring the methane concentration in the entire range of its possible values are provided. When setting up the analyzer, first of all zero setting and thermal balancing of the bridge with the thermal conductivity sensor is performed, and then zero setting and thermal balancing of the bridge with the thermocatalytic sensor is performed.

It should also be noted that the use of a two-chamber sensor also eliminates the mutual thermal influence of thermoelements when changing the spatial position of the sensor. Besides, placement of only one element in the reaction chamber and absence of the screen installed in single-chamber sensors to reduce the mutual thermal influence of the elements, allows to significantly reduce the volume of the reaction chamber and, consequently, to reduce the time constant of the thermocatalytic sensor and to increase the analyzer performance.

### 3.7. Conclusions

Based on the research performed in this section, the following conclusions can be drawn:

1. To ensure the safety of methane-air mixtures disposal captured by mine degasification systems, methane content measurement error, due to changes in the moisture content of the mixture, may not be taken into account when controlling the gas mixture explosion hazard by thermoconductometric gas analyzers.
2. Methane thermoconductometric sensors, that operate at the sensitive elements temperature up to 120 °C, have a large measurement error from carbon dioxide. Increasing the sensitive elements temperature of the sensor decreases this error, but in order to prevent oxidation of combustible gases on the thermocouples their temperature should be more than 300 °C. Taking this into account, it is reasonable to set the sensitive element temperature of the thermoconductometric sensor in the range of 210 °C – 250 °C.
3. The measurement error of the thermal conductivity sensor, due to the presence of carbon monoxide, is insignificant and is no more than 0.1% per 1% of the volume fraction of carbon monoxide in the analyzed mixture.
4. To reduce the safety margin due to the presence of flammable impurities in mine gas, the effect of hydrogen on explosion hazard controls can be disregarded.
5. The presence of carbon dioxide in gas mixtures increases the safety reserve provided for by regulatory documents, which is undesirable when using co-opted gas mixtures as fuel, because it leads to an increase in the volume of forced discharge of substandard gas mixtures through candles into the atmosphere and deterioration of economic performance of the equipment. Therefore, in order to reduce losses of explosion hazard control of gas mixtures in degassing systems it is advisable to control the volume fraction of carbon dioxide in mixtures used for energy purposes and to adjust the readings of methane analyzers depending on the content of CO<sub>2</sub> in the disposed mixture.
6. The use of a single-chamber thermoconductometric sensor with unequal electrothermal parameters of sensitive elements for measuring high concentrations of methane allows to simplify the design of the analyzer sensor, to exclude long transients arising from changes in the temperature of the gas mixture, eliminates the disadvantages of two-chamber analyzers associated with violations of the tightness of the comparison chamber. To ensure stability of the bridge zero at changing ambient temperature when designing analyzer sensors, it is necessary to choose platinum thermocouples with the same initial resistance and stable bridge current supply mode.
7. When using a single-chamber thermoconductometric sensor with unequal electrothermal parameters of sensitive elements and powering the bridge from a stable voltage source, the equality of initial resistances of the elements does not ensure temperature stability of zero. At fluctuations of medium temperature the resistance change of the less heated comparative element is greater than that of the working one. Zero stability of the bridge in this case is ensured by including a shunt resistor in parallel to the comparative thermocouple with subsequent selection of its value.

8. In the single-chamber thermoconductometric sensor, in case of using the comparative element as a temperature sensor of the measuring chamber body and introducing a heating element into the analyzer circuit and stabilizing the temperature of the measuring chamber surface and the working thermocouple, an unambiguous relationship between the methane concentration and the current increment through the working thermocouple is provided.
9. It is possible to provide operability of methane analyzers at emergency mine gasification by using different thermal modes of sensitive elements in thermocatalytic sensors. When choosing the temperature of the working element 400 °C, and the temperature of the comparative element below 300 °C, carbonization of both elements is actually excluded, the stability of zero and sensitivity of the sensor is ensured, and the low temperature of the comparative element excludes the possibility of methane and combustible components oxidation, characterized by low ignition temperature on it at emergency gassing of mine workings.
10. It is possible to provide the specified thermal modes of sensing elements by making thermocouples with different resistances, different surface areas or by shunting a comparative thermocouple of an existing commercially available symmetrical thermocatalytic sensor.
11. When shunting the comparative element of the existing commercially available symmetrical thermocatalytic sensor, the bridge is thermally unbalanced at any mode of its power supply, so this solution can be only implemented with additional introduction of a temperature sensor into the analyzer and correction of the analyzer zero based on the readings.
12. Temperature stability of the bridge with a thermocatalytic sensor, characterized by the use of thermocouples with the same initial resistance and different surface area, is provided under the condition of symmetry of the measuring bridge by including an additional resistor in the bridge branch with a comparative element and its power supply from a stable current source. When the bridge operates in the mode of voltage stabilization on the working element, the temperature stability of the bridge is achieved by introducing an additional resistor in the branch of the bridge with the comparative thermocouple, the resistance of which is comparable to the initial resistance of the thermocouple, which leads to a significant asymmetry of the bridge and a significant additional power loss on the additional resistor.
13. When using thermoresistors with the same surface area but with different initial resistance, temperature stability of the bridge with thermocatalytic sensor is provided in the voltage stabilization mode on the working element under the condition of bridge symmetry by introducing an additional resistor into the bridge arm with the comparative element. When powering the bridge from a stable current source, the stability of the bridge is achieved by introducing an additional resistor, the resistance of which is insignificant, into the branch of the bridge with the comparative thermocouple, which makes it possible to slightly reduce the power consumed by the sensor, but the measuring bridge remains asymmetrical.
14. When using two-chamber sensors, there is a possibility of separate control of the diffusive conductivity value of the filters while maintaining the electrothermal analogy of the elements. To ensure high sensitivity and small time constant of the analyzers, the diffusive conductivity of the filter of the sensor chamber in which the working element is installed, should be commensurate with the effective diffusive conductivity of the working element, and the diffusive conductivity of the sensor chamber filter in which the comparative element is installed, can be set several orders of magnitude less than that of the first chamber.
15. Designing two-chambered thermocatalytic sensors with diffusive conductivity of the chamber filter, in which a comparative element of significantly lower diffusion conductivity of the chamber filter with a working element is installed, allows to significantly improve metrological and operational characteristics of gas analyzers, to exclude cases of their ambiguous function after long-term operation and in the presence of components in gas mixtures capable to oxidize on the comparative element at the temperature of preheating of elements.
16. The technique of simultaneous experimental optimization of design and technological parameters of sensitive elements and combustible gas sensor is proposed; it allowed to choose optimal parameters of methane analyzers based on the ranking of influencing factors on the characteristics of sensitive elements and sensors.

17. The use in general-purpose wide-range methane analyzers as a thermal conductivity sensor of the comparative element of a single-chamber thermocatalytic sensor operating at the heating temperature of the thermocouple up to 400 °C is inadmissible, since in the presence of high methane concentration, its higher homologues, hydrogen and carbon monoxide in the mine atmosphere their intensive oxidation on this element is observed, which leads to the appearance of large measurement errors.

18. When using a single-chamber thermocatalytic sensor operating at the heating temperature of the thermocouple 210 °C – 250 °C as a thermal conductivity sensor of the comparative element, the measurement error due to differences in the gas composition in the reaction chamber and the analyzed gas mixture increases significantly.

19. The unambiguity of the gas composition in the reaction chamber of the single-chamber sensor and the analyzed gas mixture is provided by turning off or shunting the catalytically active element, but this leads to the appearance of long transient thermal processes.

20. It is possible to exclude transient thermal and gas-dynamic processes at shutdown or shunting of the catalytically active element in thermocatalytic sensors of gas analyzers at separate supply of the analyzed mixture to sensitive elements of sensors, i.e. at placement of sensitive elements under separate gas-diffusion filters.

21. When the bridge with a two-chamber thermocatalytic sensor is powered by a stable current source and its comparative element is used as a thermal conductivity sensor, the methane volume fraction is determined by the voltage on this element. In this case it is obligatory to have a temperature sensor in the analyzer and to correct the measurement results based on its readings.

22. Placement of sensitive elements under separate filters and the use of different temperature modes of the elements allows, without changing the analyzer power supply parameters, to simultaneously use two bridges for measuring low and high methane concentrations. When using the proposed bridge with the calculated parameters of the elements and powering the bridge from a stable current source, the thermal stability of the analyzer and the possibility of measuring methane concentration in the entire range of possible values are ensured.

23. When using a two-chamber sensor, the mutual thermal influence of thermoelements is eliminated when changing the spatial position of the sensor. Placement of only one element in the reaction chamber and absence of the screen installed in single-chamber sensors to reduce the mutual thermal influence of elements, allows to significantly reduce the volume of the reaction chamber and, consequently, to reduce the time constant of the thermocatalytic sensor and to increase the analyzer's performance.

## References

- [1] Karpov E.F., Ryazanov A.V. (1974) Thermal method of control of methane concentration in degassing pipelines. *Scientific reports of the A.A. Skochinsky Institute of Mining Engineering*, (121), 138-143 [in Russian]
- [2] Bretschneider S. (1966) *Properties of gases and liquids*. M.-L.: Khimiya [in Russian]
- [3] Karpov E.F., Ryazanov A.V. (1983) *Automation and control of degassing systems*. M.: Nedra [in Russian]
- [4] Kotlyarov, A.K. (2008) Influence of gas mixture uncontrolled parameters on their explosive properties and gas analysers measurement error. *Zbirka naukovykh prats NSU*, (30), 272-279 [in Russian]
- [5] *Safety regulations in coal mines*. (2010) DNAOP 1.1.30-1.01-10. Kyiv: Osnova [in Ukrainian]
- [6] Frundin, V.E. (1999) Single-chamber thermoconductometric sensor. *Collection of scientific articles NGA Ukraine*, (5), 168-171 [in Russian]
- [7] Holinko V.I., Kotlyarov A.K., Belonozhko V.V. (2004) *Control of explosion hazard in mine workings* D.: Nauka i Obrazovanie [in Russian]
- [8] Holinko, V.I.; Kotlyarov, A.K. (2006) Theoretical substantiation of thermoconductometric methane sensor

- parameters with non-isolated comparative element. *Collection of scientific articles of NSU*, (26), 60-67. [in Russian]
- [9] Holinko V.I., Kotlyarov A.K. (2006) Study of heat exchange process in thermoconductometric methane sensors / Ways and means of creating safe and healthy working conditions in coal mines. *Collection of scientific articles*, (18), 301-314. Makeevka-Donbass: MakNII [in Russian]
- [10] Holinko, V.I.; Kotlyarov, A.K. (2007) Development and research of single-chamber thermoconductometric methane sensor. *Naukovy visnik NSU*, (6), 85-89 [in Russian]
- [11] Holinko V.I. Belonozhko A.V. (2006) Improvement of thermocatalytic method of control of methane content in mine atmosphere. *Girnycha Elektromechanika ta Avtomatika*, (77), 81-87. [in Russian]
- [12] Holinko, V.I.; Kotlyarov, A.K.; Belonozhko, A.V. (2008) Improvement of stationary means of explosion hazard control of gas mixtures. Development of ore deposits. *Nauchno-tekhnicheskyy sbornik*, (92), 222-225.
- [13] Bilonozhko, V.V., Bilonozhko, V.P., Bilonozhko, V.I., Holinko, V.I., Kotlyarov, A.K. et al. *The system for monitoring the content of combustible gas in the mine atmosphere* Pat. Ukraine 61611A, MK G01N25/22, E21F17/18. Published 17.11.03. Bulletin No. 11 [in Ukrainian]
- [14] Kotlyarov A.K., Holinko V.I., Bilonozhko O.V., Bilonozhko V.V. The analyzer of combustible gases Pat. 79969 Ukraine, MPK G01N 25/22, E21 F17/18. Published. 10.08.07. Bul. No. 12 [in Ukrainian]
- [15] Holinko, V.I.; Romanenko, V.I.; Frundin, V.Yu. (2003) *Justification of the bridge circuit in thermocatalytic gas analysers*. Collection of scientific articles of NSU. 17, vol. 2. (pp. 352-357) [in Russian]
- [16] Holinko, V.I.; Belonozhko, A.V. (2006) Study of thermocatalytic methane sensors performance after their long-term operation. *Naukovy visnik NSU*, (10), 72-75 [in Russian]
- [17] Holinko, V.I.; Belonozhko, A.V. (2008) Study of hydrocarbon thermal degradation products accumulation on the surface of thermocouples. *Naukovy visnik NSU*, (7), 60-65 [in Russian]
- [18] Holinko, V.I.; Kotlyarov, A.K.; Belonozhko, A.V. (2008) *Development of methane control methods to ensure the performance of analysers in case of emergency gasification of mine workings: materialy mizhnarodnoyi naukovo-praktychnoyi konferentsiyi "Forum Girnikiv-2008"* (pp. 33-43). D.: National Mining University [in Russian]
- [19] Holinko, V.I.; Kotlyarov, A.K. (2006) Study of temperature modes of thermocouples in bridge circuits of thermoconductometric methane analysers. *Naukovy visnik NSU*, (12), 55-58 [in Russian]
- [20] Holinko, V.I.; Kotlyarov, A.K. (2006) Theoretical substantiation of thermoconductometric methane sensor parameters with non-isolated comparative element. *Collection of scientific articles of NSU*, (26), 60-67 [in Russian]
- [21] Sobolev, V., Bilan, N., Dychkovskiy, R., Caseres Cabana, E., & Smolinski, A. (2020). Reasons for breaking of chemical bonds of gas molecules during movement of explosion products in cracks formed in rock mass. *International Journal of Mining Science and Technology*, 30(2), 265-269. doi:10.1016/j.ijmst.2020.01.002
- [22] Holinko V.I., Kotlyarov A.K., Belonozhko A.V. Investigations of thermocatalytic methane sensors with different thermal modes of sensitive elements: *materialy mizhnarodnoyi naukovo-praktychnoyi konferentsiyi "Forum Girnikiv-2009"* (pp. 7-14). D.: National Mining University [in Russian]
- [23] Pivnyak, G., Falshtynskiy, V., Dychkovskiy, R., Saik, P., Lozynskiy, V., Cabana, E., & Koshka, O. (2020). Conditions of Suitability of Coal Seams for Underground Coal Gasification. *Key Engineering Materials*, (844), 38-48. doi:10.4028/www.scientific.net/kem.844.38

#### **4. Monitoring of explosion hazard control devices and the ways of their further improvement (written with the participation of Oleksandr Holinko)**

##### **4.1. Development of zero-readings automatic control methods of thermocatalytic gas analyzers**

Operation of the existing stationary methane content control devices is associated with significant costs due to the need to periodically check their performance. The issues of automatic diagnostics of such devices have not yet found a satisfactory solution, especially in the diagnostics of the main element of control devices, the thermogroup, the reliability of which is significantly lower than the reliability of other elements.

In general, diagnostics can be done either automatically, with an internal timer, or by an external request, for example, a request from the surface during a repair shift. For existing stationary control equipment having individual telemetering channels, it is most simple to perform diagnostics by request from the surface. However, the wide introduction of microprocessors for processing information from primary transducers determines that the most promising is the implementation of diagnostics of gas analyzers performance in automatic mode.

The conducted studies of thermocatalytic methane control devices allowed to significantly improve their reliability and stability of such gas analyzers [1, 2]. However, difficult operating conditions of gas analyzers (accidental impacts, flooding, extreme factors, etc.) as well as unauthorized interference in the analyzers' operation can affect the performance and stability of the analyzers, and this, in turn, can lead to failure of explosion protection devices, which is one of the causes of accidents in mines. An example of this is the accident with numerous fatalities caused by the explosion of methane - air mixture, which occurred on March 2, 2017 at the mine "Stepova" SE "Lvivvuhillia", where, despite the presence of the hazard control system UTAS, there was no protective shutdown of the electrical network in the presence of explosive concentration of methane, which was one of the causes of the explosion.

According to the current operating instructions for the existing stationary methane control devices, it is necessary to perform daily checks of their operability and periodically test them in mine conditions using certified gas mixtures, which causes significant operating costs.

When operating gas analyzers, zero-readings are checked by supplying clean ambient air to the sensors. It is difficult to perform this check automatically. Another way to check zero is to briefly switch the thermogroup of the gas analyzer to such a mode of operation when no methane oxidation occurs on the working element [1]. Attempts to develop such a method of automatic diagnostics were made back in the eighties [3], however, taking into account the relatively low level of electronics development and insufficient study of the processes occurring in thermocatalytic sensors, all of them were unsuccessful. Aforementioned is caused by the fact that during thermocatalytic sensors manufacturing it is impossible to provide absolutely identical parameters of thermocouples in the thermogroup, so the reduction of current through the elements always leads to a significant shift of zero of the bridge.

The second way of diagnosing the zero of the gas analyzer can be implemented only when the bridge zero is provided at least in two modes of its operation, one of which is nominal and the other is verification mode, which differs from the first one by the fact that methane oxidation on the sensing element does not occur. In fact, this means that bridge balancing should be such that the voltampere characteristics of the working and comparison elements coincide or intersect at least in two points (Fig. 4.1).

It is impossible to ensure both the identity of the voltampere characteristics of the working and comparison elements and their intersection at two points when using typical thermocatalytic sensor inclusion circuits into a bridge [1].

Application of the thermocatalytic sensor inclusion circuit proposed in [4] (Fig. 4.1) makes it possible to significantly converge the voltampere characteristics of the elements. Since the proposed circuit has two control elements and allows us to change the steepness of the voltampere characteristics of the elements, the question arises, can we achieve the intersection of the voltampere characteristics of the thermocouples at the two points of interest and thus realize automatic diagnostics of the zero of the bridge when using such a circuit.

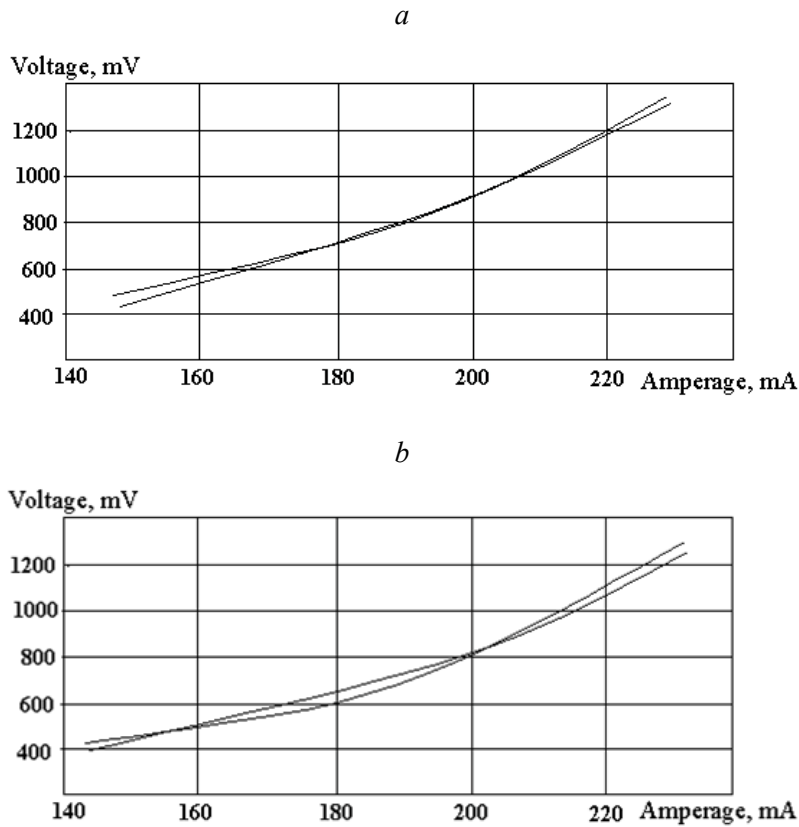


Fig. 4.1. Voltampere characteristics of thermocouples:  
*a* – in a real measuring bridge; *b* – intersecting in two points

To simplify the analytical calculations, we will analyze the operation of the thermocatalytic sensor inclusion circuit with thermal balancing of elements for a simplified version of the circuit, when the shunt chain is included in parallel to the element with a steeper voltampere characteristic (Fig. 4.3). This circuit provides bridge balancing similarly to the circuit shown in Fig. 4.2, but its use assumes the necessity of preliminary identification of the thermal element having a steeper voltampere characteristic.

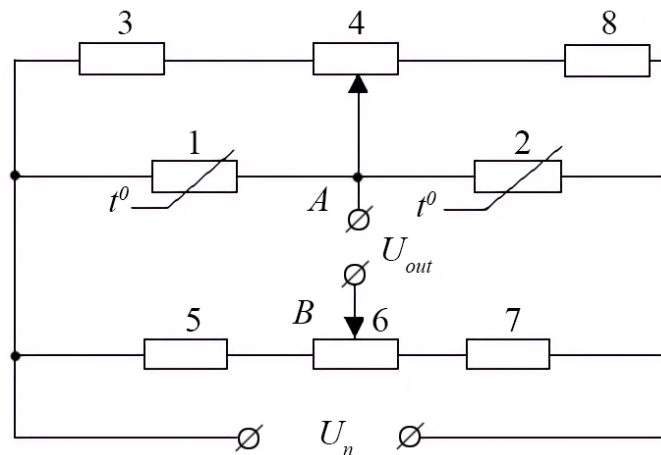


Fig. 4.2. Thermocatalytic sensor inclusion circuit with element thermal balancing:  
 1, 2 – thermoelements; 3, 4, 8 – shunt resistors; 5, 6, 7 – ballast resistors

Let's present the voltage dependence on the thermocatalytic sensor thermocouple on the current (2.71)

$$U_e = I_e R_{0e} (1 + \beta t_t) + \beta b_e R_{0e} I_e^3. \quad (4.1)$$

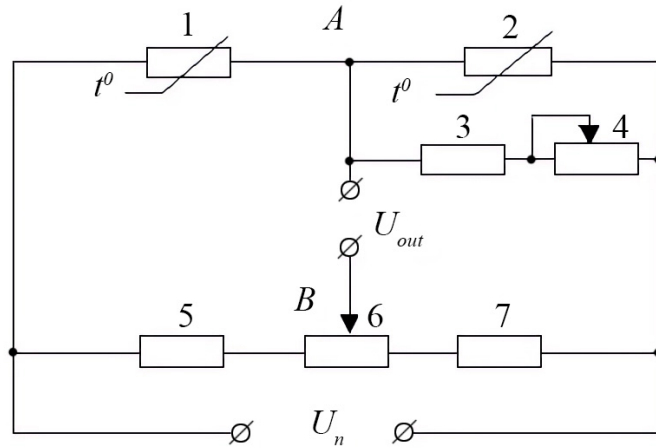


Fig. 4.3. Bridge circuit with shunt chain inclusion in parallel to the element with higher steepness of voltampere characteristic: 1, 2 – thermoelements; 3, 4 – shunt resistors; 5 – 7 – ballast resistors

Let us assume that the steepness of the voltampere characteristic of thermocouple 2 is greater than that of thermocouple 1 (Fig. 4.4). In this case, in a conventional bridge (without shunt resistors 3, 4 in Fig. 4.3), zero adjustment is carried out by shifting the potential of point B (Fig. 4.3) in the bridge arm formed by ballast resistors by the value of  $U_{ic}$ , which is equivalent to shifting the voltampere characteristic of thermocouple 1 by the same voltage.

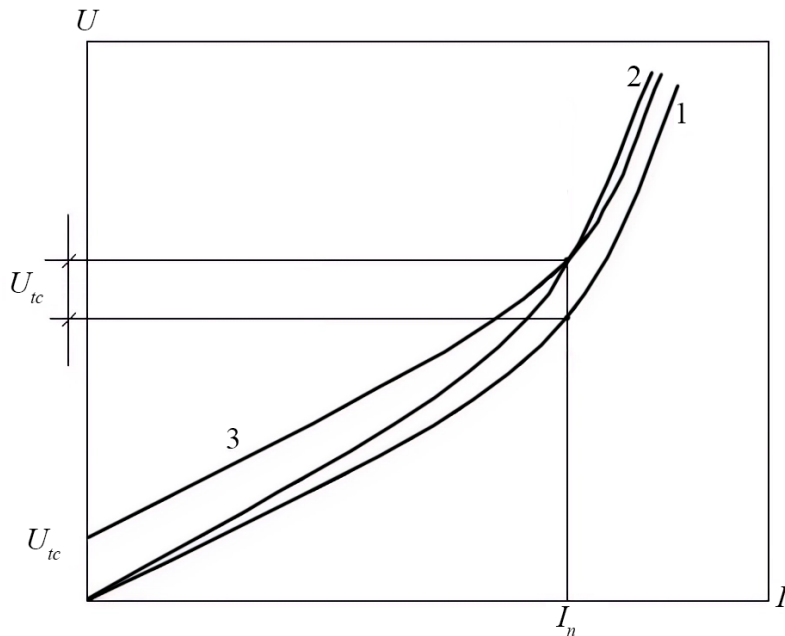


Fig. 4.4. Voltampere characteristics of thermocouples in the absence of shunt resistors: 1 – of the 1st element; 2 – of the 2nd element; 3 – of the 1st element at displacement by  $U_{ic}$

In this case, in the absence of shunt resistors, the voltampere characteristic of thermocouple 2 and the shifted characteristic of thermocouple 1 will be described by the equations

$$U_1 = U_{ic} + I_e R_{01} (1 + \beta t_t) + \beta b_1 R_{01} I_e^3; \quad (4.2)$$

$$U_2 = I_e R_{02} (1 + \beta t_t) + \beta b_2 R_{02} I_e^3; \quad (4.3)$$

where:

$I$  – current through thermocouples in the absence of shunt resistors, A.

When shunt resistors are connected to thermocouple 2, the following system of equations can be written to determine the voltampere characteristic of the bridge branch with resistors connected in parallel

$$U_2 = I_2 R_{02} (1 + \beta t_t) + \beta b_2 R_{02} I_e^3; \quad (4.4)$$

$$U_2 = I_{sh} R_{sh}, \quad (4.5)$$

where:

$I_2$  and  $I_{sh}$  – current through thermocouple 2 and shunt chain, respectively.

Given that

$$I_2 = I - I_{sh} = I - \frac{U_2}{R_{sh}} \quad (4.6)$$

the equation implicitly describing the voltampere characteristic of the bridge branch with the thermocouple and shunt resistors in parallel, we obtain in the form

$$U_2 = \left( I - \frac{U_2}{R_{sh}} \right) R_{02} (1 + \beta t_t) + \beta b_2 R_{02} \left( I - \frac{U_2}{R_{sh}} \right)^3. \quad (4.7)$$

Let's disclose the last component in expression (4.7)

$$\left( I - \frac{U_2}{R_{sh}} \right)^3 = I^3 - 3I^2 \frac{U_2}{R_{sh}} + 3I \left( \frac{U_2}{R_{sh}} \right)^2 - \left( \frac{U_2}{R_{sh}} \right)^3. \quad (4.8)$$

Realistically, when balancing the thermocouple, the shunt resistance is 20 or more times higher than the initial resistance of the thermocouple, so the last two components in expression (4.8) can be neglected due to their smallness. In this case, equation (4.7) takes the following form

$$U_2 = \left( I - \frac{U_2}{R_{sh}} \right) R_{02} (1 + \beta t_t) + \beta b_2 R_{02} \left( I^3 - 3I^2 \frac{U_2}{R_{sh}} \right). \quad (4.9)$$

Having made the necessary transformations, we finally obtain the equation explicitly describing the voltampere characteristic of the bridge branch with the thermocouple and shunt resistors connected in parallel

$$U_2 = \frac{R_{sh} (I R_{02} (1 + \beta t_t) + I^3 \beta b_2 R_{02})}{R_{sh} + R_{02} (1 + \beta t_t) + 3I^2 \beta b_2 R_{02}}. \quad (4.10)$$

Analysis of expressions (4.2) and (4.10) describing the voltampere characteristics of thermocouples, shows that at real parameters of thermocouples by selecting  $U_{st}$  and  $R_{sh}$  it is always possible to achieve the intersection of the voltampere characteristics at two points. They correspond to the nominal current through the thermocouple and the current at which the catalysis process stops. This is clearly shown in Fig. 4.5, where the voltammetric characteristics of a real thermogroup are presented. For clarity, a defective thermogroup with significantly different parameters of thermoelements was chosen.

In Fig. 4.5, the voltampere characteristics of the elements intersect at current values of 150 mA and 200 mA. At the initial section of the characteristics and at currents above 200 mA, the offset characteristic of the 1st element is located above the characteristic of the bridge branch with the 2nd thermocouple and shunt resistor in parallel. At currents of 150-200 mA the mutual position of the characteristics changes. Physically it can be explained by the fact that at low current through the 2nd thermocouple resistance is low and the presence of a shunt chain does not significantly affect the steepness of the characteristic, with increasing current the resistance of the thermocouple increases significantly and the influence of the shunt on the steepness of the characteristic is significantly increased. Selection of the bias voltage value and parameters of shunt resistors allows to control the position of voltampere characteristics and ensure their intersection at the required points.

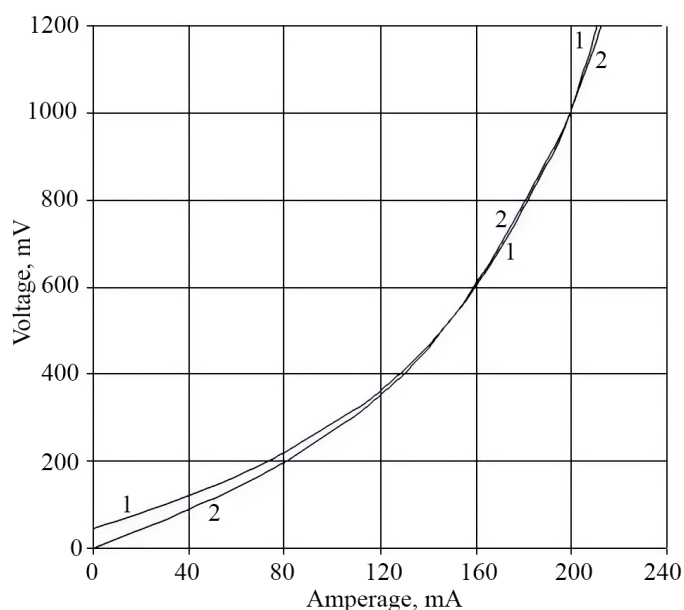


Fig. 4.5. Voltampere characteristics of the elements: 1 – 45 mV offset characteristic of the 1st element; 2 – characteristic of the bridge branch with the 2nd thermocouple and shunt resistor included in parallel

In practice, the adjustment of the characteristics of thermocouples for automatic zero diagnostics of the measuring bridge can be carried out similarly to the order of the bridge thermal balancing proposed by us [4]. Manual adjustment of the bridge is carried out in the absence of methane in the following sequence:

- voltage is applied to the bridge, at which the working element heating is still insufficient for the catalytic reaction of methane oxidation  $U_{pov}$ .
- variable ballast resistor 6 (see Fig. 3.7) sets the zero of the measuring bridge;
- nominal supply voltage  $U_n$  is applied to the bridge;
- after the end of the transient process ( $\approx 5$  s), the bridge zero is adjusted by the variable resistor of the shunt chain 4 (see Fig. 3.8);
- in the specified sequence, the operations are continued until (5-6 cycles of adjustment) the bridge zero does not shift at the transition from nominal supply voltage to  $U_w$ .

The proposed bridge balancing method allows to achieve the current reduction through the thermocouple to exclude the bridge zero offset by repetitively offsetting the bridge zero and selecting the resistance included in parallel to the thermocouple with a steeper voltampere characteristic. However, such a balancing procedure turned out to be rather long and complicated and required the introduction of additional elements for controlling the steepness of the voltampere characteristic (variable resistors) and special personnel training. This did not allow to implement the proposed solutions in practice. Besides, giving access to the bridge zero and thermocouples steepness control settings to the personnel during methane analyzers operation in mine conditions is undesirable. Therefore, to implement this method of automatic diagnostics of gas analyzers zero-readings it is necessary to exclude the balancing process and restrict access to the regulation elements of their zero and sensitivity. Therefore, let us consider the possibility of implementing such diagnostics using modern information processing equipment [5].

Fig. 4.6 shows the voltampere characteristics of thermocouples in the absence of methane in the gas mixture. For clarity, these characteristics are chosen to be significantly different, although in reality the characteristics offset is an order of magnitude smaller. At the value of current through the thermocouples  $I_e$ , corresponding to the sensors operating mode, the voltage on the working (W) and comparison (Comp) elements in series will be:

$$U_w = I_e R_{0w} (1 + \beta t_t) + \beta b_w R_{0w} I_e^3; \quad (4.11)$$

$$U_n = I_e R_{0n} (1 + \beta t_t) + \beta b_n R_{0n} I_e^3. \quad (4.12)$$

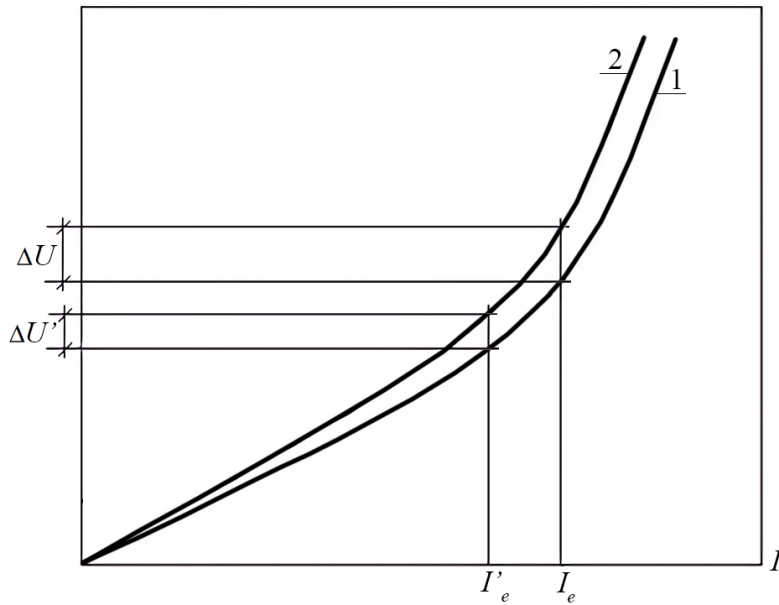


Fig. 4.6. Voltampere characteristics of thermocouples in the absence of methane in the gas consistency

The analysis of expressions (4.11) and (4.12) shows that the change in  $\Delta U$  can occur due to fluctuations in gas temperature, as well as instability of resistance of thermoelements or their thermoresistive coefficients. As for the latter two reasons, they both can occur during long-term sensor operation due to accumulation of hydrocarbon thermal degradation products on the sensing element surface [6] and due to the impact of significant mechanical impulse loads on the elements, which can lead to thermoelement spatial mixing in the reaction chamber or changes in their parameters (cracks appearing, carrier crumbling, etc.). Such overloads can occur due to accidental impacts or falls [7].

Fluctuations of gas temperature in mine workings can occur both due to changes in meteorological conditions and due to changes in ventilation modes of mine workings. When assessing the analyzer zero-reading stability, these fluctuations can be taken into account by software when additionally introducing a gas temperature sensor into the methane analyzer. Besides, reduction of dependence of analyzer zero-readings on temperature can be achieved by controlling the power supply mode of the sensing elements, which should ensure independence of  $\Delta U$  from temperature change. Analysis of expressions (4.11) and (4.12) shows that this can be provided by controlling the current through the elements so that the voltage on the comparative element remains unchanged when the gas temperature changes, which, in the absence of methane, simultaneously provides voltage stability on the working element and independence of  $\Delta U$  from temperature change. In the latter case, the practical independence of the element temperature mode from the medium temperature is simultaneously ensured, which is important for maintaining constant analyzers sensitivity over the entire range of possible changes in the medium temperature [1].

Let us represent expressions (4.11) and (4.12) in the form

$$\Delta U = I_e a + I_e^3 b; \quad (4.13)$$

$$\Delta U' = I'_e a + I_e'^3 b, \quad (4.14)$$

where:

$$a = (R_{0w} - R_{0n})(1 + \beta t_t); \quad b = \beta(b_w R_{0w} - b_n R_{0n}).$$

Availability of information about the value of element resistances obtained in the analyzer debugging mode and gas temperature allows to calculate the value of coefficient  $a$ . Based on equation (4.14) it allows the software to calculate the coefficient  $b$  while in checking analyzer zero-reading mode, based on certain current values  $I'_e$  and  $\Delta U'$ . This allows, when operating the analyzers automatically, based on equation (4.13), not only to check the stability of the analyzer zero-readings, but also to correct these readings when they change within predetermined limits.

Based on the conducted research, an analyzer model with the automatic zero-reading diagnostics function was made and both the algorithm and the analyzer operation program were developed.

There are no elements for regulating the “zero” and the sensitivity in the methane analyzer built with the use of modern microprocessors, in which the function of automatic diagnostics of zero-readings is implemented. The analyzer has two operating modes: debugging mode and working mode. All debugging and testing operations are performed without operator intervention according to the developed analyzer operation program. In the debugging mode the remote sensor of the analyzer is installed in a small-sized chamber, which is alternately filled with atmospheric air or certified gas mixture with methane content of 1.0% by command from the analyzer display. When clean air is supplied, the analyzer sets the current of specified value through the sensing elements, determines and records in the analyzer memory the values of voltages on thermoelements and their difference, determines the values of coefficients  $a$  and  $b$  in the equations. When supplying the certified gas mixture to the remote sensor of the analyzer, the voltage on the comparison element, previously determined for clean air, is determined and set, the voltage on the working element is determined and the sensitivity of the analyzer sensor,  $\text{mV}/\% \text{CH}_4$ , is calculated.

In the working mode, the following operations are continuously performed: measurement of voltages on the elements, support of a certain voltage value on the comparison element, determination of voltage difference on the elements, calculation and transfer of information on methane content. The analyzer zero-readings are checked and corrected on a regular basis or upon operator's request, according to the time defined by the analyzer operation program and in case of stable and safe gas situation in the monitored place. At that, the current through thermocouples is set so the methane oxidation reaction on the working element does not occur. After the end of the transient process following actions are performed: the voltages on the elements and their difference are determined, the values of coefficients  $a$  and  $b$  are specified, the degree of “zero” displacement of the sensor in the absence of methane oxidation reaction on the working element is estimated, and the decision is made whether it is necessary to inform the operator about the need to check and debug the analyzer or to correct the zero-readings of the analyzer. Then the operating current through thermocouples is set, and at the end of the transient process the voltages are measured on the elements, the voltage on the comparative element is adjusted, the voltage difference on the elements is determined, the analyzer zero-readings are corrected based on the results of the check, calculation and transfer of information on the methane content.

Our research established a method for automatic diagnostics of stationary thermocatalytic methane analyzers. This method involves remote, automatic zero-reading control by reducing the thermogroup's supply voltage to a level where methane oxidation on the working thermocouple is prevented. We demonstrated that modern microprocessor capabilities enable both automatic zero-reading stability checks and correction of these readings. Based on these findings, we developed an algorithm and program for analyzer operation with integrated automatic zero-reading diagnostics.

#### **4.2. Development of automatic control methods of thermocatalytic sensor sensitivity**

The issue of automating sensitivity control for thermocatalytic methane sensors is considered in [8]. The authors propose a diagnostic solution: analyze changes in output voltage surge amplitude after a timed pause during which methane oxidation is prevented on the working element of the analyzer's measuring bridge. The authors demonstrate that the normalized surge in bridge output voltage after a pause (caused by methane buildup in the sensor's reaction chamber) directly relates to the working thermocatalyst's effective diffusive conductivity. This finding allows for diagnosing changes in analyzer sensitivity using this indicator. Such diagnostics of thermocatalytic analyzers' sensor sensitivity can be combined with the process of zero-readings control. However, as the authors of this work note, changes in the normalized value of the bridge output voltage surge after a pause occur in case of pollution of the metal-ceramic filter of the sensor, as well as in violation of the reaction chamber integrity. The transient processes arising in this case in various designs of thermocatalytic sensors are considered in [9]. In this case, the analysis of the change in the relative value of the surge amplitude of the bridge output voltage after a continuous pause does not allow us to identify the change in the sensitivity of the sensor and to automatically correct the analyzer readings.

Other approaches to the implementation of automatic diagnostics of methane analyzers sensitivity using modern means of information storage and processing are proposed in [10], and the proposed solutions allow not only to carry out sensitivity control, but also to carry out its correction.

At low methane concentration and oxidation reaction on the working element of the thermo-catalytic sensor in the diffusion area, the methane flux to its surface depends linearly on the methane concentration in the reaction chamber and the effective diffusion conductivity of the element.

$$Q_{m_1} = \gamma_e C_{mk}, \quad (4.15)$$

where:

- $\gamma_e = 10^{-2} K_e \beta_{br} F_e$  – effective diffusive conductivity of the element,  $m^3/s$ ;
- $C_{mk}$  – methane concentration in the reaction chamber;
- $K_e$  – methane oxidation efficiency coefficient;
- $\beta_{br}$  – mass transfer coefficient,  $m/s$ ;
- $F_e$  – surface area of the element,  $m^2$ .

The bridge output voltage at low methane concentrations can be determined by the expression [8]

$$U_{out} = \frac{R_{e0} I_e \beta_e Q_m \gamma_e C_{mk}}{2K}, \quad (4.16)$$

where:

- $R_{e0}$  – resistance of the element at zero temperature, Ohm;
- $I_e$  – current flowing through the elements, A;
- $\beta_e$  – temperature coefficient of element resistance,  $1/^\circ C$ ;
- $K$  – thermal conductivity of the element,  $W/^\circ C$ ;
- $Q_m$  – lower heat of methane combustion,  $J/m^3$ .

In thermocatalytic methane sensors, including those used in stationary methane control equipment, thermocouples are placed in a reaction chamber, which is formed inside a porous ceramic or metal-ceramic gas exchange filter. In this case, the methane flux to the surface of the working element of the thermocatalytic sensor is defined as [1]

$$Q_{m_1} = C_{ma} \gamma_e \gamma_f / \gamma_e + \gamma_f, \quad (4.17)$$

where:

- $C_{ma}$  – concentration of methane in the atmosphere;
- $\gamma_f$  – conductivity of the filter,  $m^3/s$ .

From expression (4.17) it is clear that the methane flux to the catalytically active element and the output voltage of the bridge at a constant methane concentration depends on the conductivity of the filter and the catalytic activity of the working element. Change of these values is possible at change of the bridge power supply mode, under the influence of harmful gases, in the process of aging and accumulation of products of thermal destruction of hydrocarbons on the surface of sensitive elements, filter clogging, etc.

To improve the stability of methane analyzers, an improved design of a sensor with a double diffusion filter was proposed [1]. Sensing elements in this sensor are placed in an additional chamber made in the form of a gas-tight beaker with a calibrated orifice in the partition with diffusion conductivity. It is located inside of the volume separated from the atmosphere by a filter. In this case, the methane flux to the surface of the working element of the sensor is defined as [1]

$$Q_{m_1} = C_{ma} \gamma_e \gamma_f \gamma_{hole} / (\gamma_f \gamma_e + \gamma_e \gamma_{ot} + \gamma_f \gamma_{ot}). \quad (4.18)$$

At the choice of  $\gamma_{hole} \ll \gamma_f$  and  $\gamma_{hole} \ll \gamma_e$  the flow of methane oxidized on the working element is determined by the diffusion resistance of the orifice and the bridge output voltage is practically not affected by the filter element clogging and the change in the sensitivity of the working element of the thermocatalytic sensor.

However, fulfillment of such a condition is accompanied by decrease of the bridge output voltage and sensor's constant time increase. Therefore in practice  $\gamma_f$  is chosen in the range from  $2\gamma_{hole}$  to  $6\gamma_{hole}$ . The bridge output voltage is within  $10^{-4}$  mV/vol.% and the sensor's time constant is kept within 15 s [1].

The peculiarity of the sensor with a double diffusion filter is that the bridge output voltage in a significant current range through the thermocouples practically does not depend on the change of its value. For example, Fig. 4.7 shows the characteristics of the sensor with an additional diffusion filter obtained experimentally at the concentration of methane in the atmosphere  $C_{ma} = 1.02$  vol.% [1].

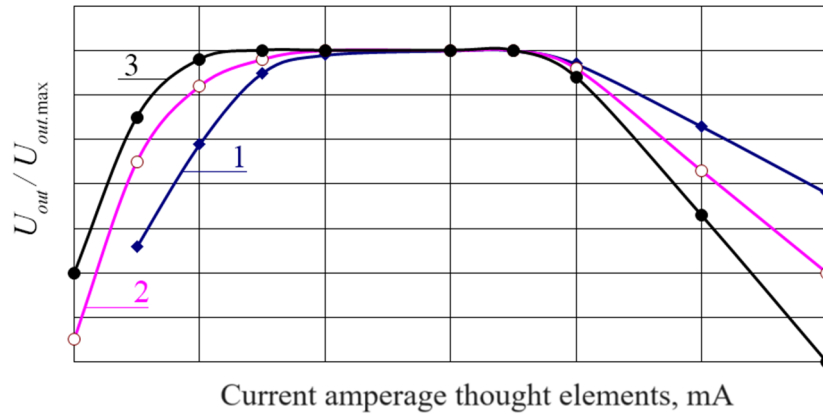


Fig. 4.7. Output characteristics of the sensor with additional diffusion filter ( $C = 1.02$  vol.%):

$$1 - \gamma_e = 2\gamma_{hole}; \quad 2 - \gamma_e = 4\gamma_{hole}; \quad 3 - \gamma_e = 6\gamma_{hole}$$

This nature of dependence of the bridge output voltage on the current through the thermocouples is explained by the fact that the flow of methane oxidized on the working element is practically determined by the diffusion resistance of the orifice. Thus the growth of the current through the elements and the effective diffusion conductivity of the working element cause the growth of the bridge output voltage, but at the same time they cause the decrease of methane concentration in the measuring chamber. In addition, at high heating temperatures of the sensing element, methane oxidation processes occur not only on the surface of the catalyst, and this causes additional dissipation of reaction energy and reduction of the real value of the bridge output voltage [11]. In this case, the power supply mode of the measuring bridge is chosen so that at minimum power consumption the operating point is on the plateau (horizontal part) of the characteristic. In this case, at a gas mixture temperature of 20 °C for the sensor with the characteristics shown in Fig. 4.7, this corresponds to a current through the thermocouples of 190 mA and the voltage on the comparative thermocouple of about 750 mV.

Proceeding from (4.18) at constant value of  $\gamma_{hole}$  and constant methane concentration, reduction of effective diffusivity of the working element from  $6\gamma_{hole}$  to  $2\gamma_{hole}$  leads to reduction of methane flux to the surface of the working element and analyzer sensitivity up to 20%.

Let us consider the possibility of analyzer sensitivity automatic control by changing the power supply mode to the sensing elements. Let's assume that when debugging the analyzer using certified methane-air mixture with methane concentration  $C = 1.02$  vol.%, the power supply mode to the sensitive elements was chosen so that the operating point was at the beginning of the characteristic plateau. This corresponds to the current through the thermocouples of 190 mA. Let's assume that the initial effective diffusion conductivity of the working element was  $\gamma_e = 6\gamma_{hole}$ . If we reduce the current through the thermocouples to 180 mA, then, based on the sensor characteristic (Fig. 4.7) the bridge output voltage will decrease by 2%. If the effective diffusivity of the working element decreases three times (to  $\gamma_e = 2\gamma_{hole}$ ), for example, due to catalyst poisoning, a similar change in the power supply mode of the sensing elements will lead to a 22% decrease in the bridge output voltage. Thus, while maintaining  $\gamma_e = 6\gamma_{hole}$ , the change of the power supply mode within the specified limits practically does not affect the bridge output voltage. A decrease in the effective diffusion conductivity of the working element leads to a significant decrease in the bridge output voltage when changing the power supply mode.

Such change of the bridge output voltage at change of the sensing elements power supply mode allows not only to automatically detect the decrease of the effective diffusion conductivity of the working element and changes in the analyzer sensitivity, but also to automatically carry out the sensitivity correction. When selecting the power supply mode of sensitive elements it should be taken into account that their temperature mode is influenced by both the current and the gas temperature. Generally, the temperature of the element in air can be estimated by the expression [1]

$$t_e = b_e I_e^2 + t_i. \quad (4.19)$$

The thermoresistive coefficient  $b_e$  for the working element is a constant and for the investigated pellister-type thermoelements is about  $9 \cdot 10^3 \text{ Ohm} \cdot \text{°C/W}$ . On this basis, in order to ensure a stable temperature regime of thermocouples when the gas temperature changes, the value of the current through the elements should be corrected as

$$I_e = \sqrt{I_{en}^2 - \frac{1}{b}(t_i - t_m)}, \quad (4.20)$$

where:

$I_{en}$ ,  $t_m$  – current and gas temperature at analyzer setting.

Our research led to the development of an algorithm and program for an analyzer with automatic zero-reading diagnostics. Built on the ATMEGA8 microprocessor [5], this system includes a module for automatic sensitivity diagnostics of the thermocatalytic sensor, enabling correction of analyzer readings when sensitivity changes.

The essence of the sensitivity diagnostic and correction process for the thermocatalytic sensor involves the following steps. In debugging mode, a certified gas mixture (1.0% methane content) is supplied to the analyzer's remote sensor. The current through the sensitive elements is adjusted (180-200 mA) until the bridge output voltage reaches a plateau (Fig. 4.7). The system then determines and stores the relative decrease in bridge output voltage  $\Delta U_{an}$  when the current is reduced by 5%. This value serves as a reference point to detect and correct changes in the analyzer's sensitivity

$$\Delta U_{an} = \frac{U_{1n} - U_{2n}}{U_{1n}}, \quad (4.21)$$

where:

$U_{1n}$  and  $U_{2n}$  – value of the bridge output voltage in the tuning mode when operating on the plateau of the characteristic and reducing the current through the elements by 5%.

The moment when the output voltage of the bridge reaches the plateau of the characteristic is fixed when the current increase by 1 mA does not lead to the increase of the bridge output voltage by more than 1%. The value of the set current and gas temperature during the analyzer setup is stored in the analyzer's memory and is further used to set the analyzer operating mode.

In the operating mode the following operations are continuously performed: stable temperature mode maintenance of thermocouples when the gas temperature changes accordingly (4.20), voltage measurement on elements, determination of voltage difference on elements, calculation and transfer of information on methane content. Upon operator's request or on a regular basis according to the timeframe defined by the analyzer operation program, the sensor sensitivity is checked and the analyzer readings are corrected in case of its change. For this purpose, the current through the sensitive elements is reduced by 5% relative to the set operating mode and the output voltage reduction relative value of the analyzer's bridge is determined.

$$\Delta U_{aw} = \frac{U_{1w} - U_{2w}}{U_{1w}}, \quad (4.22)$$

where:

$U_{1w}$  and  $U_{2w}$  – value of the bridge output voltage when operating on the plateau of the characteristic and reducing the current through the elements by 5%.

The relative magnitude of the output voltage reduction  $\Delta U_{aw}$  is determined and compared to  $\Delta U_{an}$ . If  $\Delta U_{aw} = \Delta U_{an}$ , the sensor retains its initial sensitivity and no adjustment is required. If  $\Delta U_{aw}$  decreases relative to  $\Delta U_{an}$  up to 10%, the analyzer sensitivity is corrected by increasing it by  $\Delta U_{an} - \Delta U_{aw}$ . Otherwise, the operator is notified about the need to check and debug the analyzer.

It should be noted that when changing the power supply mode of the sensor sensitive elements there are transient thermal and gas-dynamic processes, so the readings should be taken after the end of the transient process. For the primary transducers under study it lasts about 5s from the moment of current reduction through the thermocouples. In mine conditions, where methane concentrations may fluctuate during the diagnostic process, the relative decrease in output voltage  $\Delta U_{aw}$  should be measured multiple times. The collected data must then be processed to identify consistently repeated values, while random outliers are disregarded.

Our research established a method for automatic sensitivity diagnostics in stationary thermocatalytic methane analyzers. This method involves remotely analyzing the initial characteristics of primary converters. We do this by observing changes in bridge output voltage (when the current through sensitive elements shifts) while the voltage remains on the characteristic plateau. Modern microprocessor technology enables both automatic sensitivity checks of primary converters and correction of gas analyzer readings when sensitivity changes. Based on our research, we developed an algorithm and program specifically for analyzers with remote control of thermocatalytic methane sensor sensitivity.

### **4.3. Improving the speed of automatic gas protection systems**

Reducing the probability of methane-air mixture explosions requires increasing the reliability of methane control systems and protective shutdowns [12]. However, even with reliable systems, the limited speed of control mechanisms may still allow ignition during sudden releases of coal, rock, and gas.

Ukraine, along other countries, has accumulated significant experience in developing and operating automatic gas control equipment [1, 9]. In Ukrainian mines, particularly those susceptible to sudden coal outbursts, ATB methane analyzers are widely used. These analyzers provide continuous centralized monitoring of methane concentration and its rate of increase within mine workings. Additionally, they trigger power shutoffs in controlled areas when methane levels or their growth rate exceed permissible limits. However, the frequent occurrence of false alarms from ATB analyzers in the absence of actual gas surges leads to unnecessary equipment downtime and significant economic losses [13]. Given these limitations, there's a clear need to either improve existing fast-acting methane control systems or develop entirely new approaches. To prevent methane-air mixture explosions, further research must focus on both enhancing the reliability and increasing the speed of these systems.

The analysis of existing methods of methane content control has shown that the best performance of gas control equipment can be provided by the application of optical absorption method. However, the disadvantages of this method include a significant influence of temperature, pressure, humidity and various gas impurities on the measurement results. High dust levels in mine air significantly hinder the use of this measurement method at analyzer installation points.

Recent studies of the optical method have made it possible to develop sensitive compact methane sensors [14, 15, 16]. These sensors use a metal mesh as a filter, inside which the measuring optical channel is located. With the thickness of the metal wire of 0.1 mm and the area of the filter orifices 0.01 mm<sup>2</sup> the constant time is about 1s. In the experimental designs of methane analyzers based on the optical adsorption method, the dynamic performance of analyzers is improved by the software [16] and the influence of the mentioned factors on the measurement results, including dustiness, is partially compensated [14]. However, this leads to a significant analyzer complication, including those requiring the use of additional optical sensors with changed spectral characteristics. In addition, the issues of automatic diagnostics of methane analyzers based on the optical adsorption method have not been solved yet.

Currently, almost all methane analyzers used in automatic gas protection systems are based on a relatively inert thermocatalytic measurement method [1, 8]. This is due to the high selectivity of thermocatalytic sensors, minimal influence of gas composition, air humidity, dust, temperature, etc. factors on their operation. The studies of this method [1, 8] and thermocatalytic devices of methane control have allowed to significantly improve the reliability and stability of such gas analyzers.

An advantage of thermocatalytic sensors is that their operation can be monitored by adjusting power supply parameters. This functionality, combined with modern microprocessors, enables computerized diagnostics of control devices and protective shutdown systems. Our research [5] established a method for automatic diagnostics of stationary thermocatalytic methane analyzers. This method involves remote control of analyzer zero-readings by reducing thermogroup supply voltage until methane oxidation ceases on the working thermocouple. Modern processors enable both automatic stability checks of analyzer zero-readings and the ability to correct those readings if they change. An algorithm and program that implement automatic zero-reading diagnostics in analyzers were developed. A method for automatic remote sensitivity control of primary converters has been substantiated. This method involves analyzing their initial characteristics as the current through the sensitive elements is changed within the plateau region of the bridge's output voltage characteristic [10]. Utilizing contemporary information processors, it has become feasible to not only employ automated verification of the sensitivity stability of primary converters, but also to rectify the readings of the gas analyzer in the event of sensitivity variations [10]. An algorithm and program with the capability for automatic analyzer performance diagnostics have been developed.

Dynamic characteristics have been improved by redesigning sensors and minimizing the size of sensitive elements. The speed of gas control equipment has been somewhat increased by reducing the time constant of thermocatalytic sensors and utilizing additional information features [8]. However, this issue remains unresolved.

It is obvious that high speed performance of an optical sensor can be provided by installing radiation sources and receivers directly in the analyzed gas flow. However, in this case, dust is intensively deposited on the radiation source and receiver, which leads to significant measurement errors and to analyzers failure. Considering the intensive dust deposition where sensors for fast-acting gas control equipment are installed (bottom-hole spaces, cleaning/preparatory interfaces), where dust concentration can reach 500 mg/m<sup>3</sup> or more, unprotected sensing elements are quickly impacted by dust accumulation. This renders them practically unusable. Protective elements, while necessary, present a challenge. They increase sensor response time and complicate maintenance procedures. These factors have hindered the development of reliable, fast-acting gas control systems using optical measurement methods. An alternative solution to this issue could be the development of methane analyzers that utilize two sensors simultaneously: a main thermocatalytic sensor and a low-inertia optical sensor for support [17].

Fig. 4.8 depicts a structural diagram of gas control equipment designed with two methane sensors. In this analyzer, the main sensor is a highly stable and relatively inert thermocatalytic sensor. Its output signal is used for several purposes: generating a telemetering signal, triggering power cutoff, and correcting the output of the auxiliary low-inertia optical sensor. This optical sensor, in turn, provides a power cutoff signal when it detects unacceptable levels of methane concentration or an unacceptable rate of change.

A drawback of this solution is that dust accumulating on the optical sensor elements not only alters its readings but also affects its sensitivity. Unfortunately, adjusting the sensor's output signal cannot compensate for this sensitivity change. This poses a potential risk of premature protection activation under certain conditions.

This disadvantage can be eliminated by using the optical sensor to measure the methane concentration increment during gas dynamic phenomena, rather than the absolute concentration value. According to Bouguer's Law, the relationship between the incident radiation flux intensity ( $J$ ) and the amount of energy absorbed  $J_n$  by an infinitely thin layer  $dx$  of the analyzed gas within a specific spectral interval  $dv$  is expressed by the following equation

$$J_n = -KJdx dv, \quad (4.23)$$

where:

$K$  – absorption coefficient.

At constant radiation wavelength, thickness of the mixture layer  $x$  with methane concentration  $C$ , the solution of equation (4.23) has the form

$$J_n = J_0(1 - \exp(-ACx)), \quad (4.24)$$

where:

$A$  – absorption coefficient at wavelength  $\lambda$ , characteristic of the absorbing gas molecule, independent of its concentration.

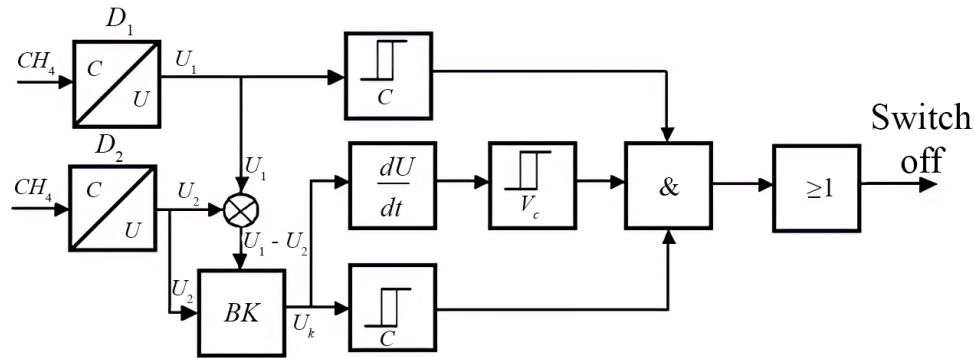


Fig. 4.8. Structural diagram of a fast methane analyzer [17]

When controlling pre-explosive methane concentrations and the distance between the radiation source and receiver is up to several decimeters, expression (4.24) can be represented as a linear dependence

$$J_n = J_0(1 - ACx). \quad (4.25)$$

Based on expression (4.25), a change in gas concentration by the value  $\Delta C$  will lead to a change in radiation flux by the value of

$$\Delta J_n = A\Delta CxJ_0. \quad (4.26)$$

Whence we have

$$\Delta C = a \frac{\Delta J}{J_0}, \quad (4.27)$$

where:

$a = 1/Ax$  is a constant value depending on the absorption capacity of the gas and the distance between the radiation source and receiver.

Expression (4.27) indicates that if the initial intensity of the incident radiation flux and its intensity after a selected time interval  $\Delta t$  are known, the increase in methane concentration during gas dynamic phenomena (within a small time interval) can be calculated with certainty. Importantly, the relative value of absorbed energy remains independent of fluctuations in the incident radiation flux's absolute intensity. This ensures that measurement results are not affected by gradual processes like temperature shifts, pressure changes, or dust accumulating on optical elements.

This allows us to take a different approach to the issue of creating a methane analyzer for fast-acting gas protection systems with simultaneous use of thermocatalytic and optical methane sensors (Fig. 4.9). Essentially, this approach means that in the absence of significant methane fluctuations caused by gas-dynamic phenomena, information about methane concentration and the signal to trigger electrical equipment shutdown are generated based on measurements taken by the thermocatalytic sensor  $D_1$ .

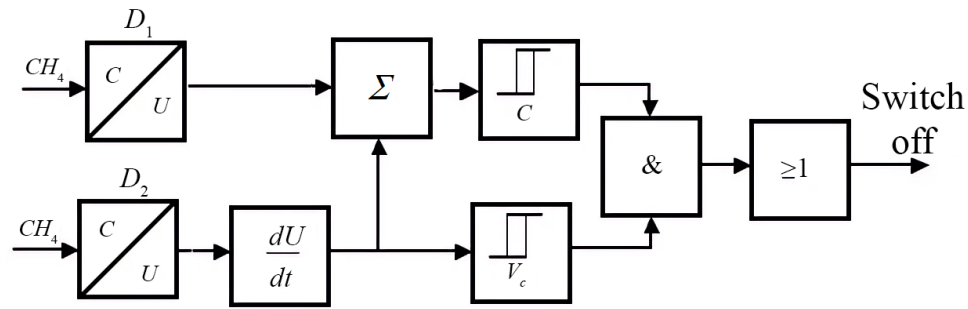


Fig. 4.9. Structural diagram of the analyzer for fast-acting gas protection systems

Low-inertia optical sensor  $D_2$  is used only to determine the value of methane concentration increase in a short period of time during gas-dynamic phenomena. If the increase in methane concentration exceeds a permissible value (e.g. 1%/c), regardless of the current value of methane concentration in the mine, a signal to shut down the electrical equipment is instantly triggered. Alternatively (for example, within the  $0.2\%/s \leq dC/dt < 1.0\%/s$  range of concentration increase), the sum of the current methane concentration (measured by the thermocatalytic sensor) and the concentration increase over a specific period is calculated. If this sum exceeds the unacceptable concentration threshold, a signal to shut down electrical equipment is generated.

The proposed method for increasing the speed of automatic analyzer systems can be implemented by supplementing our existing analyzer with several features. These include: automatic diagnostics and correction of zero-readings and sensitivity for primary thermocatalytic converters [5, 11, 18], a low-inertia optical sensor, and the necessary algorithm and program modifications [19, 20].

This fast methane analyzer, built on the ATmega8 microcontroller, features two operating modes: debugging and working. The debugging process runs automatically without external input or operator intervention, utilizing clean air and a certified gas mixture (e.g., with 1% methane) for calibration.

After entering debug mode, the analyzer's display shows "Air" and a countdown to program initiation. Subsequently:

- methane sensors are placed within a special small-sized chamber;
- the chamber is filled with clean air;

Fig. 4.10 illustrates the analyzer's operation algorithm for debugging the fast optical sensor.

In this mode, the following actions are performed programmatically, with necessary time delays to allow for transient completion:

- the rated current through the light-emitting diode is set;
- the voltage value ( $U_0$ ) at the output of the optical sensor is determined;
- the  $U_0$  value is stored in the microcontroller's memory.

After a time delay (for thermocatalytic sensor debugging), the analyzer displays "Tested Mixture" and a countdown. The chamber is filled with certified gas mixture (e.g., 1% methane). Subsequently:

- the light-emitting diode current is checked and corrected if necessary;
- the optical sensor output voltage  $U_w$  is determined;
- $\Delta U = U_0 - U_w$  is calculated;
- the relative voltage change  $K_0 = \Delta U / U_0$  is determined;
- if the certified mixture's methane concentration  $Ca$  deviates from 1%,  $K_0$  is adjusted to a 1% equivalent  $K_1 = K_0 / Ca$ ;
- the  $K_1$  value, representing optical analyzer sensitivity based on relative output voltage change, is stored in the microcontroller's memory.

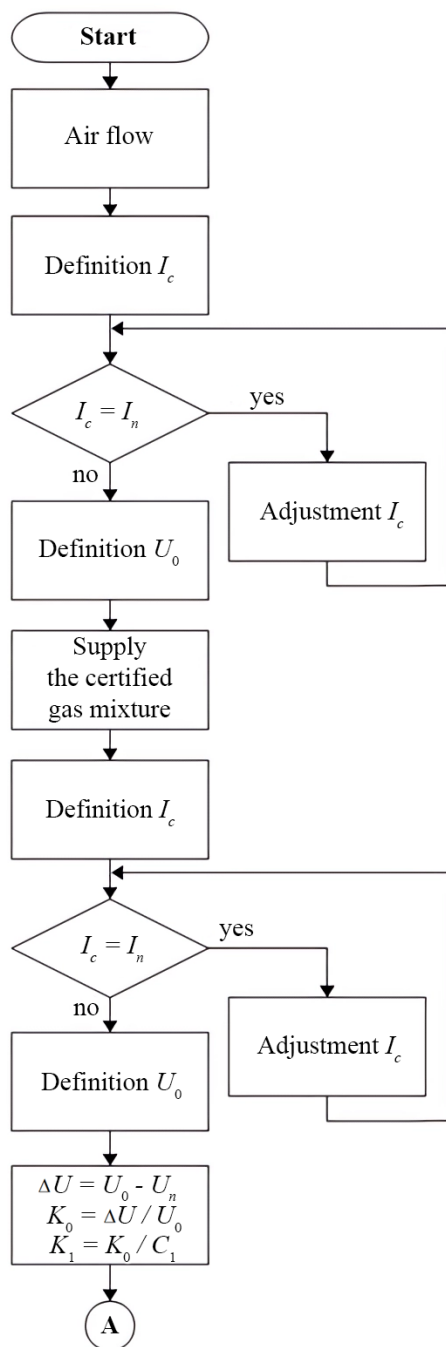


Fig. 4.10. Algorithm of the analyzer operation in the debugging mode

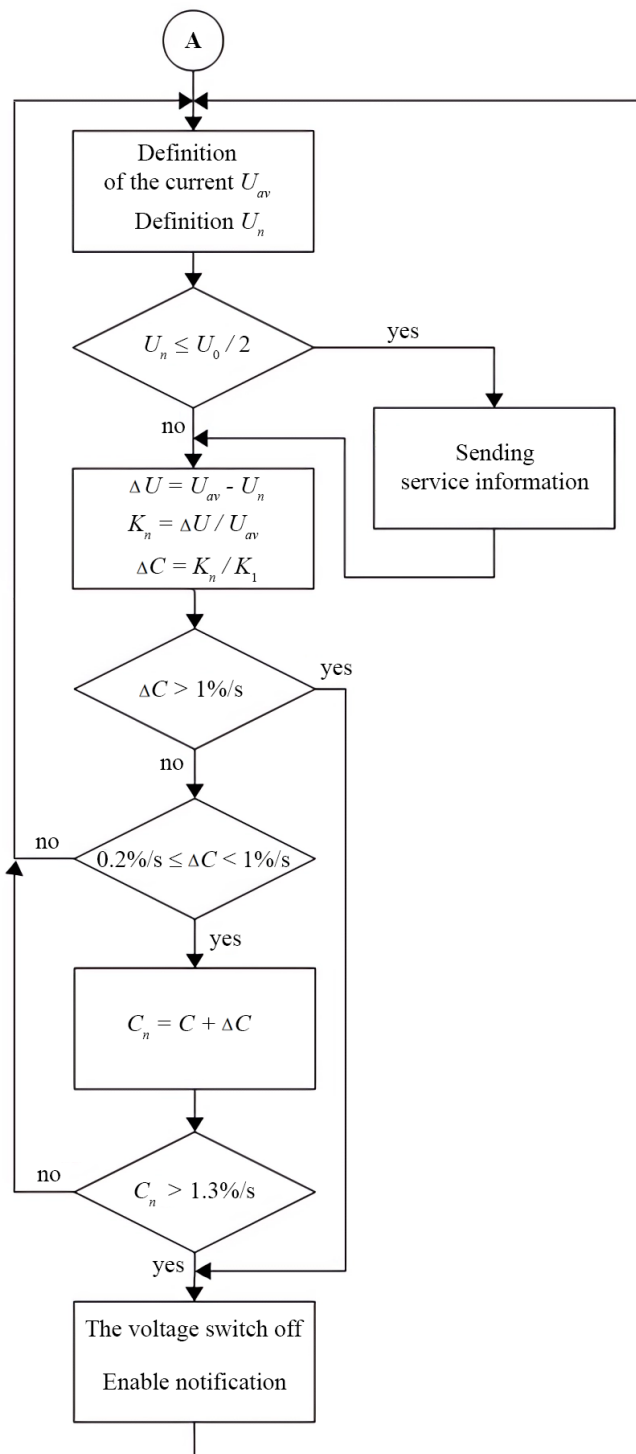


Fig. 4.11. Algorithm of the analyzer in the operating mode

Upon debugging program completion, the analyzer enters operating mode (algorithm shown in Fig. 4.11). In this mode:

- the optical sensor's output voltage  $U_w$  is measured at regular intervals (e.g., every 0.5 seconds, aligning with protective shutdown system requirements per [5]);
- the current average value of  $U_{avg}$  at the optical sensor output is determined based on the last 10 measurements (this averaging time accounts for the thermocatalytic sensor's time constant);
- the difference between the current average value of  $U_{comp}$  and the result of the last measurement  $\Delta U = U_{comp} - U_{const}$  is determined;

- the relative voltage change  $K_{const} = \Delta U / U_{comp}$  is determined;
- the change (increase or decrease) in methane concentration over the last time interval  $\Delta C = K_{const} / K_1$  is calculated;
- if  $\Delta C > 1.0$  %/s, a command to turn off the electrical power is given;
- provided that  $0.2\%/c \leq \Delta C < 1.0$  %/c, the corrected current value of methane content  $C_{corrected} \geq 1.3\%$  is determined as the sum of the thermocatalytic sensor reading and the concentration increase for a certain time interval;
- if  $C_{corrected} \geq 1.3\%$ , a command to cut off the electric power is given;
- by the value of  $U_{const}$  the state of optical channel pollution is evaluated, in case  $U_{const} \leq U_0 / 2$  the operator sends a message about the necessity of methane analyzer maintenance.

#### 4.4. Conclusions

Based on the research carried out in the section, the following conclusions can be drawn:

1. Automatic diagnostics for stationary thermocatalytic methane analyzers can be achieved through remote zero-reading control. This involves reducing the thermogroup's supply voltage to a level where methane oxidation on the working thermocouple is halted. Modern microprocessors enable not only automatic verification of zero-reading stability but also the correction of these readings if deviations occur. To utilize these findings, an algorithm and program for analyzer operation with automatic zero-reading diagnostics have been created.
2. This method enables automatic diagnostics of stationary thermocatalytic methane analyzers for remote sensitivity control of primary converters. It analyzes initial characteristics when altering the current through sensitive elements – specifically, at the plateau of the bridge's output voltage characteristic. Modern microprocessors allow for automatic verification of primary converter sensitivity stability and the correction of gas analyzer readings when sensitivity shifts. To apply these findings, an algorithm and program have been developed for analyzer operation, featuring automatic remote control of thermocatalytic methane sensor sensitivity.
3. It is possible to increase the speed and reliability of gas control equipment by simultaneously using two sensors, one of which is highly stable but relatively inertial, for example, thermocatalytic, and the other, optical, has low-inertia. We justified a method of explosion hazard detection that relies on the fact that in the absence of significant disturbances caused by gas-dynamic phenomena, the information on methane concentration and the formation of a signal to shut down electrical equipment is based on the concentration measurement by a thermocatalytic sensor. A low-inertia optical sensor is used exclusively to detect rapid methane concentration increases during gas-dynamic disturbances. Provided that the methane concentration increment exceeds the permissible value, the electrical equipment is shut down regardless of the methane concentration in the mine workings. Otherwise, the sum of the current value of methane concentration determined by the thermocatalytic sensor and the concentration increase for a certain period of time is determined. If this sum exceeds the unacceptable concentration, the electrical equipment is shut down. It is shown that the value of methane concentration increase for a short period of time can be unambiguously determined by calculating the relative value of the incident radiation flux intensity change, which ensures the independence of the methane concentration increase measurement results from slow processes associated with changes in temperature, pressure and dust accumulation on the optical elements.

#### References

- [1] Holinko V.I., Kotlyarov A.K., Belonozhko V.V. (2004) *Controlling explosion hazards in mine workings* D.: Nauka i Obrazovanie [in Russian]
- [2] Belonozhko V.V. (2003) *Investigation of temporal stability of thermocatalytic methane sensors*. (pp. 76-79), Naukovyi visnik NSU, 11, Dnipropetrovsk [in Russian]
- [3] *Equipment for testing thermochemical sensors of automatic gas protection system "Accord". Operation Manual*. (1979) (p 81) Konotop: NPO "Krasny metallist"[in Russian]

- [4] Bilonozhko V.V., Bilonozhko V.P., Bilonozhko V.I. et al. Ukrainian Patent 62861A, MK G01N27/18 (15.12.03) *Thermocatalytic sensor inclusion circuit and its balancing method Bulletin No. 12* [in Ukrainian]
- [5] Alekseev M.O., Holinko O.V. (2018) *Automated diagnostics of stationary thermocatalytic gas analyzers* (pp. 223-229). Collection of scientific papers of NSU. D.: NGU, 53 [in Ukrainian]
- [6] Holinko, V.I.; Belonozhko, A.V. (2008) Study of hydrocarbon thermal degradation products accumulation on the surface of thermocouples. *Naukovy visnik NSU*, (7), 60-65 [in Russian]
- [7] Holinko, V.I.; Belonozhko, A.V. (2006) Study of thermocatalytic methane sensors performance after their long-term operation. *Naukovy visnik NSU*, (10), 72-75 [in Russian]
- [8] Holinko V.I., Kotlyarov A.K. (2004) *Developing a method to control the sensitivity of thermocatalytic methane sensors* (pp. 54-60). *Girnycha Elektromechanika ta Avtomatika*, (73). [in Ukrainian]
- [9] Holinko V.I., Kotlyarov A.K. (2010) *Control of explosion hazard environment in mine workings and equipment of coal mines*. Monograph. Dnepropetrovsk: "Lira" [in Russian]
- [10] Alekseev M.O., Holinko O.V. (2020) Automatic control of sensitivity of sensors of stationary thermocatalytic methane analyzers (pp. 16-22). *Girnychiy visnik*, (107) [in Ukrainian]
- [11] Holinko V.I. Belonozhko V.V. (2003) Methane oxidation process study in thermocatalytic sensors. *Naukovyi visnik NSU*, (7), 62-65. Dnipropetrovsk [in Russian]
- [12] Kolosyuk A.V., Kolosyuk V.P. (2017) *Explosion hazard of power supply systems for mining machinery in mines hazardous for sudden coal and gas emissions*. Monograph. Kremenchuk: KrNU imeni Mykhaila Ostrogradskoho [in Ukrainian]
- [13] *Mine gas analysing devices. General requirements, test methods: DSTU GOST 24032:2009. from 2009-02-01.* (2009) K.: Derzhspozhzhivstandart [in Russian]
- [14] Vovna, A.V.; Zori, A.A. (2013) Fast methane concentration meter in coal mines. *Visnyk Kremenchutsk. Natsionalnogo universytetu im. Mykhaila Ostrogradskogo*, 6(83), 114-119. Kremenchuk [in Russian]
- [15] Vovna O.V., Zori A.A., Akhmedov R.M. (2017) Improving the accuracy of an optoelectronic methane concentration meter for coal mines. *Visnyk Natsionalnogo tekhnichnogo universytetu "KPI", "Power engineering and conversion technology"*, 4(1226), 19-24. Kharkiv: NTU "KPI" [in Ukrainian]
- [16] Vovna O.V., Zori A.A., Khlamov M.G. (2010) Dynamic error compensation method for infrared methane concentration meter for coal mines. *Visnyk Natsionalnogo tekhnichnogo universytetu "KPI", "Power engineering and conversion technology"*, (12), 65-70. Kharkiv: NTU "KPI" [in Ukrainian]
- [17] Holinko, V.I. (2013) *Improvement of dynamic characteristics of methane analyzers*. Collection of scientific papers. Issue 1 "Aerology and safety of mining enterprises" (pp.88-100), M.: Izdatelstvo "Gornoe Delo" LLC "Cimmeria Center" [in Russian]
- [18] Pivnyak, G., Falshtynskyi, V., Dychkovskyi, R., Saik, P., Lozynskyi, V., Cabana, E., & Koshka, O. (2020). *Conditions of Suitability of Coal Seams for Underground Coal Gasification. Key Engineering Materials*, (844), 38-48. doi:10.4028/www.scientific.net/kem.844.38
- [19] Golovchenko, A., Dychkovskyi, R., Pazynich, Y., Edgar, C.C., Howaniec, N., Jura, B., & Smolinski, A. (2020). *Some Aspects of the Control for the Radial Distribution of Burden Material and Gas Flow in the Blast Furnace*. *Energies*, 13(4), 923. doi:10.3390/en1304092
- [20] Holinko V.I., Holinko O.V., (2021) *Algorithms and methods for performance improvement of automatic gas protection systems*. Scientific works of Donetsk National Technical University, series "Problems of modeling and automation of design", 1(17), 79-87 [in Ukrainian]

## **Abstract**

This book, *Methane from Underground Coal Mines in Ukraine: Elements of Acquisition and Management Processes*, provides a comprehensive analysis of methane emissions from underground coal mines in Ukraine. It explores the multifaceted aspects of methane management, including the processes of acquisition and handling of this potent greenhouse gas.

By delving into the specific conditions and challenges faced by the Ukrainian mining sector, this book offers insights into the technical, environmental, and economic considerations necessary for effective methane management. Key elements include the assessment of current methane emission levels, strategies for methane capture and utilization, and policy recommendations to enhance safety and environmental performance in coal mines.

This book serves as a crucial resource for industry professionals, policymakers, and researchers interested in sustainable mining practices and greenhouse gas mitigation. It is also of interest to teaching staff and students of higher education institutions in the teaching of mining disciplines, and in the completion of coursework and diploma projects.



## Vasyl Holinko

Doctor of technical sciences, professor

### Areas of scientific research:

- problems of mine ventilation and labor protection;
- mine atmosphere control,
- industrial sanitation and civil safety;
- methane and dust suppression.

Author and co-author of about 300 published works, including 16 monographs, 3 textbooks, 17 training manuals. In 2008, in view of the significant scientific achievements for the work "Scientific and technological foundations, development and implementation of highly effective geomechanical monitoring of geotechnical systems of mines and mines" as part of the scientific team, he was awarded the State Prize of Ukraine in the field of science and technology.



## Roman Dychkovskyi

Doctor of technical sciences, professor

### Areas of scientific research:

- extracting the thin and very thin coal seams, including reserves with different structural changes;
- substantiation the mining technologies in zones of geologic infringements and stress borders;
- underground coal gasification;
- management of mining pressure;
- simulation the mining processes and other problems related to mining activity.

Author and co-author of more than 260 publications (including 21: monographs, reference books and textbooks, 73 scientific articles in scientometric databases Scopus and WoS, and 28 patents for intellectual property rights). Dychkovsky Roman is an honored worker of education of Ukraine.



## Artur Dyczko

Doctor of Philosophy (PhD) in Technical Sciences

### Areas of scientific research:

- mining of ore and non-ore deposits;
- planning of mining production;
- geomechanics and management of mining pressure;
- simulation the mining processes;
- AI in mining;
- neural networks in data processing and other problems related to mining activity.

Author and co-author of about 100 publications, including monographs, reference books and textbooks and scientific articles in scientometric databases Scopus and WoS. Dyczko Artur honored in recognition of special merits with the Badge of Honor "Merit for Safety in Mining".



## Marcin Popczyk

Doctor of technical sciences PhD employed at Silesian University of Technology, Faculty of Mining, Safety Engineering and Industrial Automation since 2002

### Areas of scientific research:

- underground mining of hard coal deposits
- underground waste management in mining
- prevention of underground fires in hard coal mines
- utilization of fine-grained waste from energy production in the mining industry
- pipeline hydrotransport of hydromixes based on fine-grained materials

Author and co-author of about 80 publications, including monographs, reference books and textbooks and scientific articles in scientometric databases Scopus and WoS, Co-author of 2 patents. In 2016, he was awarded the Prime Minister's award for scientific activity in 2011.